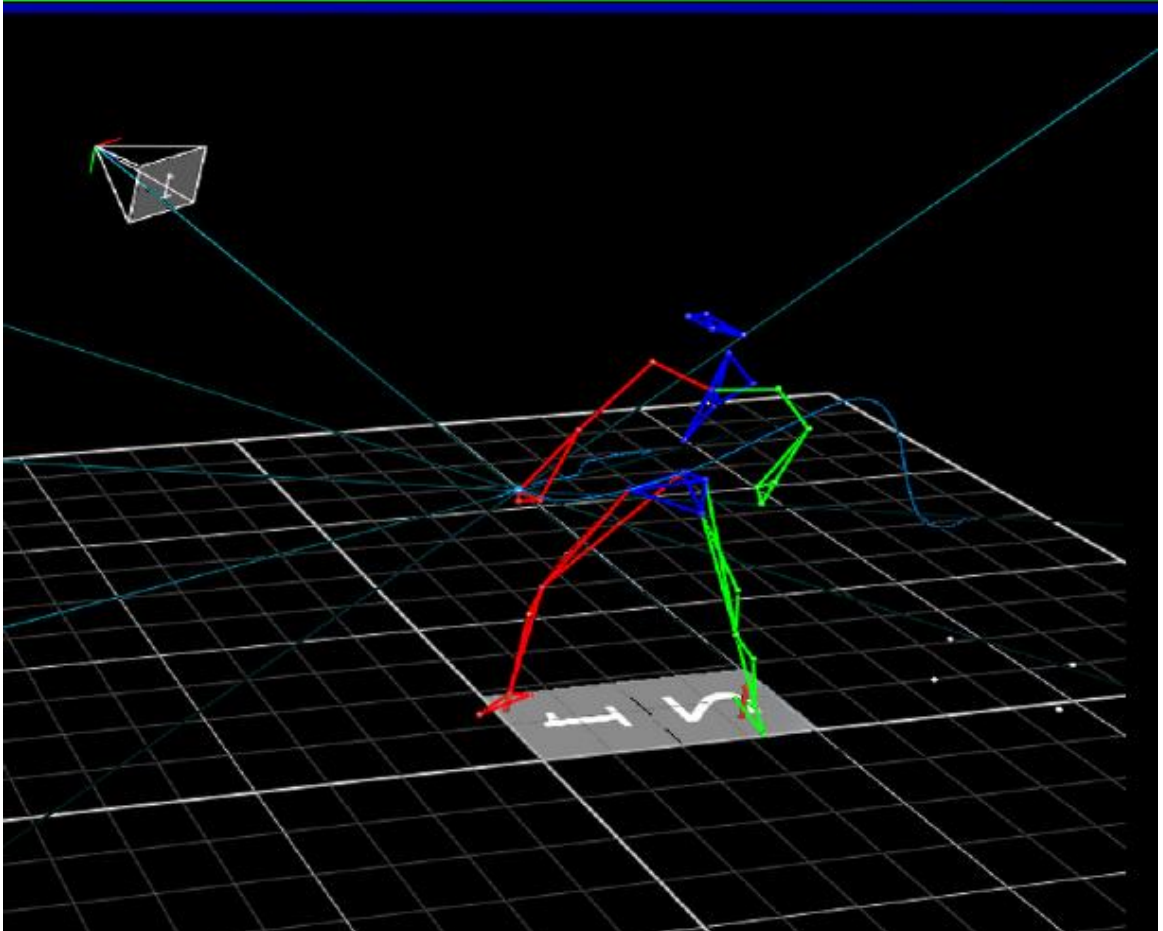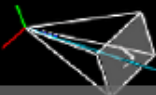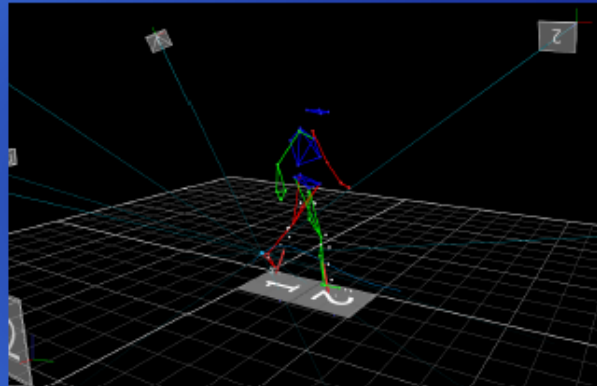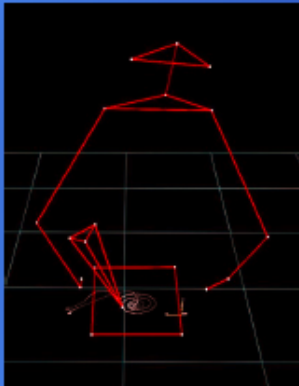# Andrea Ancillao

Stereophotogrammetry in human movement analysis

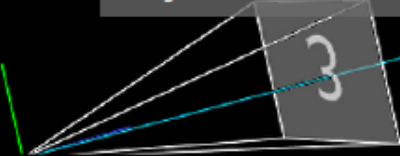Novel methods for the quality assurance, biomechanical analysis and clinical interpretation of gait analysis

The study of movement has always fascinated artists, photographers and researchers. Across the years, several attempts to capture, freeze, study and reproduce motion were made. Nowadays, motion capture plays an important role within many fields, from graphical animation and film making to virtual reality and medicine.

Quantitative data obtained from measurements may support the diagnosis and treatment of many pathologies, allowing to take clinical decisions and supporting the follow-up of treatments or rehabilitation. This approach is nowadays named "evidence based medicine".

In this work, advanced signal processing and motion capture techniques were exploited in order to design: a protocol for validation and quality assurance of clinical strength measurements; an algorithm for clinical gait analysis data interpretation; some user-friendly software tools to be ued in clinical settings to process data and to aggregate the results into reports.

Andrea Ancillao received the Master's degree in Clinical and Biomedical Engineering from "Sapienza" University of Rome, Italy, in 2010, where he is currently Ph.D. candidate in Industrial Production Engineering. He has years of experience in the field of functional evaluation, motion analysis, biomechanics and he is author of several international publications. This book contains the results of his award-winning research about the quality assurance of clinical strength measurements and his recent work about clinical gait analysis.

Stereophotogrammetry in human movement analysis

Novel methods for the quality assurance, biomechanical analysis and clinical interpretation of gait analysis

Andrea Ancillao

Cover Illustration:	Screenshot of Vicon Nexus™ software, in use for the reconstruction of three-dimensional human motion
Graphical design:	Andrea Ancillao
Book editing:	Andrea Ancillao
Contact:	andrea.ancillao@hotmail.com

Stereophotogrammetry in human movement analysis: novel methods for the quality assurance, biomechanical analysis and clinical interpretation of gait analysis

Author
Dott. Ing. Andrea Ancillao

Supervisors
Prof. Ing. Paolo Cappa
Prof. Ing. Zaccaria Del Prete

Academic Year 2016-2017

Research partners:

"How I Did It"

So much has been done, more, far more, will I achieve;
treading in the steps already marked,
I will pioneer a new way, explore unknown powers,
and unfold to the world the deepest mysteries of creation.

(Victor Frankenstein)

Content

List of abbreviations

Abbreviation	Meaning
CP	Cerebral Palsy
CS	Coordinate System
CV	Coefficient of Variation
D/A	Digital to Analog converter
DDST	Denver Developmental Screening Test
EDS-HT	Ehlers-Danlos Syndrome - Hypermobility Type
EMG	Electromyography
GA	Gait Analysis
GGI	Gillette Gait Index
GDI	Gait Deviation Index
GPS	Gait Profile Score
GUI	Graphical User Interface
GVS	Gait Variable Score
HFI	Hip Flexor Index
HHD	Hand Held Dynamometer
IR	Infra-Red radiation
LFM	Linear Fit Method
LRS	Local Reference System
MAP	Movement Analysis Profile
MCID	Minimally Clinical Important Difference for GPS
MoCap	Motion Capture
OC-GVS	Offset Corrected - Gait Variable Score
OC-MAP	Offset Corrected - Movement Analysis Profile
OC-GPS	Offset Corrected - Gait Profile Score
OS	Optoelectronic System
PD	Parkinson's Disease
PIG	Plug In Gait marker protocol
R	Pearson's coefficient of correlation
RMS	Root Mean Square
RMSE	Root Mean Square Error
RoM	Range of Motion
RS	Reference System
SD	Standard Deviation
SEMLS	Single Event Multilevel Surgery
TD	Typically Developing Children

Part 1:
Background

This section contains a brief survey about the history of motion analysis and a review of the earliest experiments in biomechanics. The most famous historical works, mainly based on photography, were reviewed. Modern techniques and methods were described as well.

As most of the modern research, in the field of functional evaluation and biomechanics, is based on the use of optoelectronic systems, the working principle of optoelectronic system was reviewed as well as its applications and setup in the clinical practice.

Some modern functional evaluation protocols, aimed to the quantitative evaluation of physical performance and clinical diagnosis of motor disorders, were also reviewed. Special attention was paid to a common motion analysis exam that is nowadays worldwide standardized, i.e. the Gait Analysis. Examples of Gait Analysis studies on subjects with pathology and follow-up were reviewed.

The literature review reported in this section settled the basis of the research work described through sections 2 and 3.

1.1 - History of Motion Analysis

The study of human and animal movement is an intriguing topic that has always fascinated the curiosity of artists and researchers. Across the years, many studies and publications were made, aiming to figure out the principles of movement and its biomechanical causes and effects.

Human/animal biomechanics involves multiple anatomical systems (nervous, muscular, visual, auditory etc.) and requires a strong coordination between the systems and the limbs, resulting in smooth and elegant movements. Such motion may be very simple in the effect, but very complex from the mechanical point of view. Examples range from the animal quadrupedal walking or human bipedal walking (which requires maintaining the balance), to the most extreme sport performances.

For years, engineers tried to reproduce the natural movement strategies by means of machines or robots, but no one, has ever succeeded in equalling such complex, smooth and beautiful motor performance.

A close attempt is the one achieved by the Dutch artist Theo Jansen (Figure 1.1.1) that created some kinetic sculptures, named *Strandbeest* (that means *Beach Beasts*). These sculptures are made of PVC, wood, and fabric airfoils that collect the power given by the wind. By means of advanced mechanical design, wind power is stored in flywheels and transferred to several legs that move sequentially, achieving a walking effect (Figures 1.1.2). These beasts are able to reproduce a multi-legged walking pattern and are free to walk around by themselves (www.strandbeest.com).

Figure 1.1.1: *Theo Jansen*

Figure 1.1.2: *A Strandbeest designed by Theo Jansen.*

Studying human/animal biomechanics represents a big research challenge, aimed to understand, model and reproduce the principles of movement. Such studies may finally answer the question: how can such a perfect machine, that

is human body, achieve such smooth movements in a so simple and natural way?

The first studies in the field of biomechanics were conducted by means of photography techniques, where an effective representation of motion could be obtained by taking sequential pictures at a fixed time interval. This technique was known as chronophotography. The most known attempts were the works of the English photographer Eadweard Muybridge (9 April 1830 – 8 May 1904, Figure 1.1.3). He used advanced photographic instrumentation (for that time) to take sequential photography of animals and people performing motor tasks. His works were greatly appreciated for their artistic and scientific value.

Muybridge's most famous work, The Horse in Motion (Figure 1.1.4), was inspired by a biomechanical question that was popular in that period: is there a moment in which all the four feet of a trotting horse are off the ground at the same time? Till that time, in fact, most artists used to paint horses with one foot always on the ground. The question was intriguing, because the forward movement logically required a moment of complete loss of contact with the soil, but no one had ever observed it, as the human eye is not fast enough to catch the moment. To answer that question, Muybridge took sequential shoots of a galloping horse using an array of 12 cameras placed along a racetrack (Muybridge 1878). The images clearly showed that there was a time in the running stride when the horse did actually have all the four hooves off the ground (Figure 1.1.4, 1st line, 2nd and 3rd images).

Other famous Muybridge's works are "The Woman Walking Downstairs" and "Two women kissing", shown in Figures 1.1.5a and b, where the author used
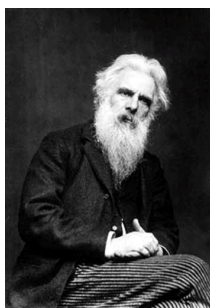
Figure 1.1.3: Eadweard Muybridge
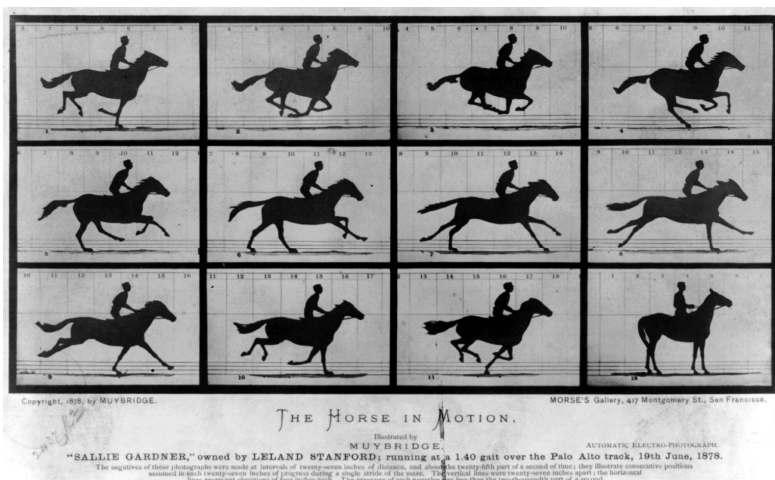
Figure 1.1.4: The Horse in Motion, by E. Muybridge, 1878.
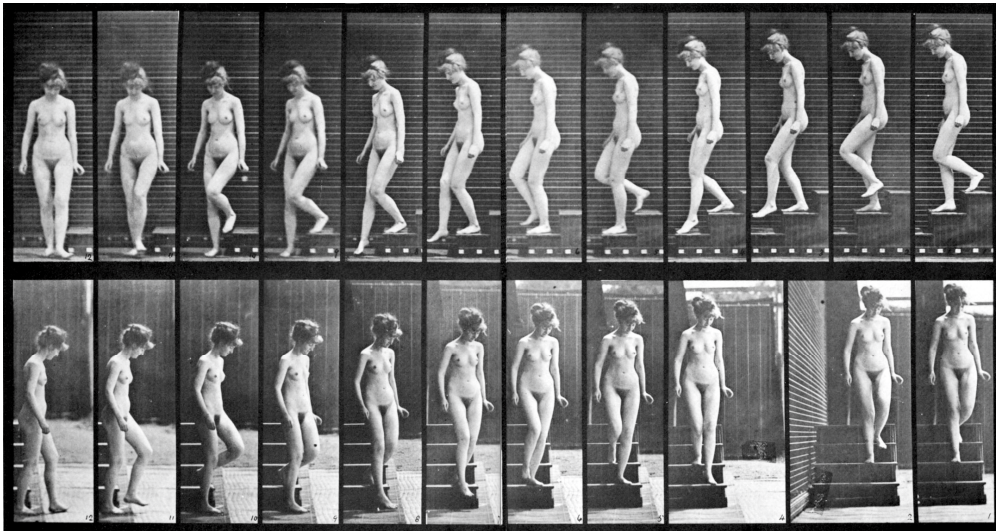
Figure 1.1.5a: *Woman Walking Downstairs, by E. Muybridge, 1887.*
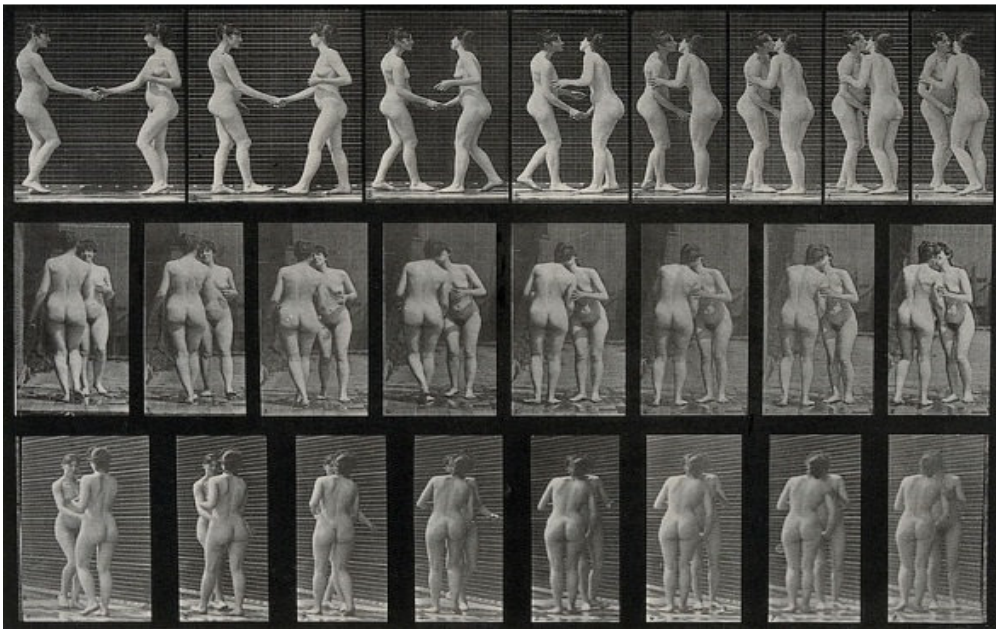
Figure 1.1.5b: *Two Women Kissing, by E. Muybridge, 1887.*

the chronophotography technique to represent the human motion, providing an objective evaluation of the posture and motor strategy involved in that action.

The "Woman Walking Downstairs" is a remarkable piece of work as it considered one of the first attempts to objectively study the biomechanics of human body while performing everyday tasks. The "Two Women Kissing" is considered the first ever filmed kiss.

In 1882, the French scientist and photographer Étienne-Jules Marey (5 March 1830, 15 May 1904, Figure 1.1.6) invented a device capable of taking 12 consecutive frames in a second. This device was a shotgun modified to capture light on a photo-sensitive disc that collected the 12 frames consecutively. The device was named chronophotographic gun (Figures 1.1.7, 1.1.8) and the resulting pictures in motion can be considered the precursor of the Cinematographer, invented by Lumière brothers in 1895.
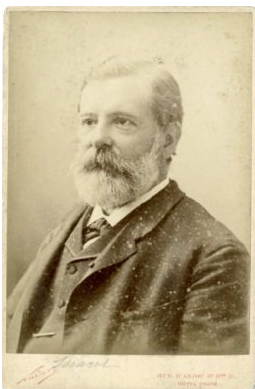
Figure 1.1.6: *Étienne-Jules Marey*

Figure 1.1.7: *The Chronophotographic Gun, by Étienne-Jules Marey*
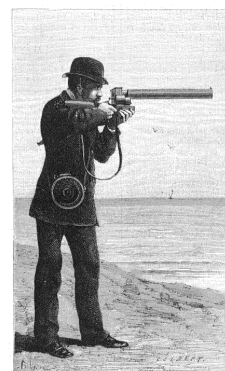
Figure 1.1.8: *Chronophotographic Gun in use.*
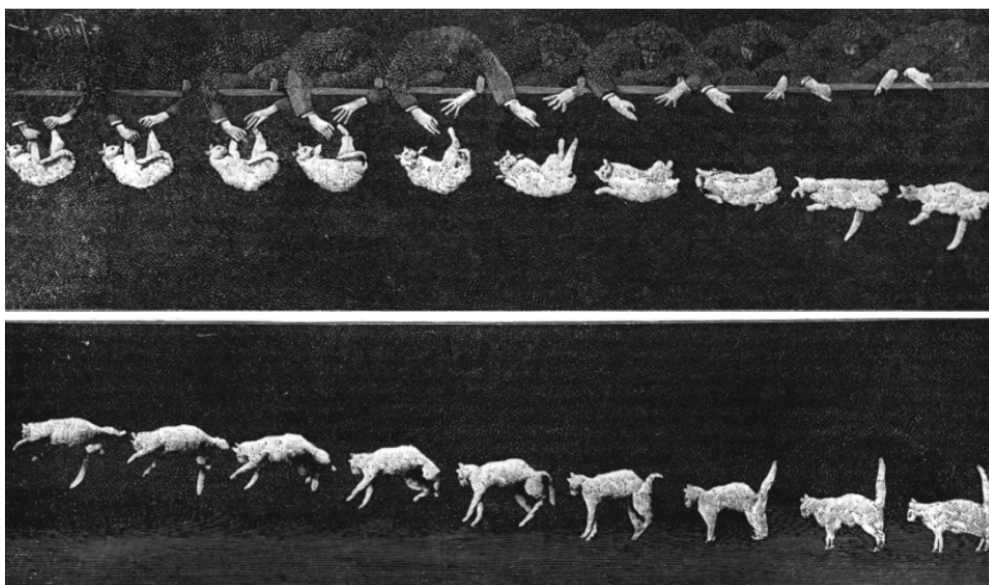
Figure 1.1.9: *Falling Cat, by Étienne-Jules Marey, 1894. Sequential shoots of a dropped cat taken with the Chronophotographic Gun.*

Marey's studies were mainly focussed on animals (horses, birds, cats and others) and human locomotion as well (Marey 1874). The most famous work is the movie that demonstrates how falling cats always land on their feet (Figure 1.1.9). He also conducted very similar studies on chickens and dogs finding out that they could do almost the same (Marey 1894). Marey conducted studies on the biomechanics of human walking (Figure 1.1.10) and improved the photographic technique by adding markers on the subject's body. These markers resulted in bright dots or lines on the developed film, allowing an accurate identification of body segments and landmarks and their evolution over time (Figure 1.1.11).
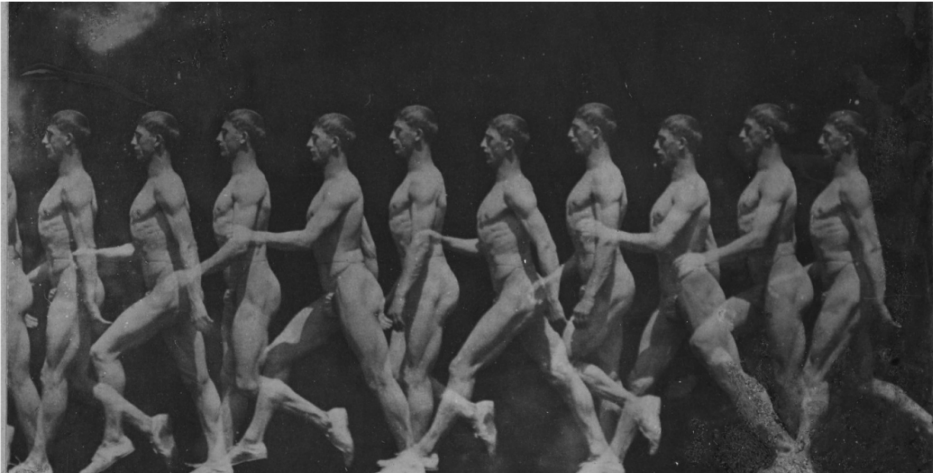
Figure 1.1.10: *Man Walking, by Étienne-Jules Marey, 1890s.*
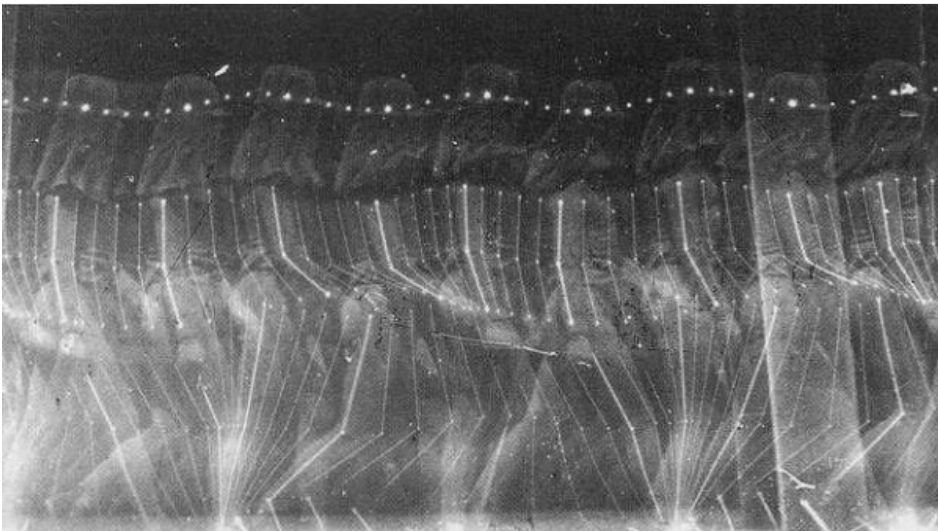
Figure 1.1.11: *Walk, by Etienne-Jules Marey, 1886. Reflecting markers and sticks were added to the subject to improve detection of motion over time.*

Following years brought several advances in photographic techniques and cinematography allowing the biomechanical analysis to become more accurate and detailed.

The possibility to obtain an objective evaluation of human motor performance has captured the interest of clinicians and today it is considered a valid method to study motor performance and to support the diagnosis with quantitative data (Whittle 1996).

The most notable advance was the introduction of stereo photogrammetry

Figure 1.1.12: *Human 3D perception* (Baker 2007)*.*

techniques, that allows to numerically reconstruct the 3D position of a point by observing it from two different points of view. It is the same process happening in the human brain that is able to reconstruct the depth of field by means of the different images provided by the two eyes (Figure 1.1.12).

More details about earlier stereo-photogrammetry techniques and other methods to record motion before the advent of modern computers can be found in Baker's work (Baker 2007).

1.2 - Leonardo da Vinci's Contribution

In a dissertation about biomechanical analysis, it is worth spending some words about the work that Leonardo da Vinci carried out in 1500s.

Leonardo da Vinci (Figure 1.2.1) was an Italian anatomist, painter, sculptor, mathematician, musician, scientist, engineer, inventor, geologist, cartographer, botanist, and writer that gained wide consideration as one of the most talented individuals who has ever lived.

Leonardo's main objective was to understand the underlying proportion of human body so that the science of man could be introduced through art. In his own words, Leonardo's artistic quests were to represent "man and the intention of his soul" and the "attitudes and movements of the limbs." (Jastifer and Toledo-Pereyra 2012). In fact, prior to the use of computers or cameras, it

17

was the artists of the time who communicated our understanding of the world, including the human body.

Leonardo understood that modelling human motion is not an easy task, as there are so many ways in which bones, muscles, and tendons can create movement. He attempted to understand and explain such processes through dissections, drawings, and notes.

Figure 1.2.1: Leonardo da Vinci
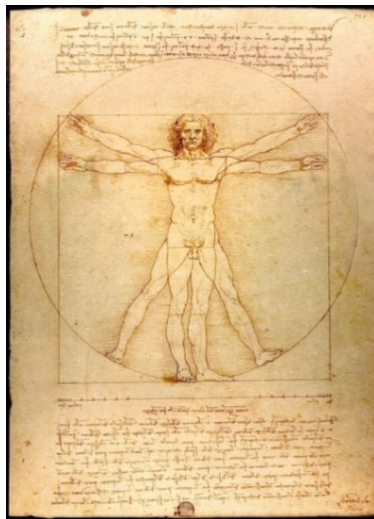
Figure 1.2.2: The Vitruvian Man, 1487, by Leonardo da Vinci.

The Vitruvian man (Figure 1.2.2) is one of the most famous and recognized drawings in the world. The significance of the image is described in the accompanying text that contains some observations about the anatomical and mechanical structure of the human body. E.g. the arm span is often equal to the height of a man, the foot is one-seventh of the height of a man, from below the foot to below the knee is one-quarter the height of man, and from below the knee to the pelvis is one-quarter the height of man. A translation of the original text beneath the drawing goes like this (Jastifer and Toledo-Pereyra 2012):

> *If you open your legs enough that your head is lowered by one-fourteenth of your height and raise your hands enough that your extended fingers touch the line of the top of your head, know that the centre of the extended limbs will be the navel, and the space between the legs will be an equilateral triangle.*

The *Anatomic Manuscript A* is another famous work by Leonardo da Vinci that contains several drawings of the anatomy of human body. A particular interest was given to the sesamoid bones of the first ray of the foot (Figure 1.2.3). Leonardo eloquently described the two primary functions of the sesamoid

bones in the human body. First, they increase the moment arm of the flexor hallucis brevis muscle. Second, they protect the flexor hallucis brevis and longus from the effects of damaging force being transferred from the base of the metatarsal head through the tendons and onto the ground during weight bearing (Jastifer and Toledo-Pereyra 2012). These are still considered the main functions of the sesamoid bones (Aper, Saltzman, and Brown 1996). Such drawings built da Vinci's argument for the sesamoid function of increasing the moment arm of the enveloping tendon and its muscle. Using a thought experiment, Leonardo explains that if one took two solid tubes and ran a string through the middle, and the string was fixed on one end, then with tension on the loose end of the string, the tubes would be stabilized together (Jastifer and Toledo-Pereyra 2012).

Figure 1.2.4 shows Leonardo's free body diagrams of standing and toe-rise that are thought to have been drawn between 1510 and 1511. Those drawings are part of a study on the distribution of body force throughout the foot and lower limb and were considered a pioneering work for the understanding of pathophysiology of disease in the foot and ankle. In fact, human locomotion requires the muscles of the body to act across the ankle joint to create movement and stable gait. Moreover body weight is transmitted through joints and the forces across joints can be significantly higher than the body weight alone (Jastifer and Toledo-Pereyra 2012).

Leonardo explains that, when the body weight is centred over the ankle joint, the Achilles tendon must create a force that is twice the magnitude of the body
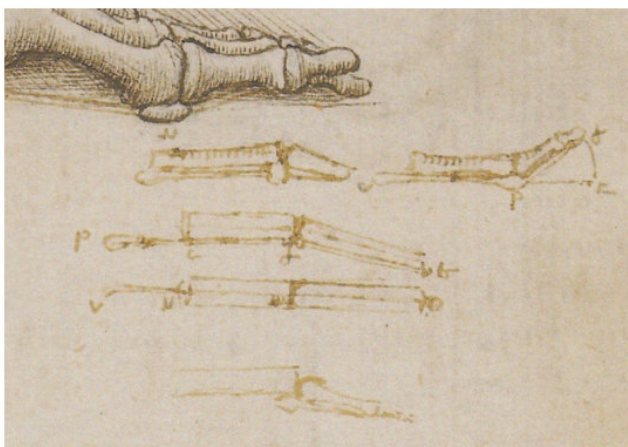
Figure 1.2.3: Illustration of foot biomechanics by Leonardo da Vinci, from Anatomic Manuscript A
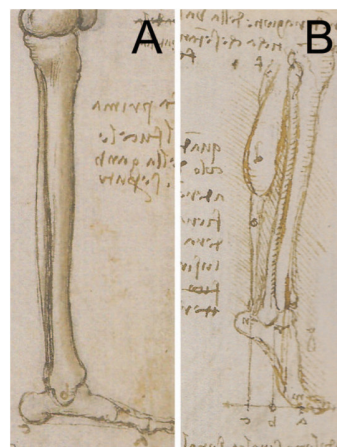
Figure 1.2.4: Illustration of leg and foot biomechanics by Leonardo da Vinci, from Anatomic Manuscript A

19

weight because the distance from the centre of rotation of the ankle to the line of pull of the Achilles is roughly twice the distance to the metatarsal heads. Leonardo's conclusions have held throughout time. While there has been progress toward a better understanding of the complex interplay between all the muscles, bones, joints of the foot and ankle, the basic principles laid out by Leonardo still hold today (Jastifer and Toledo-Pereyra 2012; Scott and Winter 1990).

1.3 - Modern Functional Evaluation

Nowadays, biomechanical analysis has switched from a purely academic discipline to a powerful clinical tool for functional evaluation and diagnosis of motor disorders. It was proved of being useful for the diagnosis of motor disorders an treatment follow-up as it provides quantitative information (Camerota et al. 2015; Sale et al. 2012, 2013).

The process of recording and reconstructing the movements of a subject, actor, animal or any moving object, is nowadays known as motion capture, or MoCap for short.

The gold standard method for MoCap is the use of an Optoelectronic System (OS) that is able to reconstruct, with high accuracy, the Cartesian coordinates of reference points on moving bodies (Cappozzo et al. 2005).

The OSs are widely used for the modelling and animation of humanoid characters in the cinema and video games industry. Their use was recently extended to medicine and sport science, for the functional evaluation of patients and athletes.

OSs use several infra-red cameras placed along the perimeter of a laboratory in order to observe the scene from different angles. Each camera has an IR strobe coaxial to the lens that lightens up the field of view (Figure 1.3.1). Light produced by the strobes bounces on the reflective markers that are placed on anatomical landmarks over the subject/object to acquire. Camera's

Figure 1.3.1: *Modern OS camera with powered strobe and lens*

sensors have a filter that allows them to collect only the infra-red radiation scattered by the markers, while the ambient light is discarded. This allows to obtain high contrast images of the markers, that are seen as white dots on a dark background. A further method to discard ambient light and to reduce artefacts (false marker detection due to reflecting objects in the room and uncontrolled lighting) is to drive the strobes at a specified frequency (flashing). The camera's shutter is then driven at the same frequency.

The two-dimensional images acquired by each camera are mixed by using stereo-photogrammetry techniques that allows to reconstruct a three-dimensional model of the object (Figure 1.3.2).

For each marker the sensor detects a white dot, whose diameter depends on the size of the marker itself, resolution of the sensor and the distance between the marker and the camera. The centroid of the white area is computed in order to define the marker positions with respect to the camera's frame (Figure 1.3.3a).

By means of parallax algorithms it is possible to reconstruct the *x,y,z* Cartesian coordinates of each marker in a 3D virtual space. The coordinates are acquired as time series representing the duration of motion. For the algorithm to work, each marker should be seen by at least two cameras. As the markers may be easily hidden during motion, many cameras are placed along the perimeter of the room, to ensure that at least two cameras see each marker during the recording. If more than two cameras see the same marker, redundancy can be used to optimize, and therefore increase, the accuracy of the reconstruction (Cappozzo et al. 2005; Chiari et al. 2005; Della Croce et al. 2005; Leardini et al. 2005).

The markers are small spheres or hemispheres with IR-reflecting coating. The most common diameters are 10 mm, 5 mm, 3 mm and 1 mm (Figure 1.3.3b).

The accuracy of the system depends on the resolution of cameras' sensor and the volume of the laboratory, which is usually a physiotherapy gym with an useable ground surface of about 100 m². To such a volume, corresponds an accuracy of ~1 mm.

Figure 1.3.2: *Reconstruction of a 3D object from two bi-dimensional field views.*
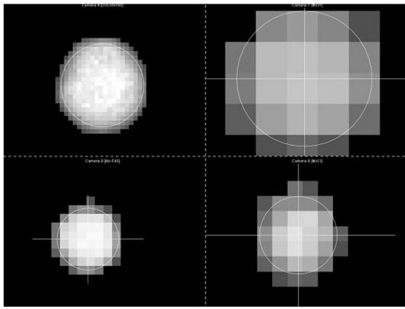
Figure 1.3.3a: *Markers seen by camera's sensor.*

Figure 1.3.3b: *IR reflective markers for motion capture.*

The Optoelectronic System may also record real time data streamed from other instrumentation, such as force platforms, electromyography and video recording systems, and synchronize it to the kinematic recording. This allows a multifactorial and multivariate analysis of motion(Ancillao et al. 2014).

The key point in motion capture is the reconstruction of a subject model from the markers coordinates (Figure 1.3.4). To obtain this, markers have to be placed on specific anatomical landmarks according to a protocol which depends on the anatomical district that needs to be investigated.

The design of a functional evaluation protocol is not an easy task, as limbs need to be modelled as rigid segments defined from the physical markers applied
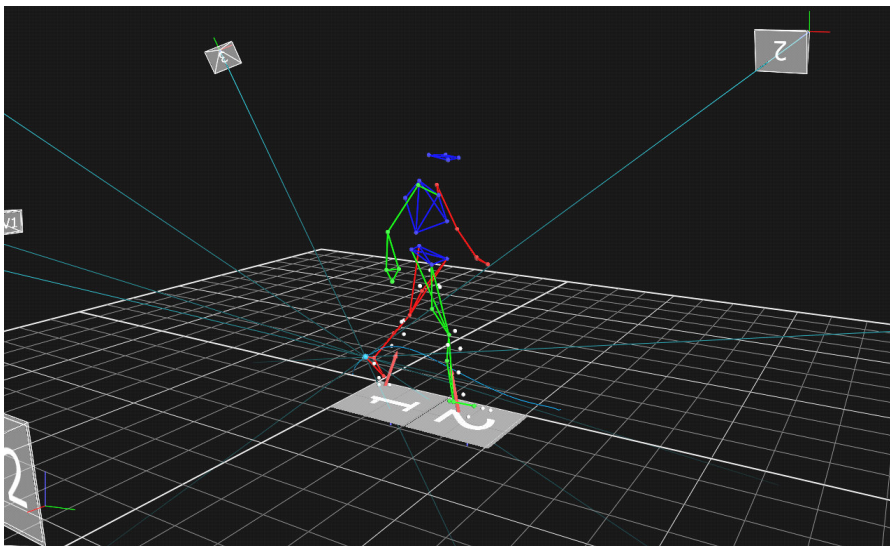
Figure 1.3.4: *3D reconstruction of motion obtained by the Optoelectronic System*

over the skin of the subject. The modelling therefore runs under the rigid body assumption, meaning that the modelled limbs are assumed to have no modifications during the motion. Under this assumption, at least three markers are required to track each segment (Camomilla et al. 2006).

It is clear that the tracking of rigid bodies is affected by artefacts and errors due to marker wrong positioning, skin sliding over the bones, etc. This kind of errors are usually addressed as "soft tissue artefacts" (Leardini et al. 2005). These effects can be reduced by: (i) marker redundancy, (ii) accurate marker placement and (iii) accurate definition of anatomical landmarks by the *ad-hoc* design of functional evaluation protocols.

The general guidelines for markers placements identify the most suitable landmarks as the point where the effect of the skin sliding over the bones is minimum. These landmarks are often identified on bone prominences, points of reference for joint rotations (elbow, knee, ankle, etc.) and limb extremities (toe, fingers, etc.).

1.4 - Functional Evaluation Protocols

Many functional evaluation protocols were developed across the years, depending on which task needs to be investigated, ranging from general motor abilities, to high level neuro-motor coordination, that reflects the brain's ability to conceive, organize, program and carry out a sequence of actions (Rosenbaum 2009).

Biomechanical analysis becomes critical when modelling small anatomical segments such as fingers. Some study were conducted about the definition and validation of biomechanical models of thumbs and wrist joints (Carpinella, Jonsdottir, and Ferrarin 2011; Cerveri et al. 2008; Chiu et al. 2000; Metcalf et al. 2008; Small et al. 1996). Cerveri et al. (Cerveri et al. 2008) validated a kinematic model of the trapezio-metacarpal joint. The motion was reconstructed by nine passive markers applied on the surface of hand and fingers, and then acquired through an OS. The model allowed representing motion of the thumb joint across the three anatomical axes. Analysis of inaccuracies showed that the model was able to reconstruct kinematics with an error of 5mm for linear distances and 6° for angles. Small et al. (Small et al. 1996) modelled and measured motion of the wrist by means of an OS and stereoradiography. The detailed kinematic analysis allowed to extract Euler angles among the anatomical planes. Angular uncertainties due to the OS were

estimated as about 6 mm in accordance with the results of Cerveri et al. (Cerveri et al. 2008).

Many research works were aimed at the design and validation of MoCap protocols for the functional evaluation of a specific anatomical district or functional task. Examples follow.

Ancillao et al. (Ancillao et al. 2012) designed a protocol for the analysis of displacements of human mandible. It was based on 12 small markers placed on the face of the subject, plus five markers on the upper body of the subject, that allowed the measurements of small displacement of the jaw and the head (Figure 1.4.1). The protocol was applied to subjects with Ehlers–Danlos syndrome and allowed a quantitative analysis of jaw dislocation and its effects on posture on subjects with pathology (Ancillao et al. 2012). The same authors designed another protocol for the evaluation of facial movements and expressions (Ancillao et al. 2016). It was based on 16 markers placed on the face of the subject (Figure 1.4.2). The high accuracy reached allowed to measure the effects of stroke on facial conformation and mobility, giving a substantial help for the diagnosis and follow up of such pathologies (Ancillao et al. 2016).

Ancillao et al. also designed a protocol for the analysis of handwriting by means of the OS (Ancillao et al. 2013). This protocol was based on 20 markers of 5mm diameter, placed on the cap of a common pen/pencil, on the corners of a
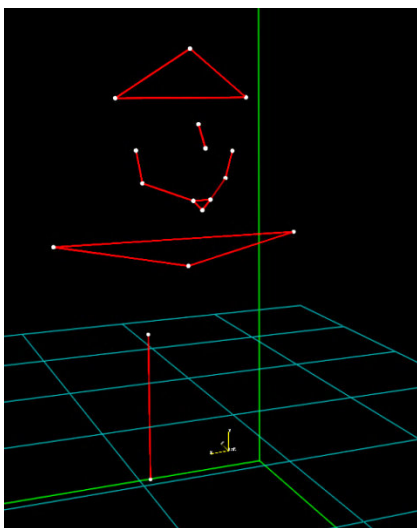
Figure 1.4.1: Marker protocol designed by (Ancillao et al. 2012) in use for the reconstruction of mandible position and motion.
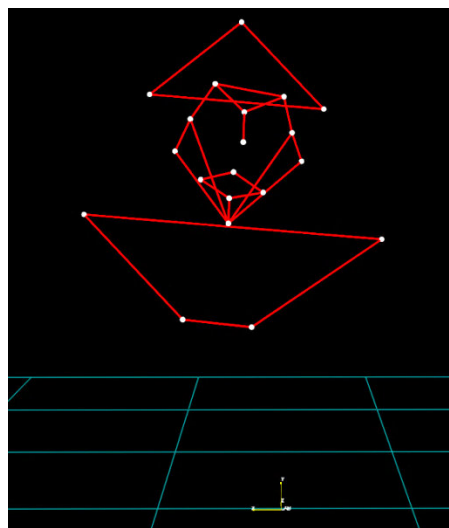
Figure 1.4.2: Marker protocol designed by (Ancillao et al. 2016) in use for the reconstruction of facial expressions.

common sheet and on the upper limbs of the subject. To capture handwriting, the subject holds the pen or pencil, equipped with markers, within the calibrated volume of the OS and simply draws on the sheet. The ad-hoc developed software reconstructs the position of the sheet, the pen, the track left on the sheet and the posture of the subject (Figure 1.4.3).

The protocol was proved to be able to reconstruct handwriting with an accuracy of ~0.6 mm, producing quantitative data that support many clinical tests that are commonly administered by the Pen-and-Sheet method. For these tests, a score is qualitatively assigned by a trained operator (Ancillao et al. 2013). Some examples are the Denver Developmental Screening Test, in which the subject is asked to draw simple geometrical figures, such as a circle, a square and a triangle (Frankenburg and Dodds 1967; Galli, Vimercati, et al. 2011; Khalid et al. 2010) and the Clock Drawing Test, in which the subject is asked to draw a clock indicating current time (Aprahamian et al. 2010; Brodaty and Moore 1997).

From the quantitative data, it is possible to obtain a detailed analysis of the handwritten track, such as computing of velocity, smoothness, coordinates of starting/ending points, position and number of touches and lifts, dimensions and length of the track, position on the sheet, anatomical angles and posture, etc. Such measurements were proved to play an extremely important role in the diagnosis and follow-up evaluation of neurological diseases, such as Parkinson's disease (De Pandis et al. 2010; Vimercati et al. 2012), Multiple Sclerosis (Longstaff and Heath 2006), or developmental disabilities (Casellato et al. 2011; Gilboa et al. 2010; Khalid et al. 2010).
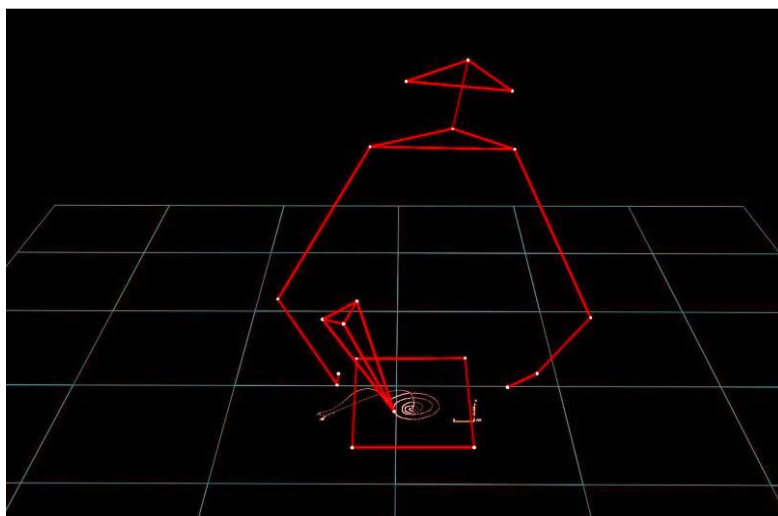
Figure 1.4.3: Marker protocol designed by (Ancillao et al. 2013) in use for drawing capture and 3D reconstruction.

The use of MoCap is preferable to the graphic tablets because it may work with a common pen and sheet without altering the writing conditions by inserting a layer between the sheet and the desk. Moreover, the MoCap protocol (Ancillao et al. 2013) may use a sheet of any size, while with the graphic tablets, the writing area is strongly limited by the size of the sensor. The OS provides additional information that is not recorded by the graphic tablet, i.e. the trajectory and speed of the pen tip while it is not in contact with the paper, the orientation of the pen in space, etc. Measures of angles and motion of anatomical joints (finger, wrist, elbow, shoulder) and general posture of the subject may also be recorded at the time of the writing (Ancillao et al. 2013; Galli, Vimercati, et al. 2011).

Such information is very valuable for clinical analysis. In fact, handwriting is a complex motor task that requires high level of coordination between fingers, arms, sight, and the central nervous system in general. Drawing and writing are the culmination of several mental steps that are required to communicate some ideas to the external world (Rosenbaum 2009). The same high-level graphic representation may be represented in different ways. It is the subject's motor control system that solves the kinematic chain of actions in order to achieve the best result with the minimum energy expenditure (Rosenbaum 2009). People's graphic outputs are, in general, different and distinctive. In fact, signatures and handwriting can be used for identification purposes. It was also suggested that writing styles may indicate personality traits (size of letters, shape. etc.), anyway this was never scientifically proved (Fischman 1987; Rosenbaum 2009).

Handwriting may be seriously affected by motor pathologies and neurodegenerative diseases that affect motor planning, coordination, and motion in general (Rosenblum and Livneh-Zirinski 2008). It was also demonstrated that children's drawings reflect their intellectual skills and development (Goodenough 1928). Therefore, handwriting and drawing analysis becomes a powerful tool to assess the skills of children with learning disabilities (Galli, Vimercati, et al. 2011).

Several graphic tests were developed for the cognitive evaluation of children. An example is the Denver Developmental Screening Test (DDST) that is able to evaluate both gross and fine motor functions (Frankenburg and Dodds 1967). In the DDST the child is asked to copy by hand the figures of a circle, a square, and a cross. In this kind of tests, the drawings are usually administered using the "pen and sheet method" and a score is given by the operator, with respect to the presence or absence of some features. Another example is the "Clock

Drawing Test", in which the subject is asked to draw a clock indicating current time (Aprahamian et al. 2010; Brodaty and Moore 1997).

The drawing protocol by (Ancillao et al. 2013) was successfully applied to children with Down Syndrome (Vimercati et al. 2014) that were evaluated by means of the DDST (Frankenburg and Dodds 1967; Khalid et al. 2010). Drawing parameters were measured, such as: size of the geometrical shapes, proportions, drawing time and velocity, drawing accuracy, distance between subject's head and table and subject's posture. The study demonstrated that children with Down Syndrome drew faster than controls but with less accuracy (Vimercati et al. 2014). The distance between head and table was lower in Down Syndrome subjects than controls, indicating that the subjects drew with the head close to the sheet.

A different protocol for the functional evaluation of the upper limb was designed by (Vimercati et al. 2013b) to investigate the strategy chosen by subjects with Down Syndrome that were asked to sequentially hit some targets by a stick hold in hand while sitting in front of a table. The protocol was composed of 12 passive markers that provided a fine reconstruction of the motor strategy chosen by the subjects with Down Syndrome that are known to have poor coordination, high rates of failure and slower reaction time, mainly due to lower muscle tone and ligament laxity (Morris, Vaughan, and Vaccaro 1982). Linear and angular velocities were measured, as well as acceleration, showing in agreement with other studies (von Hofsten 1991; von Hofsten and Rönnqvist 1993) that children with Down Syndrome moved slower and with reduced peak velocity than normally developed children. The motion of the upper limb was also studied in a patient with hemiplegia that was treated with neuromuscular taping (Camerota et al. 2013). The subject, while sitting in front of a table, was asked to reach a target with her finger on the affected arm and then bring the arm back to the resting position. The markers were placed on the head, the trunk, the arm, forearm and hand and the reaching movement was segmented into three sequential phases. The OS allowed to compute timings of the phases, smoothness of the movement, joint ranges of motion and reaching accuracy. The analysis was repeated "pre" and "post" treatment and it was proved that motion in the "post" session was smoother, faster and less segmented (Camerota et al. 2013).

A detailed study on reaching is the one by Butler et al. (Butler et al. 2010) that studied the ability of children with cerebral palsy to reach, grasp and transport objects, compared to a control group. More in details, children were asked to reach a cup of water, bring it to the mouth and simulate water drinking. The motion was studied by an OS and a marker protocol on the upper limb,

composed of 17 markers. The parameters measured were: trunk flexion/extension and rotation, shoulder elevation, elbow flexion/extension, forearm pronation/supination and wrist flexion/extension. The study showed that children with cerebral palsy had reduced elbow extension followed by increased wrist flexion and trunk motion (Butler et al. 2010).

The motion analysis of the upper limb is crucial to study the biomechanical activities that involve fast and accurate movements such as bowing to play string instruments. In the work of (Turner-Stokes and Reid 1999), the authors developed a protocol to study the motion of the bowing arm of musicians. The protocol involved an OS, reflective markers placed on the bowing arm and it was aimed to the diagnosis of neuro-motor diseases that are common among professional musicians (Turner-Stokes and Reid 1999). The authors compared motor strategies and trajectories adopted by players of different bowing instruments from cello to violin. Quantitative results were proven reproducible and demonstrated clear differences between the instruments as well as stylistic differences between the players. The range of motion of the shoulder correlated with the type of the instrument, being larger on the cello and smaller in the case of the violin. Instead, the range of motion of the elbow was

greater on the violin (Turner-Stokes and Reid 1999). The high range of motion of the shoulder was correlated to the neck and shoulder symptoms that are common among cellists. Another study on interlimb coordination in violin players was conducted by (Baader, Kazennikov, and Wiesendanger 2005). In this case, the use of the OS allowed to record finger trajectories and bowing motion providing quantitative results in terms of velocity and timings. Anticipatory mechanisms in finger-press, synchronization, and errors
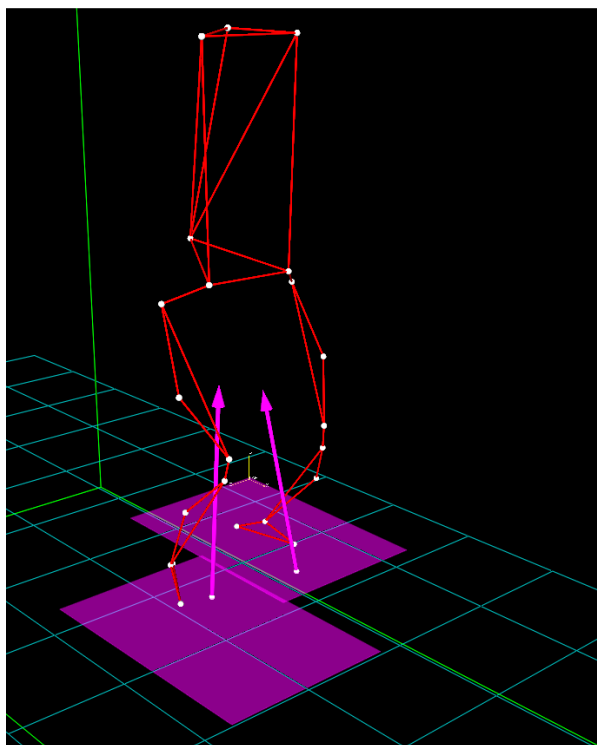
Figure 1.4.4: Biomechanical model of a subject performing a vertical jump (Ancillao et al. 2014).

in timings were also investigated, proving that the optoelectronic measurements are accurate and powerful in assessing small, fast and accurate movements (Baader et al. 2005).

A whole body functional evaluation protocol was designed by (Ancillao et al. 2014) to measure the biomechanical parameters of healthy subjects performing a vertical jump (Figure 1.4.4). The protocol required an OS to track the kinematics, two force plates to record the ground-interaction forces and an EMG recorder to study muscle activation. Subjects were asked to jump at different heights by adjusting the force on the legs. EMG data were processed by means of innovative algorithms based on fractal dimension, with the aim to filter noise and identify muscle activation (Accardo et al. 1997; Klonowski 2000; Lopes and Betrouni 2009). The main finding was a very high level of correlation between the fractal dimension of the EMG signal, assumed to be representative of the level of muscle contraction, and the height reached in the jump. The study confirmed that fractal dimension of EMG can be used together with the temporal and frequency domain analysis to characterize the EMG signal and it is representative of muscle activation (Ancillao et al. 2014). As the EMG signal is the result of superimposition of many pulse trains produced by the asynchronous firing of single motor units, the resulting EMG complexity increases as the muscle contracts. EMG complexity represents the level of cooperation and synchronous activation/deactivation of motor units, thus fractal dimension, that measures signal's complexity (Higuchi 1988; Katz 1988), can be assumed as an index of activation of the muscle under study.

An innovative MoCap study is the one by (Charbonnier et al. 2014), that designed a protocol to investigate the risk of impingement and joint instability that may occur during sexual activities in subjects that underwent total hip arthroplasty. Motion was recorded by means of an OS equipped with 24 IR cameras and 108 m^3 calibrated volume. The recorded data were applied to prosthetic hip 3D models, obtained by magnetic resonance imaging, to evaluate impingement and joint instability during motion (Figure 1.4.5). The authors used spherical retroreflective markers (14 mm diameter) placed directly onto the skin using double sided adhesive tape to record the overall kinematic of the action (Figure 1.4.5). Hip joint kinematics were computed from the recorded markers' trajectories. The study objectively demonstrated that bony or prosthetic impingement, associated with joint instability, may occur during sexual activity after total hip arthroplasty. Hence, some sexual positions could be potentially at risk (Figure 1.4.6), particularly for women, whose ranges of motion were the highest, as well as the risk of impingement (Charbonnier et al. 2014).
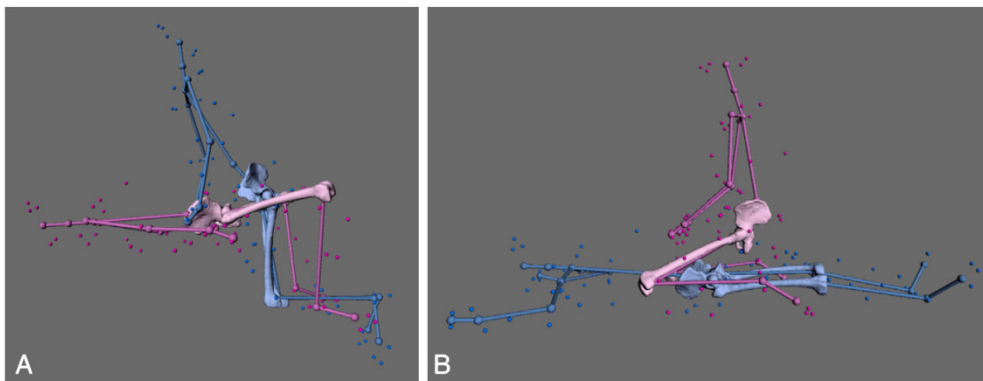
Figure 1.4.5: *Sexual positions reconstructed by* (Charbonnier et al. 2014) *showing the markers (small spheres) and the virtual skeletons: (A) Position #4, (B) Position #11. In both images, the man is represented in blue and the woman in pink.*
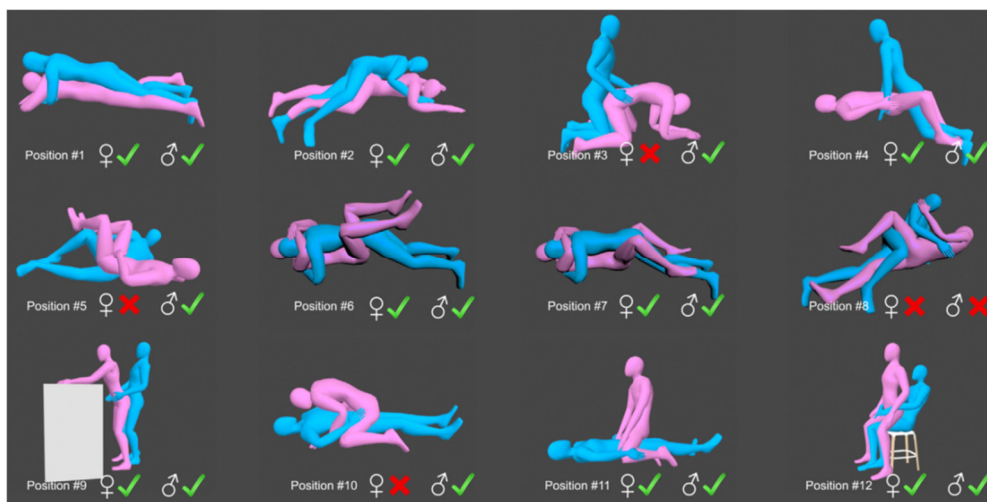
Figure 1.4.6: *Sexual positions for men (blue) and women (pink) recommended after total hip arthroplasty. A cross next to each symbol means that the position should be avoided; a tick means that the position is allowed* (Charbonnier et al. 2014)*.*

1.5 - Gait Analysis

The clinical Gait Analysis (GA) is a clinical exam that started spreading in the '90s – 2000s and it is nowadays standardized across motion analysis laboratories. It consists in the recording of the walking patterns of human subjects, allowing to study the motor strategy adopted for walking and its implications on the posture. It follows that GA plays an important role in the

diagnosis of neuro/motor pathologies related to gait and in the follow-up of rehabilitation treatments (Rigoldi et al. 2012; Rigoldi, Galli, and Albertini 2011), as the "qualitative" analysis, commonly based on direct clinical observation, video recording, etc., can be supported and integrated by "quantitative" information that is not operator-dependent and it is based on objective measurements.

A GA exam requires the simultaneous recording of different types of data (kinematic tracks, forces, EMG, etc.), therefore it implies the use of different measurement systems, whose data need to be time-synchronized and usually stored within the same database. A summary of the instrumentation commonly involved in a GA exam is shown in Table 1.5.1 and examples of data produced are shown in Figure 1.5.1.

The results of a GA exam are some sets of biomechanical parameters that provide detailed and quantitative information about the functionality of the anatomical districts: foot, ankle, knee, hip and pelvis. The functionality is assessed by measuring angular displacement of joints along their degrees of freedom and the joint stiffness/stability while walking.

Instrument	Data	Purpose
Optoelectronic System	Marker x, y, z coordinates and their evolution over time.	Track motion of the subject and computing of anatomical angles and parameters
Force platforms / pressure matrices	Force and moment vector exchanged with the ground. Coordinates of the centre of pressure.	Analysis of ground forces, joint reaction and muscle force. Computing of internal moments. CoP/Posturography analysis.
Electromyography	Time-series indicating the voltage produced by muscle contraction and collected by electrodes.	Analysis of muscle contraction patterns associated to the walking.
Video recording	Video files (avi, mpeg).	Trial documentation and reference.
Oxygen consumption	Time-series of O_2 and CO_2 levels measured in the air inhaled and exhaled.	Analysis of energy expenditure while walking or performing an exercise.
Other devices	Time-series	Dynamometers, accelerometers, etc.

Table 1.5.1: *Instrumentation needed for a Gait Analysis exam and details about the data obtained.*
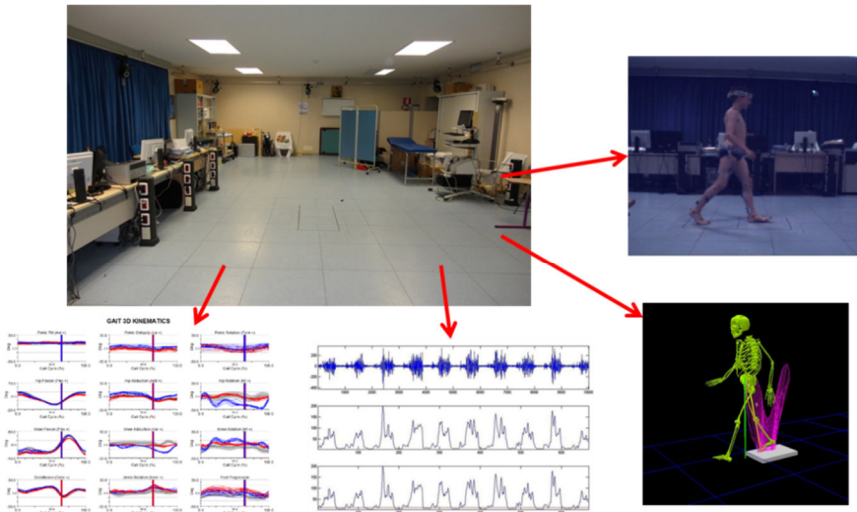
Figure 1.5.1: *A motion analysis laboratory and visual examples of data obtained in a Gait Analysis exam: video recording, kinematics, EMG and ground-reaction forces.*
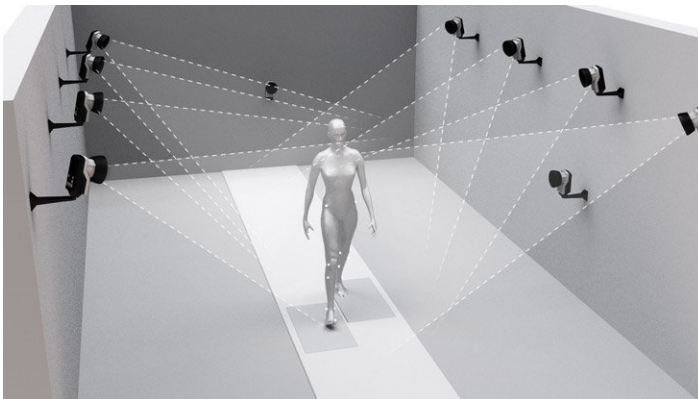
Figure 1.5.2: *Working principle of Gait Analysis conducted in a motion analysis laboratory.*
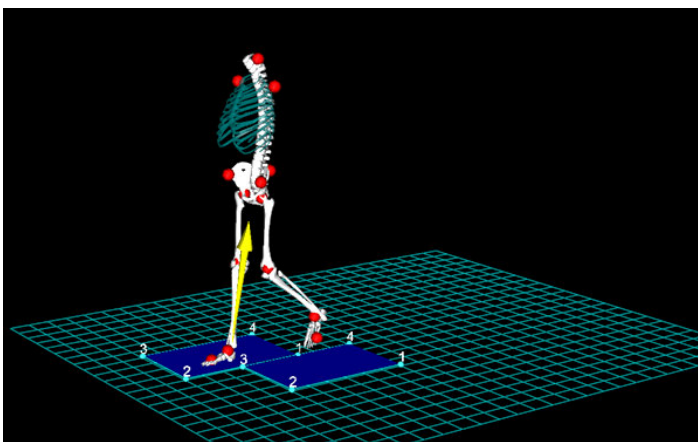
Figure 1.5.3: *Biomechanical walking model reconstructed from a Gait Analysis exam.*

During a GA, the subject is asked to walk along a pathway within the lab. The path is designed in such a way to have the subject naturally hitting the force plates (which are hidden under the floor), and, at the same time, make the subject visible to the most of the cameras of the OS (Figure 1.5.2). The walking is repeated several times, in order to reduce random errors and to increase repeatability of results. Data obtained by the OS and the force plates allow to reconstruct a biomechanical model of the walking subject, that is used to compute mechanical parameters (Figure 1.5.3).

GA works under the assumption that the segments of human lower limbs are rigid bodies.

The results of a Clinical GA are often presented as a standardized clinical report which contains the following parameters: (i) kinematics parameters: the anatomical angles and their variation across three anatomical reference planes (sagittal, coronal and horizontal); (ii) spatiotemporal parameters: cadence, velocity, step length, stance time, stride time, asymmetry in stride, etc.; (iii) kinetic parameters: ground reaction forces in three dimensions and their evolution over time; (iv) EMG tracks and other analog tracks describing muscular activation, timings and strength. A standard GA report contains information about the motion of anatomical joints along all their degrees of freedom. Graphs are usually normalized to a complete stride (Figure 1.5.4): conventionally the stride begins with an Heel Strike, namely 0%, and ends with the subsequent Heel Strike, namely 100%. The stride is divided into the "stance phase" (foot touching the ground) and the "swing phase" (foot flying). The event "Toe Off" representing the time when the foot leaves the ground, happens at about 60% of stride, in subject with no gait pathology.

Several marker protocols were proposed for the kinematic recording of a GA (Ferrari et al. 2008). These protocols can be grouped into two families: (i) anatomical protocols and (ii) technical protocols. Technical protocols require
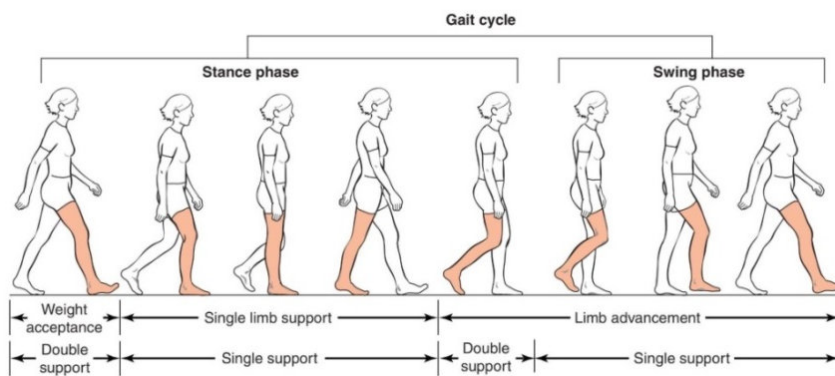
Figure 1.5.4: *Gait cycle & stride phases.*

only a cluster of markers for each rigid segments to track and use a static calibration trial to identify anatomical landmarks or joint rotation centres. Technical protocols reduce the sliding-skin effect but require a longer preparation time, therefore they are not often used in the clinical practice, as they require to repeat the calibration trials in case the markers are accidentally removed during the trials. The most famous technical protocol is the CAST (Cappozzo et al. 1995).

Anatomical protocols require markers to be placed directly on anatomical landmarks, such as bone epiphysis or limb extremities. These protocols do not require static calibration, therefore preparation time is shorter than technical protocols, but marker position can be affected by sliding skin effects. The most famous anatomical protocol is the Davis protocol (Davis et al. 1991) and its modern adaptation, i.e. the Plug In Gait (PIG, Figure 1.5.5). Davis protocol and PIG are widely used in today's clinical practice.

GA is widely recognized as a multifactorial and powerful clinical tool and it is widely adopted as a routine exam (Carriero et al. 2009; Whittle 1996). As
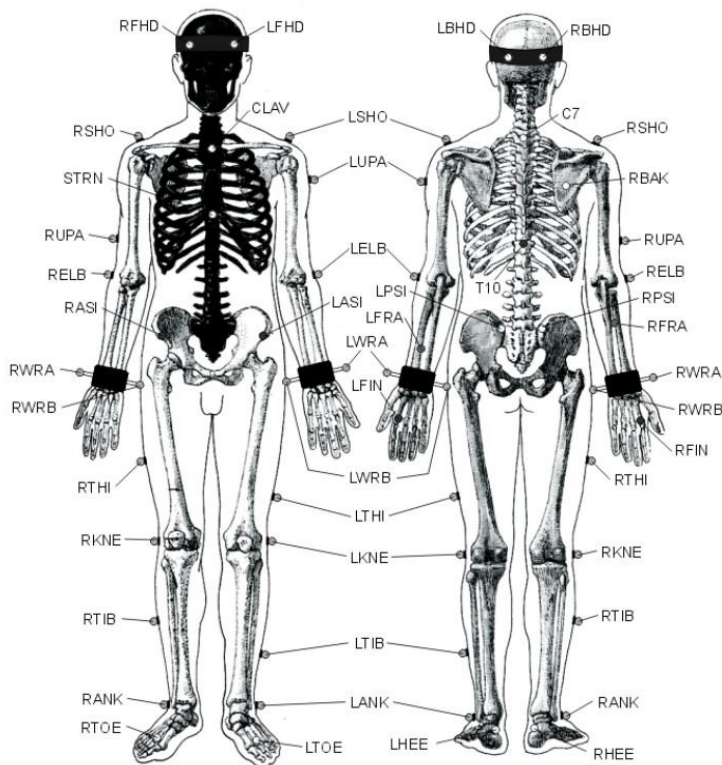
Figure 1.5.5: Anatomical landmark for Plug In Gait marker protocol.

examples, GA was used to study and characterize: Parkinson's disease (Sale et al. 2013), Down syndrome (Galli et al. 2008), Ehlers-Danlos syndrome (Rigoldi et al. 2012), Cerebral Palsy (CP) (Carriero et al. 2009; van den Noort et al. 2013) and it was widely applied to validate the effects of novel treatments in subjects with neurological disorders (Camerota et al. 2015; Sale et al. 2013; Vismara et al. 2016).

Clinical decisions, rehabilitative treatments and follow-up evaluation are often based on the results of GA exams (Assi et al. 2009; Whittle 1996), especially in the case of CP and spastic paresis that may induce motor disorders at different levels. Thus, very different gait patterns are observed in patients with CP (Galli et al. 2010; Piccinini et al. 2011). Some examples of gait abnormalities observed in CP patients are: the equinus gait pattern, that involves alteration of ankle joint functionality (van der Krogt et al. 2009); crouch gait, that is characterized by abnormal knee flexion (van den Noort et al. 2013); and pelvis abnormal anti-retroversion with overall range of motion limitation due to spasticity (van den Noort et al. 2013).

As further examples, GA was used to monitor the long term effects of orthopaedic surgery on children with CP, quantifying the improvements over the time (Galli et al. 2009). Patients with Prader-Willi syndrome were found to have a significant improvement in GA after an osteopathic treatment (Vismara et al. 2016). Sale and colleagues used GA to measure gait improvements in subjects with Parkinson's Disease undergoing a robotic treatment (Sale et al. 2013). And a treatment of neuromuscular taping was found to improve the gait of a subject with Joint Hypermobility Syndrome (Camerota et al. 2015).

1.6 - On Human Motor Control

When talking about biomechanics, it is easier to think about the experimental setups, hardware and methods needed to model and study the human motion. In other words, the focus is commonly set on the mechanical characteristics which are the *effects* of motion.

A wide research stream is being conducted about the *causes* of human motion: which is the origin of motion? Why movements are performed in a certain way? How are movements coordinated in order to achieve a global complex action?

In other words, we may say that while most of the biomechanical research is focussed on the *hardware*, it is worth to discuss and investigate also the *software* governing the biomechanical action.

The answer to the previous questions lies within the human brain, as motor control resides in the human brain and underlies all the activities we engage in. Examples are: walking, running, jumping, reaching for objects, talking, handwriting, nonverbal communication, etc.

The *core problems* of human motor control can be summarized within the following questions (Rosenbaum 2009):

1. How are movements selected to achieve a particular task when there are infinite ways to achieve it? (*degrees of freedom problem)*
2. How are behaviours sequenced in time? (*sequencing and timing problem*)
3. How are perception and control combined? (*perceptual-motor integration problem*)
4. How are motor skills acquired? (*learning problem*)

Understanding human motor control is not an easy task, as it is in general not predictable and the response may depend on several inputs. In other words, it is chaos (Rosenbaum 2009). Human brain takes decisions in a very short time, after processing, filtering and integrating several inputs coming from perception, memory and feelings. It is worth to remark that the *core problems* are "problems" for the researcher, not for the subject performing the action. In fact most of the motor control and decision making is handled by the unconscious mind (Rosenbaum 2009).

David Marr proposed three levels of understanding for the study of such systems (Marr 1982):

- The *computational* level, that represents the mathematical description of the functions that a system is supposed to achieve;
- The *procedural* level, that represents how the action is performed and how events occur and are adjusted in real time;
- The *implementation* level, that represents how single actions, composing the whole motion, are achieved (e.g. muscle contraction).

As an example, we may consider a cat jumping on a table (Figure 1.6.1). At the computational level, the cat's planning can be represented by equations and diagrams. Even though equations are not used explicitly by the cat, they are used implicitly in the performance representation within the mind (Rosenbaum 2009).

How the cat actually jumps on the table is out of the preliminary computational description, as some events may occur while the cat is performing the motion. Therefore some *adjustment*, based on sensory feedback, is needed. This is the procedural level. Finally the implementation level concerns how the cat achieve the motion, how muscles contract and relax and which brain regions are being used.
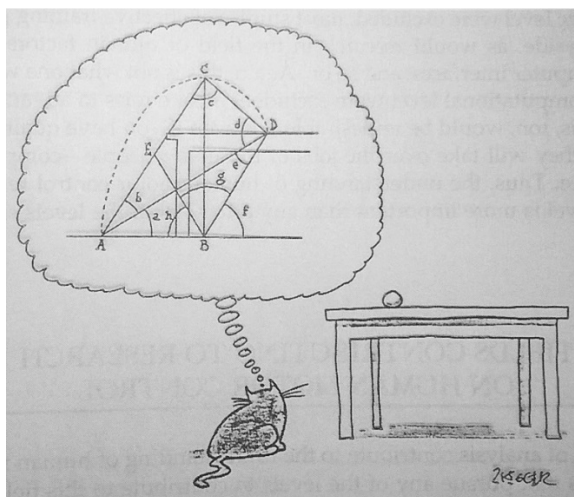
Figure 1.6.1: *The computational level of analysis in motor control.*

Several research studies were conducted to understand how the human brain does handle such levels and how integrates perception and motor control. Most of the studies about motor control and features of movement were conducted by means of OSs, accelerometers and other instrumentations able to accurately record motion.

The perceptual-motor integration is achieved mainly by two mechanisms: the *feedback* and the *feedforward*. In the feedback, information coming from the senses is used to correct the output action; once an error in the action is detected, that information is used to correct the error. In the feedforward, the back-loop is unavailable and the brain relies only on memory and learned procedures to plan the motor action. Surprisingly, a number of movement sequences can be performed relying only on feedforward: animals that were deprived of sensory feedback (by cutting the nerves that transmit sensory signals from the limbs to the spinal cord) were still able to walk, climb, grasp and point (Taub and Berman 1968).

From the engineering point of view, the feedback corresponds to a closed-loop system where the output returns to a comparator that adjusts the incoming signal; while the feedforward corresponds to an open-loop control system where feedback is unavailable, the loop is opened up and no information can get through about the success or failure of performance.

Dealing with these topics goes beyond the scope of the present work. A detailed review about Human Motor Control and motor integration strategies can be found in (Rosenbaum 2009).

Part 2:
Strength Measurements

This section contains a description of the "Strength" project, from the preliminary analysis to the final results. After a literature review about the clinical procedures commonly adopted to measure maximal muscle force, the methods and the results of the project are described.

The project was aimed to the design and implementation of a novel measurement protocol in order to identify the quality and reliability issues occurring when measuring forces and moments by means of Hand Held Dynamometers (HHD). Such analysis was needed as some reliability issues of commercial HHDs were raised in the literature.

The developed protocol provided an analysis of reliability of strength measurements allowing to investigate sources of error occurring when commercial HHDs are used. This method can be used in the clinical routine for the quality assurance of strength measurements and in those cases were high accuracy of measurements is essential.

This work was sponsored by the MD-Paedigree European Project: Work Package 6 (quality assurance of recorded data), Work Package 11 (muscle strength evaluation and modelling) and by the PRIN 2012 Project (quality assurance of measurements conducted in motion analysis laboratories).

The "Strength" project was conducted in partnership with "Bambino Gesù" Children Hospital, Rome, Italy, - Motion Analysis and Robotics Laboratory (MARLab).

The text in this section was adapted and integrated from the papers:

- Ancillao, A., Rossi, S. & Cappa, P. *Analysis of knee strength measurements performed by a hand held multi-component dynamometer and optoelectronic system.* IEEE Transactions on Instrumentation and Measurement, 66(1); pp. 85-92; 2017. DOI: 10.1109/TIM.2016.2620799.
- Ancillao, A., Rossi, S., Patanè, F. & Cappa, P. *A preliminary study on quality of knee strength measurements by means of Hand Held Dynamometer and Optoelectronic System.* MeMeA2015 pp. 595–599 (2015).
- A. Ancillao, S. Rossi, F. Patanè, A. Pacilli, P. Cappa. *Technical quality assurance for strength measurements performed with Hand Held Dynamometer.* Proceedings of 1st Clinical Movement Analysis World Conference, Rome, 1-4 October 2014.

2.1 - Introduction

Measuring strength means measuring the maximum voluntary contraction force produced by muscles.

Strength measurements are popular in the medical practice as they provide information about the healthiness of muscles and ligaments and document the effectiveness of training and rehabilitation programs (Allen, Gandevia, and McKenzie 1995; Bohannon 1990; Hughes et al. 2001; Maughan, Watson, and Weir 1983). Indeed, the joint force and torque estimation inherently describes the stability and healthiness of the joint itself (Brunner and Rutz 2013).

The study of forces and torques is also used to assess the effects of neuro-motor or genetic diseases on the musculoskeletal system. Examples are Cerebral Palsy, Prader-Willi syndrome and Ehlers-Danlos syndrome, that are characterized by gait and muscular disorders, due to poor joint stability and muscle-tendon weakness (Ancillao et al. 2012; Brunner and Rutz 2013; Galli, Cimolin, et al. 2011). Moreover, it was observed that obesity may have effects on the muscle power of lower limb, influencing everyday tasks such as raising from a chair or walking (Capodaglio et al. 2009).

It is clear that strength assessment plays an important role for the study of the previously cited pathologies and definition of rehabilitative treatments.

Several methods to measure human strength were developed across the years. The simplest ones were based on the indirect measurement of muscle force and fatigue as in the chair-stand test (Csuka and McCarty 1985); that consist in measuring the time required to stand up and sit back on a chair. The trial is repeated ten times.

As direct methods are generally to be preferred (Allen et al. 1995; Jones, Rikli, and Beam 1999) some protocols were developed, allowing the measurement of strength by means of force sensors and *ad-hoc* built mechanical systems (composed of ropes, cantilevers, etc.). E.g. these systems were used targeting the knee extensor (Figure 2.1.1) (Maughan et al. 1983) and triceps brachii (Figure 2.1.2) (Allen et al. 1995)*.*

Nowadays, the gold-standard and widespread direct method is the isokinetic dynamometer which is also commercially available (Janssen and Le-Ngoc 2009; Kim et al. 2014; Martin et al. 2006; Tsaopoulos et al. 2011).
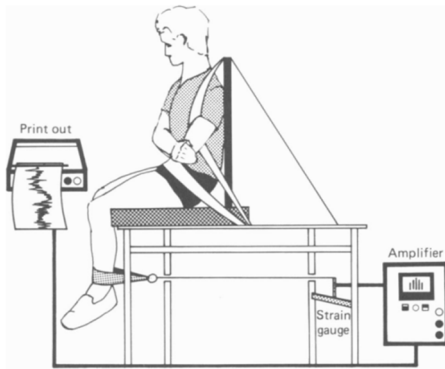
Figure 2.1.1: *Knee extension strength measurement* (Maughan et al. 1983)*.*
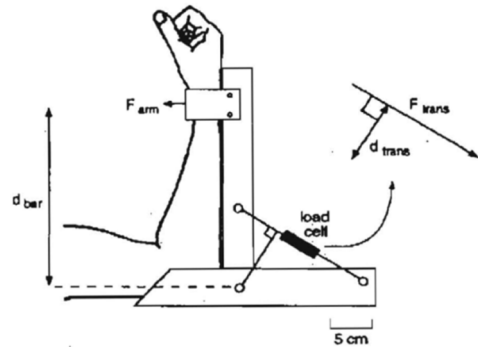
Figure 2.1.2: *Triceps Brachii strength measurement* (Allen et al. 1995)*.*

The isokinetic dynamometer (Figure 2.1.3) is composed of a seat and a moving instrumented arm that allows the gathering of force-velocity curves and the estimation of the maximum force exerted by the patient during a specified exercise.

The isokinetic dynamometer showed high inter-rater and intra-rater reliability and reproducibility for the measurement of joint forces and torques when it was applied to subjects with different age, both on the lower limb and upper limb (Fulcher, Hanna, and Raina Elley 2010; Hartmann et al. 2009; Hughes et al. 2001; Kim et al. 2014).

The main drawbacks of the isokinetic dynamometer are that it is expensive, it is not portable, it requires long time to prepare the subject as well as dedicated spaces.

Figure 2.1.3: *Isokinetic Dynamometer.*

Figure 2.1.4: *Hand Held Dynamometer in use.*

(a)

(b)   (c)
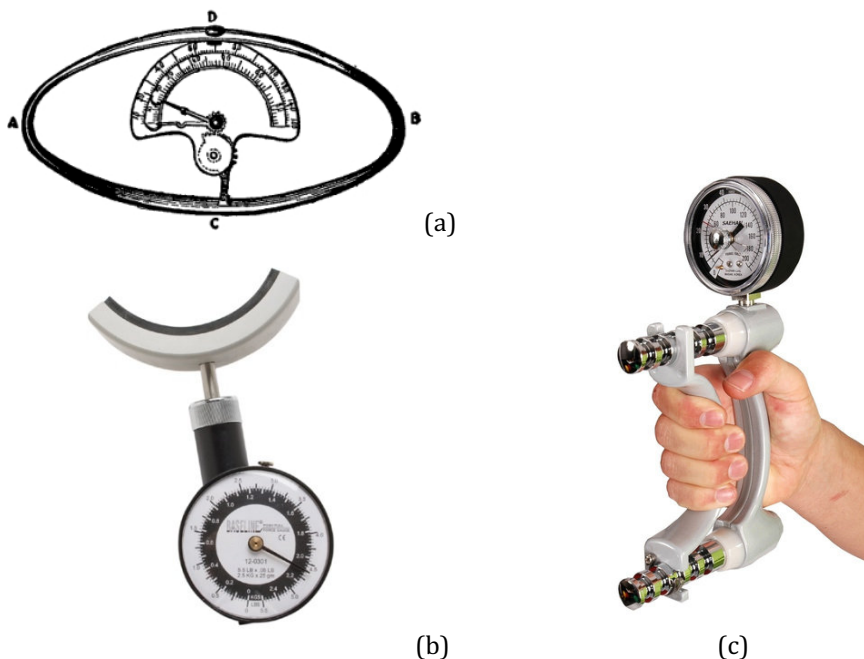
Figure 2.1.5: *HHDs for: (a) handgrip strength, based on a circular elastic element (ABCD). The force is applied between the points C and D; (b) general purpose, based on a hydraulic system; (c) handgrip strength, based on a hydraulic system.*

An alternative and modern method to directly measure strength is by using an Hand Held Dynamometer (HHD). It consists in the use of a small and portable dynamometer that can be held in hand by a clinician that applies it on some defined landmarks (Figure 2.1.4), asking the patient to exert a force against the dynamometer (Fulcher et al. 2010; Kim et al. 2014).

(a)   (b)
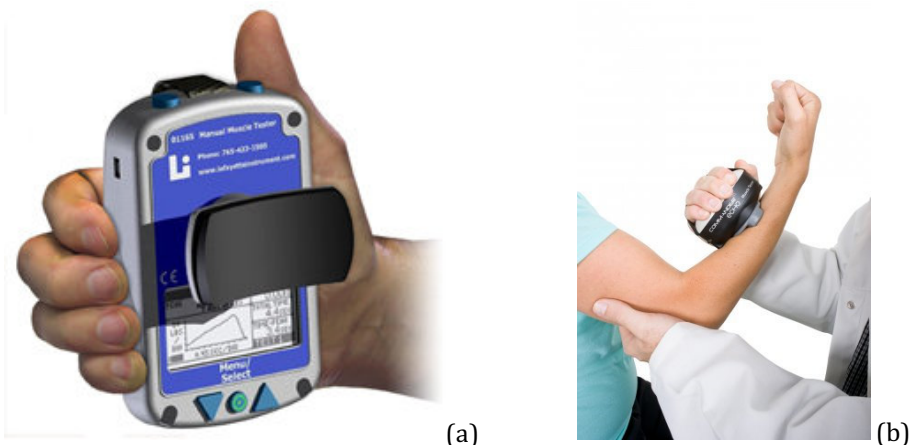
Figure 2.1.6: *Modern Hand Held Dynamometers. (a) shape and handling, (b) application to elbow flexion.*

The HHD is a low cost device, if compared to the isokinetic dynamometer, portable, easy to use and it does not require long lasting procedures or dedicated rooms for its use. Moreover, the HHD allows the indirect measurement of joint torque by knowing the distance between the positioning landmark and the anatomical joint. Maximum joint torque can then be obtained by multiplying the maximum force measured by the distance from the joint center.

The HHD may be realized with different shapes, depending on the anatomical landmark to which it is intended to be applied. Moreover HHDs can be realized according to different working principles, examples are: (i) spring/cantilever systems (Figure 2.1.5a); (ii) hydraulic systems (Figure 2.1.5b,c) and (iii) piezoelectric/strain gage load cells (Figure 2.1.6). The most of modern commercial HHDs are based on single component load cells (Figure 2.1.6) that are relatively inexpensive and allow a fast measurement, data recording and storage. Anyway the correct application by the operator is crucial to ensure that the force is effectively applied on the sensible axis of the load cell and subject's limb remains still during the measurement.

According to the literature, two methodologies were developed to measure strength by means of the HHD (Bohannon 1988): (i) the "make" test, in which the examiner holds the dynamometer stable while the subject exerts a maximal force against it, and (ii) the "break" test, in which the examiner holds the HHD in place but she/he has to overcome the maximum force exerted by the subject, making consequently the limb move in the opposite direction. The two methods were compared by (Bohannon 1988) concluding that both were reliable and repeatable if the examiner had enough force to contrast the force exerted by the patient.

Another paper comparatively examined the previously mentioned tests (Phillips, Lo, and Mastaglia 2000) and the main outcomes were: (i) the "break" test requires a larger force exerted by the examiner and some examiners may experience troubles, thus when this occurs the "make" test is preferable; (ii) both "break" and "make" test provide similar results, both are strongly operator-dependent and, as a tendency, they underestimate the maximum force exerted by the knee extensor.

The reliability and repeatability have been studied in recent years (Clark et al. 2010; Kim et al. 2014; Martin et al. 2006; Wuang et al. 2013). Wuang et al. (Wuang et al. 2013) focused the study on the measurement of strength of lower limb muscles in children with intellectual disabilities. The authors concluded that the use of HHDs could be considered practical and easy for

clinicians but the measurement protocol had some critical issues related both to the operator's training and to the positioning of the dynamometer on the subject's limb.

The operator's influence on the strength measurement was tested by Kim et al. (Kim et al. 2014) by comparing three set-ups: (i) with the HHD fixed to the distal tibia by a velcro strap; (ii) with the HHD held by the operator; and (iii) with an isokinetic dynamometer, assumed as a reference. They found that fixed and non-fixed methods showed good inter-rater reliability and the reliability of the fixed method was the highest.

According to (Martin et al. 2006), the HHD offers a feasible, inexpensive, and portable test of quadriceps muscle strength for use in healthy older people, but it was found to underestimate the absolute quadriceps strength if compared to the isokinetic dynamometer, especially in stronger subjects.

In spite of the advantages of the HHD, reports on reproducibility and inter-operator repeatability were controversial (Bohannon and Andrews 1987; Hébert et al. 2011; Marmon et al. 2013; Riddle et al. 1989). The main causes of low reliability of HHD method were identified in the poor training of operators and wrong patient's positioning (Bandinelli et al. 1999). In fact, HHD method relies on operator's strength and training in order to contrast the force exerted by the patient (Bohannon 1988).

Among the lower limb joints, special attention should be paid to the ankle, as plantar flexion/extension and inversion/eversion are important determinants of balance and general functional ability (Spink et al. 2011). Moment exerted by the ankle, as well as ankle power and stiffness play an important role in human gait. In fact, ankle kinematics and kinetics are commonly affected by motor pathologies and may improve in case of therapy (Camerota et al. 2015; Galli et al. 2008; Rigoldi et al. 2012; Vismara et al. 2016).

Ankle strength can be measured by means of HHD and studies about reliability of such measurements were conducted. Ankle strength of healthy subjects was measured by means of HHD and then compared to an electromechanical dynamometer, i.e. a fixed dynamometer that allowed evaluation of isometric force (Marmon et al. 2013). Results showed that HHD measurements were not correlated to the fixed dynamometer, that was assumed as reference, and statistical differences were found between the two sets of measurements. This was attributed to the low strength of the examiner and his inability to position and hold steady the HHD. The conclusion was that HHD strength measurements of the plantar-flexors should not be considered valid (Marmon et al. 2013). Such results were in disagreement with the results observed by

Spink et al. (Spink et al. 2011), that found high reliability of ankle and foot HHD strength measurements in older and younger participants. They concluded that HHD is a valid methodology for the evaluation of ankle strength. Another work about HHD reliability on ankle measurements is the one by Hebert et al. (Hébert et al. 2011). They found that among all the lower limb joints, ankle plantarflexion and ankle dorsiflexion had the lowest reliability, therefore they recommended further study in this direction, especially regarding the strength evaluation in children with neuro-motor disabilities.

2.2 – Aim of the research

What emerges from the literature survey is that the operator's skills in holding the HHD in place represent a decisive factor on the quality of the strength measurements. Moreover, reliability studies conducted on HHD produced controversial results as sometimes it was found to be "excellent" (Mahony et al. 2009) and sometimes it was found to be "low" (Verschuren et al. 2008).

A further unaddressed potential limitation in the use of HHD is that commercial HHDs acquire only the component of the force projected on the sensitive axis of HHD and, consequently, the lateral components of force and the moments exerted by subject on HHD are always ignored.

Previous reliability studies were limited to the statistical analysis of repeated measurement and, to the author's best knowledge, no other studies were conducted to quantify the effect of the two previous cited limitations and to directly measure the sources of inaccuracy occurring when commercial HHDs are used.

The aims of this work were therefore the following:

- Design and implementation of a protocol for the validation of clinical HHD;
- Measurement of the sources of inaccuracy:
    - actual dynamometer position with respect to the joint;
    - undesired motion of the limb;
    - actual forces and torques exerted between patient and operator;
- Testing the strength measurements by targeting the knee joint on healthy subjects.
- Propose a quality assurance protocol for HHD clinical strength measurements.

This work represents a first step in a long range research aimed to model muscle physiology and to ensure quality of strength measurement in children with neurological diseases.

2.3 – Preliminary Setup and results

Acquiring preliminary trials was necessary to test and improve the early design of the protocol. Preliminary testing was conducted in the Motion Analysis and Robotics Laboratory of "Bambino Gesù" Children Hospital of Rome, IT (Figure 2.3.1).

Healthy adult subjects were recruited according to the inclusion criteria: healthy adult subjects of both sexes from 18 to 35 years old. Subjects must not have any neurological or orthopedic disorders and must not have undergone surgery to the lower limb joints. All the subjects were evaluated by a trained clinician before inclusion.

Ten healthy adult subjects were enrolled in this study: 6 males, 4 females, mean age 27.3±1.4 years, average height 169.2±11.2 cm, average body mass 65.4±11.2 kg. They were all right handed even though this was not an inclusion criterion. The subjects were informed and signed consent prior to the participation. This study was approved by the ethical review board of Children's Hospital Bambino Gesù Rome.

Figure 2.3.1: *The Motion Analysis and Robotics Laboratory of "Bambino Gesù" Children Hospital of Rome, IT.*

To track position and motion of the subject, the operator and the force sensor, we used a Vicon MX Optoelectronic System (Oxford Metrics, UK) equipped with 8 IR cameras and strobes, Nexus 1.7 software, sampling frequency of 200 Hz and a calibrated volume of about 4 m³. The overall inaccuracy was estimated as ~1 mm.

Force was measured by means of a commercial MicroFet™ Hand Held Dynamometer (HHD) (Figure 2.3.2, Hoggan Scientific, Salt Lake City, US). The dynamometer was set up to transfer real time data by means of wireless connection. HHD had a sampling frequency of 100 Hz, maximum load capacity of 1300 N, accuracy 1% of full range.

According to classical clinical protocols, the HHD is meant to be held in-hand by a trained clinician that applies it on some defined landmarks on subject's limb and asks the patient to exert a force against it. The result of the measurement is the maximum force that occurs during the trial and the effective duration of the trial, that should be about 5 s. (Bohannon 1986; Fulcher et al. 2010; Kim et al. 2014; Martin et al. 2006; Phillips et al. 2000).

The HHD working principle is based on a one-axis load cell that collects and records the force applied over the sensing surface.

The microFET2® HHD used for this project was provided by "Bambino Gesù" Children Hospital of Rome, IT, where it was already in use it for other research activities related to the MD-Paedigree European Project.

The HHD was equipped with reflective markers, diameter was 10 mm, in order to reconstruct its position and orientation within the calibrated volume of the Vicon System. Three markers were placed on sticks and a fourth marker was placed at the centre of the sensing surface, as shown in Figure 2.3.2. The central marker was used only for the static trial and was removed during force measuring trial. The central marker was necessary to reconstruct a reference position for force origin on the sensing surface. The reconstruction was made possible by a localization procedure based on a local reference system built on the three fixed markers (Ancillao et al. 2013). More details of the reconstruction procedure will be discussed later.

The subject was equipped with a marker set based on the PlugInGait (PIG) protocol with the addition of markers on the internal epicondyle of the femur and of the ankle, in order to easily locate the knee and ankle joint centers and a cluster composed of three markers applied on the thigh (in correspondence of the *quadriceps femoris*) that allowed optimal reconstruction of thigh anatomical markers in case they are covered.

Markers were applied on both sides of the body even though strength was measured only on the dominant side. Full marker protocol, including markers on the HHD, is depicted in Figure 2.3.3.

HHD markers were placed on sticks rigidly fixed to the HHD in order to avoid covering by the operator's hand (Figure 2.3.2).

Figure 2.3.2: *The microFET2® Hand Held Dynamometer equipped with passive motion capture markers.*
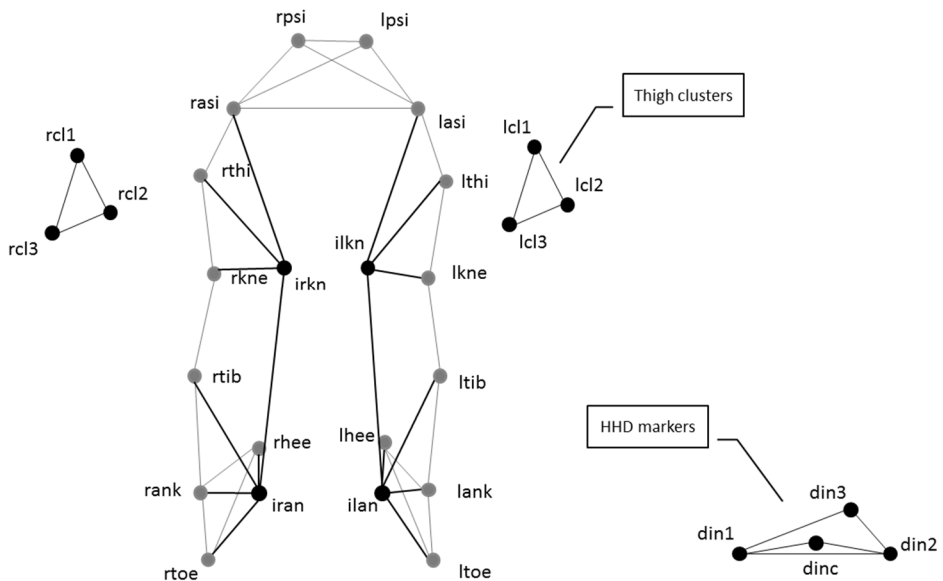
Figure 2.3.3: *The full marker set used for this study. Gray lines/dots represent the P.I.G. model, black lines/dots are the markers added to the P.I.G.*

The designed protocol required the acquisition of a static trial before the set of dynamic trials. In the static trial the subject had to stand up still in the calibrated volume for about 5s. The HHD was also kept still in the calibrated volume (Figure 2.3.4). This allowed the recording of the position of the central marker, corresponding to the sensing surface, with respect to the other three markers. The dynamic trials (Figure 2.3.5) consisted in the use of the markerized HHD to measure knee strength according to the standard clinical protocol, that described in the following.

An attempt to collect real time data produced by the HHD and to synchronize it with kinematic data was done. As the HHD transmits data through an USB dongle, its driver was implemented in a LabView® programming environment (National Instruments, USA). Data collected by the dongle was streamed towards the analog output port of a National Instruments® A/D board (Figure 2.3.6). The board was therefore working as digital to analog converter. Analog signal, real time generated, was sent to the analog input port of the Vicon® system.

Synchronization testing was done by simultaneously applying a variable force in series to the HHD and the force platform connected to the Vicon® system. This was achieved by vertically pushing the HHD against the surface of the force platform. Delays and differences between the signals were identified (Figure 2.3.7).

The testing showed a strong noise superimposed to the HHD signal and a stochastic delay in the signal itself that made the automatic synchronization impossible. The delay was attributed to the computing time required to collect data and to conversion speed/buffering limits of the A/D board. The delay was also probably due to delays in the commercial wireless protocol implemented by the maker of the HHD.

After some testing, the idea of data synchronization trough the analog port was dropped. A procedure for manual synchronization was implemented instead: Kinematic signals and HHD signal were recorded separately. HHD signal was collected by means of a LabView® *ad hoc* designed software that saved the digitally acquired data to a CSV (text) file. Data files were then imported in MatLab® environment and were synchronized by the user who had to visually identify events on both signals. The events to be identified were the beginning (rising) and ending (descending) of force track. This ensured an acceptable synchronization between kinematic recording and force measurement.
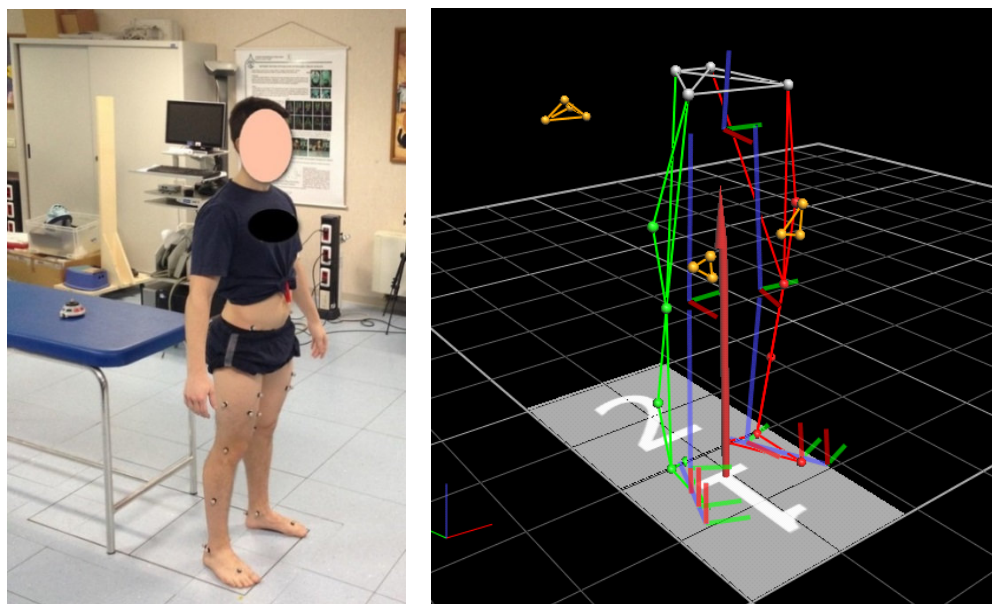
Figure 2.3.4: *Static trial for the preliminary protocol and its biomechanical reconstruction. The subject is wearing the full marker set.*
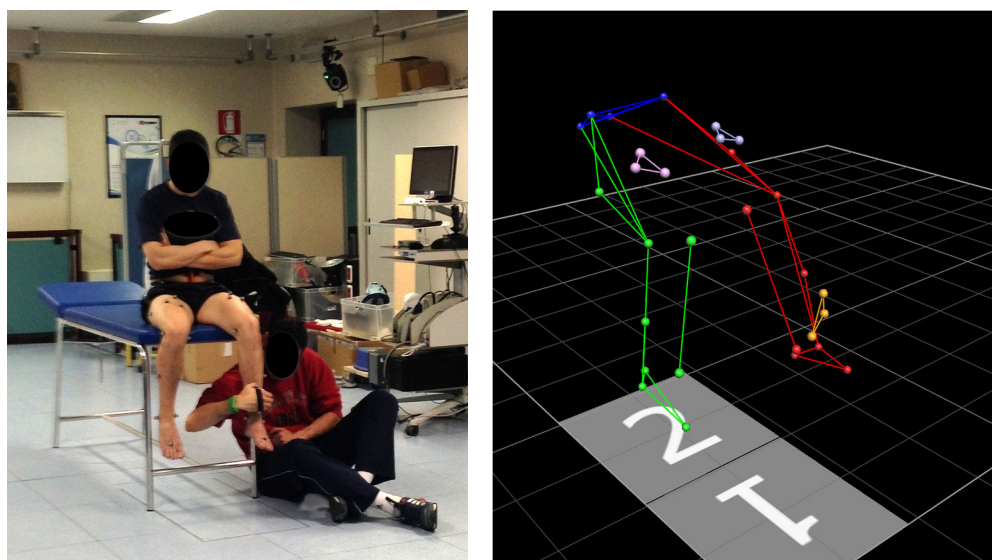
Figure 2.3.5: *Knee extension strength measurement trial for the preliminary protocol and its biomechanical reconstruction.*
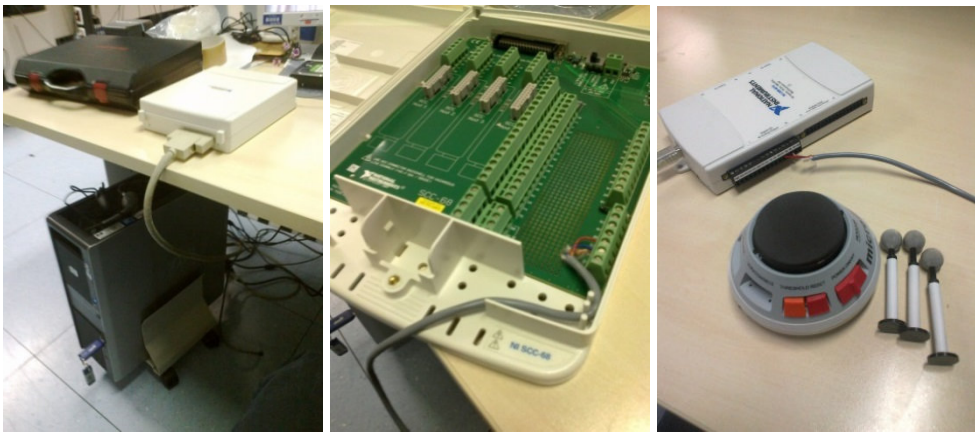
Figure 2.3.6: *System for collecting wireless HHD data and streaming to Vicon as analog signal.*
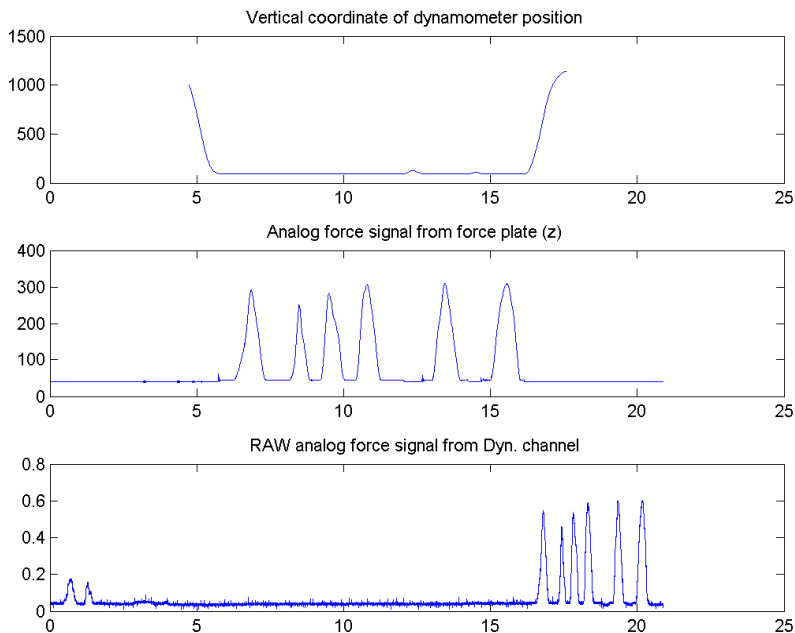
Figure 2.3.7: *Sync testing of the HHD and Vicon System. Horizontal axis has time, vertical axes are mm, N and V respectively.*

In this preliminary testing, the strength of the knee flexors and knee extensors was measured by means of a clinical protocol defined in a close cooperation with the clinical partners of the neuromuscular disease group within the FP7 MD-Paedigree project (Ancillao et al. 2015).

The protocol consisted in a "make test" method that is widely accepted in literature (Martin et al. 2006; Wang, Olson, and Protas 2002).

HHD was held by a trained clinician while the trial is performed according to the following directions:

- Extension: Subject sitting, lower legs hanging from the table with hips and knees in flexion at 90°. HHD was placed proximal to the ankle on the anterior surface of the lower leg. Manual fixation at the thigh and resistance exerted by the operator at the shank in knee flexion direction.

- Flexion: Subject sitting, lower legs hanging from the table with hips and knees in flexion at 90°. HHD was placed proximal to the ankle on the posterior surface of the lower leg. Manual fixation at the thigh and resistance exerted by the operator at the shank in knee extension direction.

The operator was required to counteract the force of the patient by trying to keep the shank still. The patient had to exert its maximum force against the HHD for about five seconds. The participants were also instructed to avoid explosive contraction but to increase force gradually to the maximum (Wang et al. 2002). Moreover, the operator also measured the distance between the knee and the HHD application landmark by using a measuring tape.

The trials were repeated 5 times for knee extension and 5 times for knee flexion with a resting time of about 30 s between trials to avoid fatigue effects.

Data recorded for each trial were pre-processed by Vicon Nexus 1.7 software (Vicon Motion Systems, UK). Pre-processing included: track labelling, interpolation, smoothing and C3D export.

C3D data were then processed according to *ad-hoc* built MATLAB (MathWorks, USA) scripts.

A local coordinate system (CS) axes was defined for the shank:

- y-axis: parallel to the main axis of the shank, directed from the ankle joint to the knee joint.

- yz plane: the plane containing the y-axis and the vector from the knee center to the lateral tibial marker. z-axis is in the medio-lateral direction, pointing to the right of the subject.

- Origin: knee center.
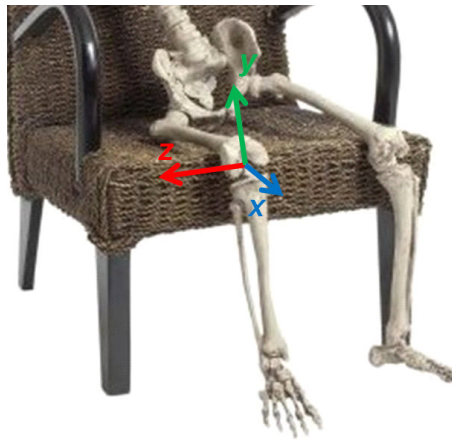
Figure 2.3.8: *Local Reference System defined for the knee joint.*

(a)

(b)

(c)

(d)
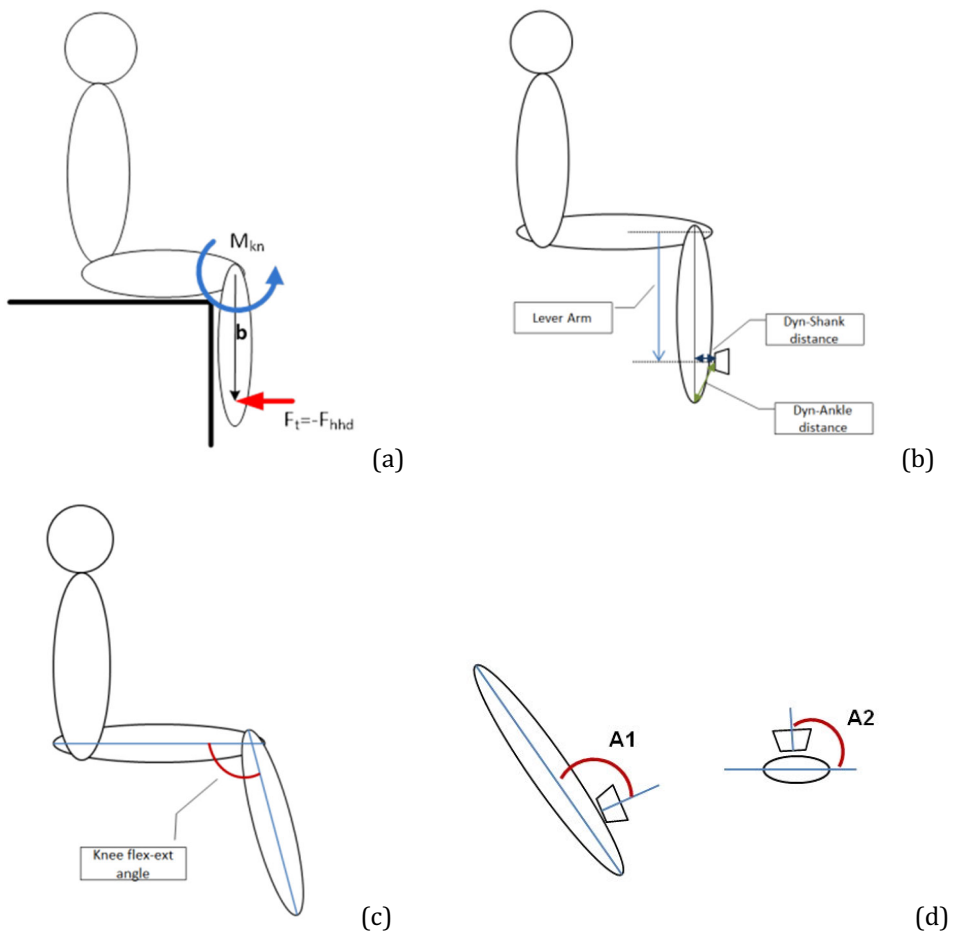
Figure 2.3.9: *Graphical representation of the measured parameters. (a) Force and Moment. (b) Distances. (c) Knee flexion extension angle. (d) HHD positioning angles with respect to the shank.*

In accordance to the literature, for each trial we recorded the maximum force measured by HHD, here addressed as nominal force (F_{nom}), and the nominal knee moment (M_{nom}) obtained simply by multiplying force to the lever arm (Figure 2.3.9 a, b).

Taking advantage of the motion capture protocol used, we also measured the following kinematic and kinetic quantities:

- Knee Range of Motion (RoM), as the angular displacement of the knee from the resting position (Figure 2.3.9c).

- Angles between the dynamometer and the shank on the sagittal plane (A1) and on the transverse plane (A2) at the instant in which the maximum force is recorded (Figure 2.3.9d).

- Ranges of Motion of the angles A1 and A2 (RoM-A1 and RoM-A2) during the whole trial.

Actual knee force and moment (F_x, F_y, F_z, M_x, M_y, M_z), computed by knowing the actual position of the HHD and the actual direction of its sensible axis.

The main component of knee moment is on the z-axis. Lateral component should be ideally ~0 Nm. Quality analysis of strength measurements is conducted on the moment results, as they take into account overall effects due to the positioning and orientation of HHD performed by the operator.

To quantify the difference between the nominal value of moment and the actual moment components (M_x, M_x and M_z), the root-mean-square error (RMSE) was computed. Since the nominal moment is assumed only on the z-axis, RMSEs were defined according to the following equations (expressed as % of the maximum nominal moment):

$$RMSE_z = \sqrt{\frac{\sum_{i=1}^{N}\left(M_z^i - M_{nom}^i\right)^2}{N}} * \left|\frac{100}{\max(M_{nom})}\right| \qquad (1)$$

$$RMSE_x = \sqrt{\frac{\sum_{i=1}^{N}\left(M_x^i\right)^2}{N}} * \left|\frac{100}{\max(M_{nom})}\right| \qquad (2)$$

$$RMSE_y = \sqrt{\frac{\sum_{i=1}^{N}\left(M_y^i\right)^2}{N}} * \left|\frac{100}{\max(M_{nom})}\right| \qquad (3)$$

$$RMSE_{xy} = \sqrt{(RMSE_x)^2 + (RMSE_y)^2} \tag{4}$$

Where: N is the number of trials recorded for each subject and max(M$_{nom}$) is the maximum value of subject's nominal moment. RMSEs were computed for each subject.

RMSEs of lateral components, that are x and y, were merged within a single parameter (eq. 4) that provide an evaluation on the magnitude of lateral components of moment that are neglected in usual clinical strength assessment.

All the parameters were averaged between the five repetitions of each subject. Coefficient of variation (CV) of each parameter, defined as the % ratio between standard deviation (SD) and mean was computed to quantify repeatability within the single subject.

$$CV\% = \left| \frac{SD}{mean} \right| * 100 \tag{5}$$

Figure 2.3.10 shows the force profiles recorded in a strength trial. In the first figure the distance between the HHD and the shank is visualized. When this distance approaches zero it means that the HHD is in contact with the shank. The green vertical lines represent the trial starting and trial ending events that were used to cut the data tracks. The graphs on the second column shows the force profile as measured by the HHD, the force projections on the directions of the CS of the shank, the moment of the knee along the three axes of the CS. On the first column the A1 and A2 angles and knee flexion angle are depicted.

Table 2.3.1 shows results of kinematic and kinetic analysis of knee extension and flexion trials. For each parameter is reported the mean value and SD between subjects.

As the *Make* method was adopted for strength measurements (Martin et al. 2006; Wang et al. 2002), subject's limb should remain still across the trial, that implies a RoM ideally near to 0°. In our analysis, the measured angular RoM was never equal to 0° and we observed a value of 32±12° across the subjects; hence, the operator was not able to hold the limb completely still. This fact affected the strength measurement, as the operator was not able to exert a correct opposing force to the subject. This result is coherent with the results of Kim *et al.* (Kim et al. 2014) that proved a better measurement validity when the HHD is fixed with Velcro fixation than it is held by the operator.
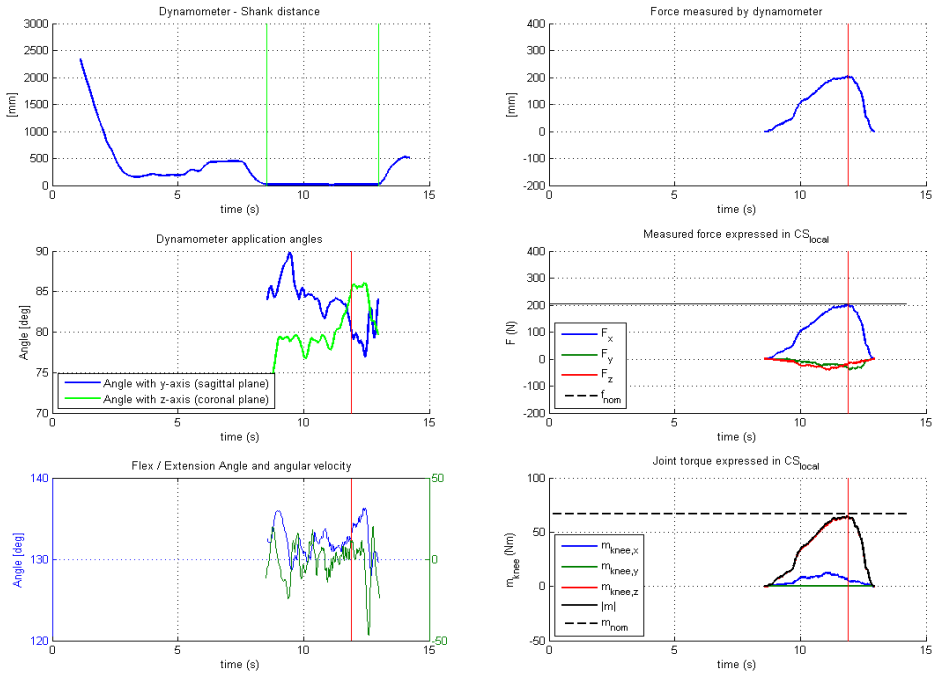
Figure 2.3.10: *Analysis of forces and position for one strength trial.*

Parameter	Knee Extension		Knee Flexion	
	Mean (SD)	CV% (SD)	Mean (SD)	CV% (SD)
Knee RoM [°]	32 (12)	20.9 (12.1)	27 (5)	16.7 (7.2)
A1 [°]	93 (7)	3.4 (2.0)	87 (8)	9.1 (11.4)
RoM-A1 [°]	14 (6)	27.3 (8.6)	20 (14)	36.3 (14.9)
A2 [°]	90 (8)	5.7 (2.1)	101 (8)	4.1 (1.9)
RoM-A2 [°]	21 (7)	27.1 (9.5)	16 (6)	34.1 (17.1)
F_nom [N]	240 (29)	7.6 (2.9)	-138 (22)	6.9 (1.5)
M_nom [Nm]	83 (13)	7.6 (3.0)	-46 (6)	6.8 (1.6)
RMSEz [%]	4.8 (1.7)		11.6 (5.7)	
RMSExy [%]	15.3 (7.6)		20.4 (11.5)	
RMSEz [Nm]	4 (2)		5 (3)	
RMSExy [Nm]	12 (5)		9 (6)	

Table 2.3.1: Numerical results of the preliminary trials. A1 is the angle on the sagittal plane, A2 is the angle on the transverse plane. F_nom is the nominal force. M_nom is the nominal moment.

From the preliminary results, we observed that Knee RoM had more variability in the knee extension trials than knee flexion, in terms of both mean value and CV. This finding can be related to the lower force exerted in flexion trials and it was in agreement with the results of Laing *et al.*(Laing et al. 1995).

Repeatability of measurements was quantified for each subject by means of the CV% of the force and moment. The average CV% was low (< 10%) for both knee extension and knee flexion trials, meaning high repeatability of measurements, coherently with previous studies (Kim et al. 2014; Martin et al. 2006; Phillips et al. 2000).

Positioning angles A1 and A2 were close to 90° with a low CV % (<10%), meaning a good positioning of the HHD on the shank. Worst results were obtained for the knee flexion trials, due to the operator's position that had to extend his arm behind the shank and therefore had a poor control of positioning.

Ranges of motion of angles A1 and A2 quantified the stability of the operator's hand across the trial. They were in the range of 20° with high CV%, >25% for knee extension and >30% for knee flexion, meaning instability and movement of the HHD during the trial. This finding confirmed the operator's dependence of the measurement quality (Bohannon 1986; Kim et al. 2014; Martin et al. 2006; Willemse et al. 2013) and also confirmed the poor control of HHD positioning in knee flex trials.

In a clinical context, only nominal force and moment are measured and they are assumed as the force and moment on the axis of flex/extension while lateral components are neglected. RMSE parameters were therefore computed in order to quantify the inaccuracy committed by neglecting the lateral components. More precisely, $RMSE_z$ represented the error between the nominal moment and the component of the actual moment on the z-axis that is the flex/ext axis, while $RMSE_{xy}$ represented the magnitude of lateral components of the actual moment.

The knee extension trials had a $RMSE_z$ <5% indicating a low error, while $RMSE_z$ for flexion was >10%. Also $RMSE_{xy}$, that represents the effect of lateral components of moment, was higher for knee flexion (20.4%) than knee extension (15.3%).

Absolute RMSEs on the main axis were comparable with the respective uncertainty level. RMSEs of lateral components were slightly higher but lower than the moment on the main axis. These findings were connected to the angular displacement observed in A1 and A2 values and confirmed that

angular misplacement induced an inaccuracy in the estimation of flex/extension moment.

The force and the moment exerted by the subjects were higher in knee extension trials with respect to knee flexion trials. Knee flexion trials had some issues due to HHD positioning. These issues were represented by angles A1 and A2 and their ranges of motion. Moreover, the operator was not able to keep the limb of the subject perfectly still. Therefore, specific attention has to be paid for HHD positioning in knee flexion and extension trials. Stability of HHD is crucial and therefore training of the operator is extremely important. Moreover, the operator should be strong enough to exert a force equal to the force produced by the subject and avoid motion of the limb.

The preliminary analysis proved that the motion capture protocol was robust and able to reconstruct the kinematics.

The main limitations observed in the preliminary trials were:

- The HHD used was a 1-componet load cell. A multi component load cell would be useful to better evaluate the effect of lateral components of force and moment;
- Need to simplify the system by removing the LabVIEW software running on a dedicated machine and the D/A board, having the whole system running on the same machine;
- Manual synchronization of data was time consuming. Synchronize data at the time of recording would dramatically reduce processing time;
- Other anatomical district should be taken into account by the protocol;
- Limited number of subjects;
- Need of a software to batch-process a large amount data with reduced user action;
- Need to "summarize" results in a few parameters.

2.4 – Final experimental setup

The final setup and the whole data acquisition were conducted in the Motion Analysis and Robotics Laboratory of "Bambino Gesù" Children Hospital of Rome, IT (Figure 2.3.1).

To overcome the limitations observed in the preliminary analysis, the materials and methods of the research were modified as follows (for more details see: (Ancillao et al. 2015; Ancillao, Rossi, and Cappa 2017).

Subjects

Thirty healthy adult subjects were enrolled in the study: 18 males, 12 females, age 26.2 ± 2.1 years, height 173.6 ± 7.2 cm, body mass 68.1 ± 8.7 kg. Subjects must not have had any neurological or orthopedic disorder and must not have undergone surgery to the lower limb joints. All the subjects were evaluated by a physiatrist before the trials. All the subjects were right handed even though this was not an inclusion criterion. This study complied with the principles of the Declaration of Helsinki, and it was approved by the Ethical Committee of the Children's Hospital "Bambino Gesù" Rome, IT.

Instrumentation

In order to overcome the limitations observed for the one-component HHD (as used for the preliminary analysis) a multi-component analog load cell was used. Specifically, the limitations of a one-component HHD were identified as: (i) data synchronization issues, (ii) loss of information about the lateral components of force and (iii) no direct measurement of torque.

The sensor chosen was a six-components HHD based on a Gamma F/T load cell, ATI Industrial Automation, USA, shown in Figure 2.4.1. Measurement ranges and metrological characteristics are shown in Tables 2.4.1 and 2.4.2. This model was chosen because the sensing range on the z-axis was compatible with the range of strength measurements to be conducted. Moreover, the physical dimensions (Table 2.4.2) were comparable to the MicroFET2 dynamometer, therefore the load cell could be held by hand and used as an HHD.

Figure 2.4.1: *ATI Gamma 6-components F/T Sensor*

Sensing Ranges			
Fx,Fy	**Fz**	**Tx,Ty**	**Tz**
130 N	400 N	10 Nm	10 Nm

Resolution			
Fx,Fy	**Fz**	**Tx,Ty**	**Tz**
1/40 N	1/20 N	1/800 Nm	1/800 Nm

Table 2.4.1: *Ranges and resolution of the ATI Gamma F/T Sensor*

Single-Axis Overload	
Fx, Fy	±1200 N
Fz	±4100 N
Tx, Ty	±79 Nm
Tz	±82 Nm
Stiffness	
X-axis & Y-axis forces (Kx, Ky)	$9.1x10^6$ N/m
Z-axis force (Kz)	$1.8x10^7$ N/m
X-axis & Y-axis torque (Ktx, Kty)	$1.1x10^4$ Nm/rad
Z-axis torque (Ktz)	$1.6x10^4$ Nm/rad
Resonant Frequency	
Fx, Fy, Tz	1400 Hz
Fz, Tx, Ty	2000 Hz
Physical Specifications	
Weight*	0.255 kg
Diameter*	75.4 mm
Height* ** Specifications include standard interface plates*	33.3 mm

Table 2.4.2: *technical specifications and metrological characteristics of the ATI Gamma F/T Sensor.*
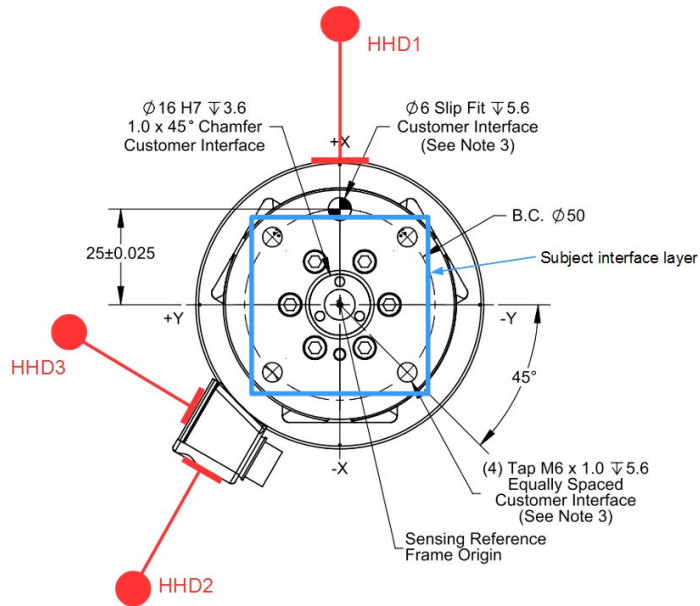
Figure 2.4.2: *Geometrical specifications of the ATI Gamma F/T Sensor and application of the Vicon markers (red).*
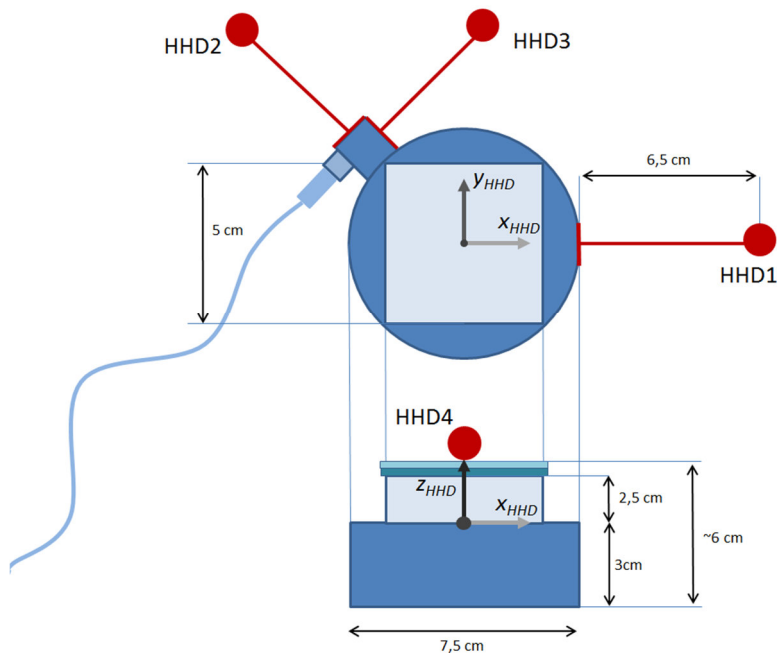
Figure 2.4.3: *Design of force transferring layers and their dimensions. Landmarks for Vicon markers are visualized in red. The local reference system is also indicated.*

The load cell was equipped with an *ad-hoc* designed aluminum force-transferring layer and a foam layer on the side that was in contact with the subject's limb in order to maximize subject's comfort during the measurement. Mass of the load cell was 0.255 kg, diameter 75.4 mm and height 33.3 mm. Geometrical details of the layers are shown in Figures 2.4.2 and 2.4.3.

The load cell was connected through a shielded cable to a pre-amplifier box, powered by 5V DC current. Downstream of the pre-amplifier box, analog voltage output of each channel was available. Each channel delivered its output by a couple of wires. A total of 12 wires plus ground and shield were connected to the analog input box of the Vicon® system and acquired in differential mode (Figure 2.4.4).

The load cell and the acquisition system were tested by applying a known load to the cell and the force platform in series (Figure 2.4.5). Results of this test showed the proper operation of the measurement chain.

The motion was recorded by means of a Vicon MX Optoelectronic System (OS) (Oxford Metrics, UK), equipped with 8 cameras. The OS was able to reconstruct the *x,y,z* coordinates of markers and their motion in a 3D virtual environment.

Static and dynamic calibration tests, performed in accordance with the manufacturer's indications, were conducted before each participant's trial session and they showed that overall RMS error of marker coordinates in three-dimensional space was less than 1 mm in a calibrated volume of about 2x1x2 m^3.

Calibration allowed to build a local reference system for each camera and to define the position in space of each camera with respect to an absolute reference system.
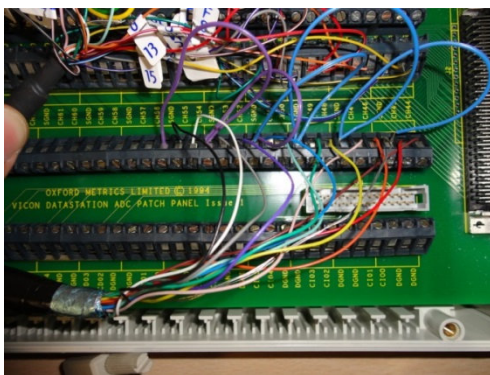
Figure 2.4.4: *Vicon analog junction box and connection of the 6 channels and ground (13 connectors) from the load cell.*

Figure 2.4.5: *Testing of the load cell by applying a known load in series to the load cell and the force plate.*

Figure 2.4.6: T-shaped calibration wand for the Vicon MX system.

The calibration procedure adopted by the Vicon MX system is named *DynaCal3.* It uses a T-shaped wand, with markers on it, for both dynamic and static calibration procedures. Markers are placed in such a way to univocally determine wand's position and orientation in space (Figure 2.4.6).

Dynamic calibration consists in randomly moving the wand along the volume to be calibrated, paying attention to have each camera recording an adequate amount of frames containing the full visible wand. This procedure allows to define the boundaries of the acquisition volume and computation of camera parameters and relative position. This is made possible by comparing the measured distance between wand's markers and their actual distance that is known.

Static calibration consist in placing the wand on the floor and recording its position. This allows to define the absolute reference system of the lab and to compute the position of each camera with respect to this reference system. The crossing point of the wand's arm becomes the origin of the Cartesian space, while the arms define the axes. By convention, z-axis is defined pointing upwards from the floor.

Vicon Nexus software allowed to acquire and process the system calibration, to view in real time the acquisition volume as well as the output of each camera. At the end of the recording, the software could reconstruct the *x, y, z* coordinates of markers, allowing their labelling and construction of the biomechanical model.

The signal produced by the load cell was recorded and synchronized to the kinematic data and t the force platforms of the lab. Signal was stored within the same file container of Kinematic and force platform data, i.e. C3D format.

Motion Capture Protocol

The 6-component HHD was equipped with four passive markers as shown in Figure 2.4.7. Markers were placed on sticks rigidly fixed to the HHD to avoid covering by the operator's hand. The central marker was placed in the midpoint of the patient-interface area of the HHD needed to locate its center

with respect to the other markers that were used to build a local reference system (Figures 2.4.3 and 2.4.7). The central marker was removed during the measurement of strength and its position was reconstructed by using a non-optimal localization procedure based on the three fixed markers (Ancillao et al. 2013).

Markers on the subjects were placed according to an *ad-hoc* defined marker protocol composed of 26 markers placed on the subject's skin surface (Figure 2.4.8a and b). Landmarks were identified as follows: posterior and anterior iliac spines (4 markers), lateral thighs (2 markers), lateral and medial epicondyles (4 markers), lateral and medial malleoli (4 markers), lateral shanks (2 markers), second metatarsal head (2 markers), and calcaneous (2 markers). Finally, two clusters of three markers (6 markers) were applied on the thighs (in correspondence of the quadriceps femoris).

Positions of knee and ankle centers were computed as the midpoint between the two markers on epicondyles and on the malleoli, respectively. Hip center was reconstructed solving the Plug-In-Gait model, which is a modified version of the Davis protocol (Davis et al. 1991), when the subject is in the upright position. Instead, the position of hip center when the subject assumed the seated position, was reconstructed by means of an optimal localization procedure (Cappozzo et al. 1997) using the markers on the thigh, as the markers on the pelvis were not always visible to the OS cameras.

A static trial was recorded for each subject before the trials for strength quantification. In the static trial, the subject was asked to stand up still in the calibrated volume for about five seconds. At the same time HHD was kept still on the laboratory floor in calibrated volume of the OS, while zero input was applied. The static trial allowed to evaluate: (i) the position and the orientation of local reference systems of each body segment and the HHD; and (ii) the offset signals gathered by the HHD.
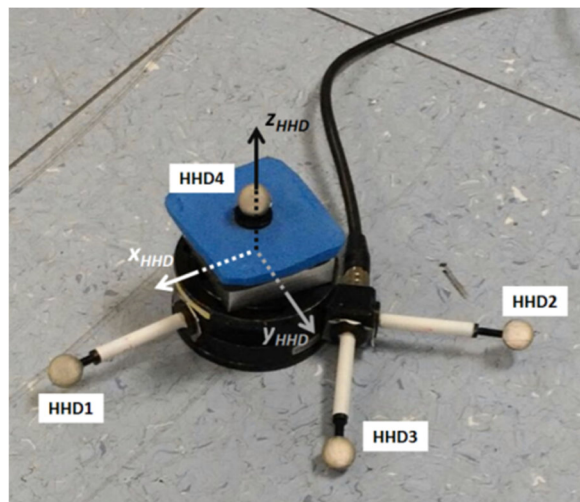
Figure 2.4.7: *Six-components load cell equipped with force transferring layers. Markers are identified by their names and the local reference system is represented.*
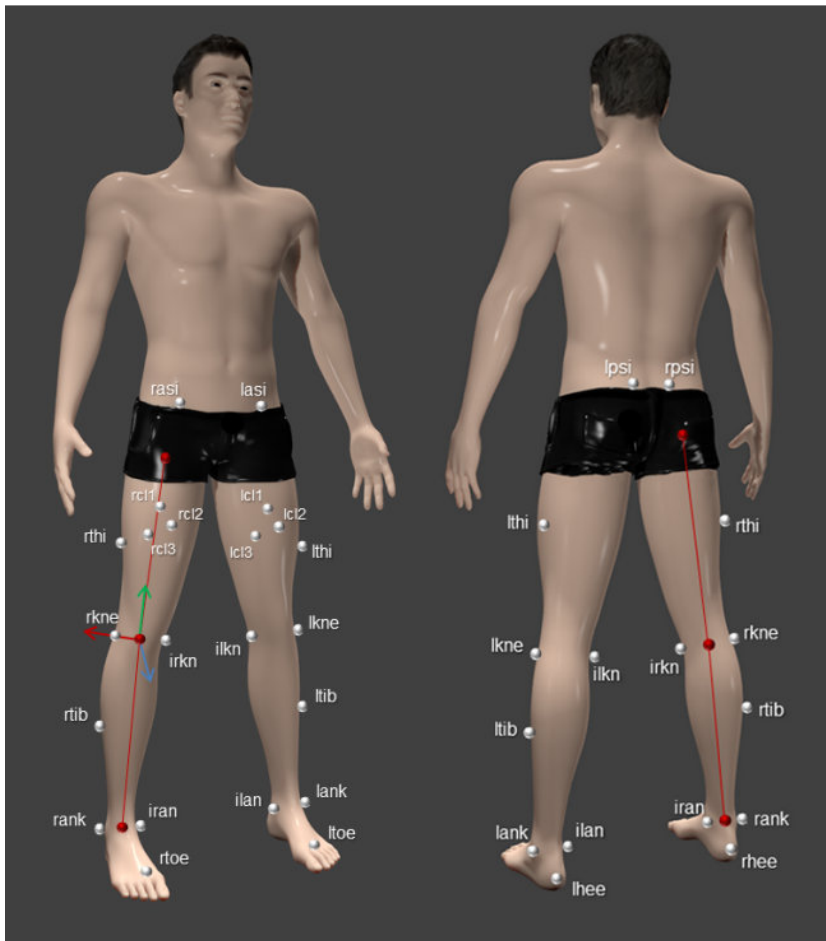
Figure 2.4.8a: *The marker protocol used to reconstruct position of subjects' lower limb. White dots represents the markers used with the optoelectronic system; red dots are the computed joint centers (virtual markers). Local reference system of the shank is shown. High resolution rendering of human figure was obtained by graphic software (see page 79 for details).*

Strength protocol

Strength of the knee flexors and knee extensors muscles was measured by a protocol defined in a close cooperation with the clinical partners of the neuromuscular disease group within the FP7 MD-Paedigree project. This protocol consisted in a "make test" method (Bohannon 1988; Laing et al. 1995; Martin et al. 2006; Wuang et al. 2013). The HHD was held by a trained clinician and the trials were performed in accordance to (Eek, Kroksmark, and Beckung 2006): Subjects were sitting on a bench, lower legs were hanging with hips and knees in flexion at about 90°. They were stabilized to reduce compensation from other muscle groups and the movements of thigh were impeded by a belt connected to the bench.
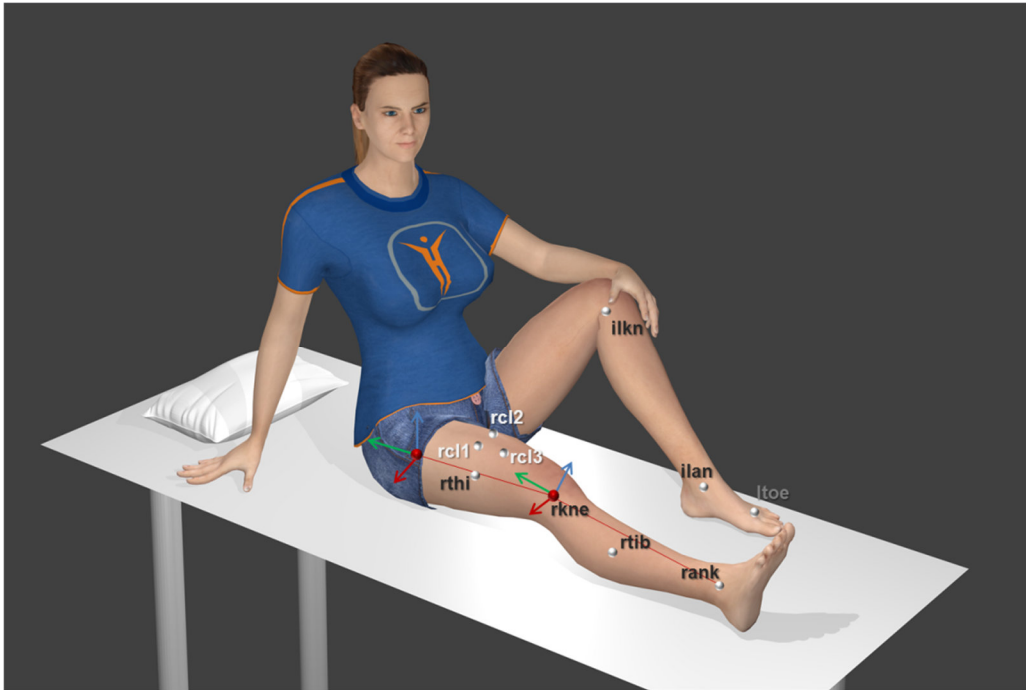
Figure 2.4.8b: *Another representation of the anatomical landmarks used for lower limb kinematic analysis. The markers allowed to reconstruct a biomechanical model of the lower limb and its motion. Local reference systems of thigh and shank are shown.*
High resolution rendering of human figure was obtained by graphic software (see page 79 for details).

The HHD was placed proximally to the ankle on the anterior or posterior surface of the lower leg for the extension (Figure 2.4.9) and flexion (Figure 2.4.10) trials, respectively. The operator had to exert a force in the opposite direction of patient's one (Figure 2.4.11).

The markers placed on the subject and on the HHD allowed to reconstruct a numerical biomechanical model of the action (Figure 2.4.12) that was used to compute the parameters of interest.

The subjects were instructed to exert their maximal force against the HHD for about five seconds while the operator counteracted the force trying to keep the shank still. The participants were also instructed to avoid explosive contraction but they were invited to increase force gradually from zero to the maximum achievable value (Wuang et al. 2013). Participants were tested individually by a single operator. Trials were repeated five times for both knee extension and knee flexion with a resting time of about 30 s between trials to avoid fatigue effects in both subject and operator. The session for each participant lasted approximately 30 minutes.
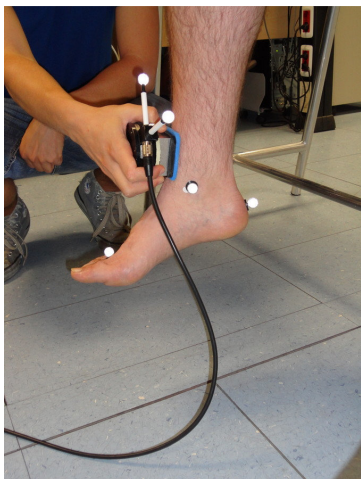
Figure 2.4.9: *HHD placement for knee extension trials.*

Figure 2.4.10: *HHD placement for knee flexion trials.*

Figure 2.4.11: *Graphical rendering of the correct positioning for a knee extension trial.*
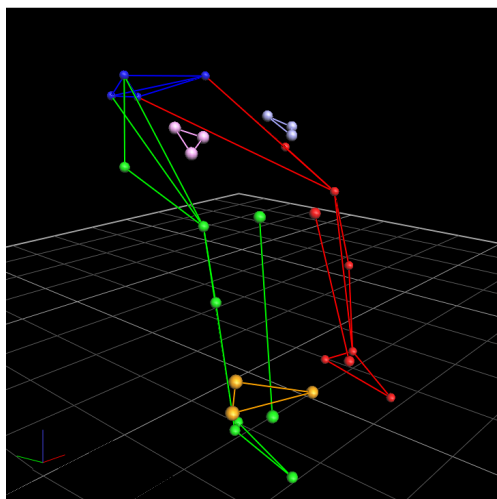
Figure 2.4.12: *Biomechanical model of the lower limb with the HHD (yellow triangle) placed in proximity to the right ankle.*

2.5 – Data processing

The kinematic data and the force signal from the load cell were recorded simultaneously and stored within the same data file. The data from each trial were stored within a C3D file that served as container for motion capture data.

Preprocessing, which included: signal denoising, track labelling, artifact removal and data compression, was done in Vicon Nexus 1.7 (Oxford Metrics,

UK). At this stage, the C3D format was maintained, containing the preprocessed data for each trial.

Further data processing was achieved by means of *ad hoc* designed algorithms implemented in Matlab (MathWorks, USA). C3D data file were imported within the Matlab environment by means of ad hoc designed libraries, and then processed as explained in the following.

Calibration (a.k.a. static) trials were processed first. The static parameters were required by the dynamic processing script, namely dynamic engine. The purpose of the dynamic engine was to interpret motion capture and HHD data in order to obtain some kinematic and kinetic indices that were used to describe the quality of strength measurements.

The flowchart of data processing is depicted in Figure 2.5.1. Static processing and dynamic processing are explained through Figures 2.5.2 and 2.5.3.

Computing of parameters was based on the definition of anatomical local reference systems (LRS) on the basis of external markers placed on the skin of the subject.

LRS were defined for the shank, LRS_{SH} (Figure 2.5.4), and for the HHD, LRS_{HHD} (Figure 2.4.7).

LRS_{SH} was defined as:

- y_{SH}, the unit vector from ankle center to knee center, directed upwards;
- x_{SH}, the unit vector perpendicular to the plane defined by the knee medial and lateral epicondyles and the ankle center, and pointing forwards;
- z_{SH}, the unit vector perpendicular to xSH and ySH;
- origin, located at the knee center.

LRS_{HHD} was defined as:

- vmkr, the virtual marker defined as the projection of HHD4 on the plane represented by HHD1, HHD2 and HHD3;
- x_{HHD}, the unit vector from vmkr to HHD1;
- z_{HHD}, the unit vector perpendicular to the plane defined by HHD1, HHD2 and HHD3, pointing upwards;
- y_{HHD}, defined as cross product between z_{HHD} and x_{HHD};
- origin, the virtual marker on the line between vmkr and HHD4 with an offset from HHD4 of 2.7 cm, that is the sum of thickness of the force coupling layers and the marker's radius.

The LRSs allowed to compute Euler's angles between rigid bodies and a set of parameters describing the motion of the limb and HHD placement.

Parameters were classified as kinematic indices and kinetic indices.

The <u>kinematic</u> indices were:

- Range of Motion of knee angle (RoM), defined as the difference between the maximum and minimum of knee angle measured throughout the trial. Specifically, the knee angle was defined as the angle between the vector from knee center to hip center and the vector from knee center to ankle center (Vimercati et al. 2013a). RoM is an index to quantify the quality of strength measurements (low values of RoM represent higher adherence to the selected protocol, actually the limb had to ideally remain still during the trial).

- A1 and A2, representing the angles between z_{HHD} and y_{SH} and between z_{HHD} and z_{SH}, respectively (Figure 2.5.4). A1 and A2 were evaluated at the instant in which the measurement of strength was gathered, that is when the maximal force was recorded. A1 and A2 should be ideally equal to 90° and their deviations from this value, namely δA_1 and δA_2 , represent indices of incorrect positioning of HHD.

The previously defined indices were computed for both knee extension and knee flexion trials and they were averaged between the five repetitions of each subject.
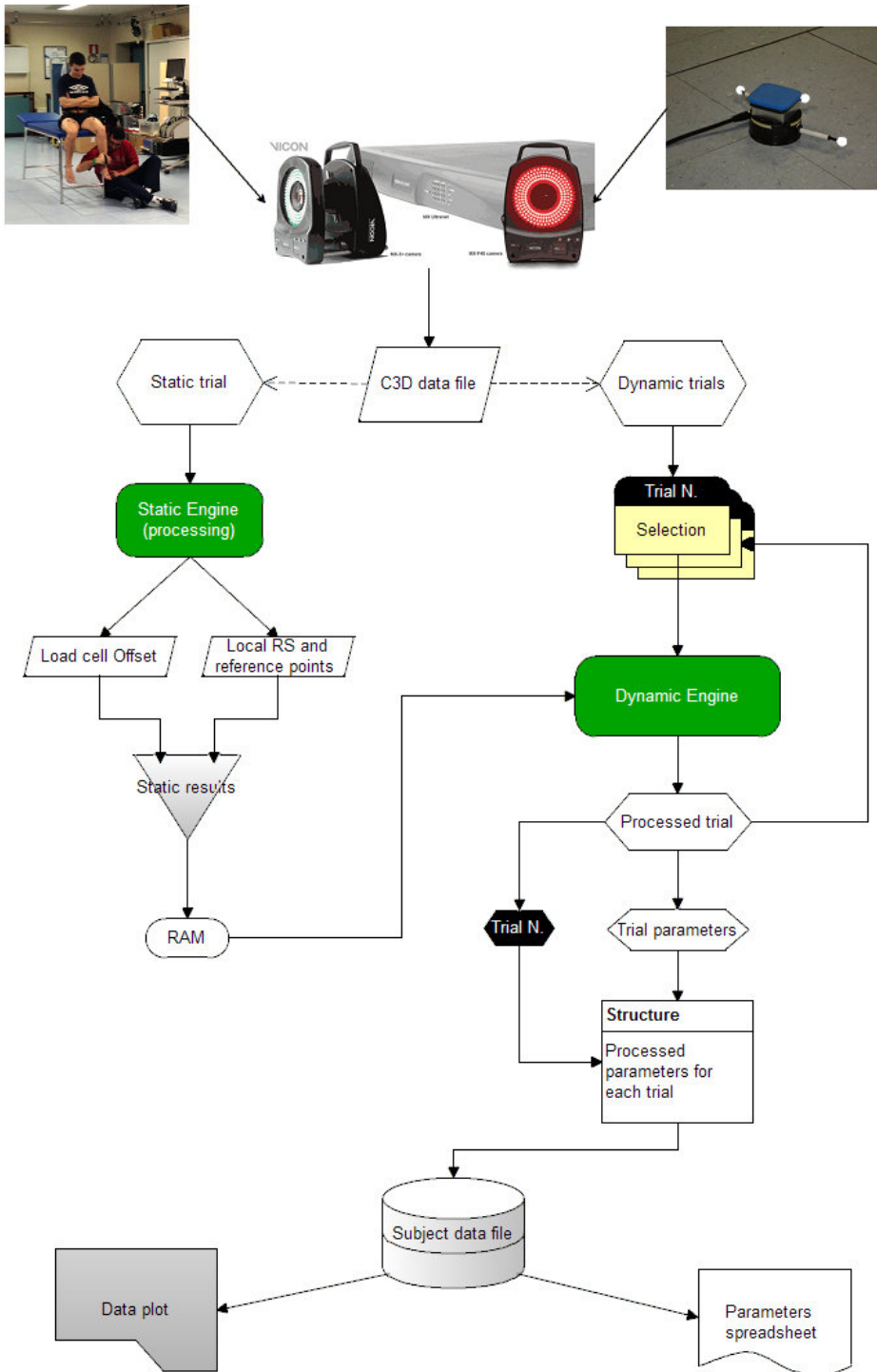
Figure 2.5.1: *Overall data processing flowchart.*
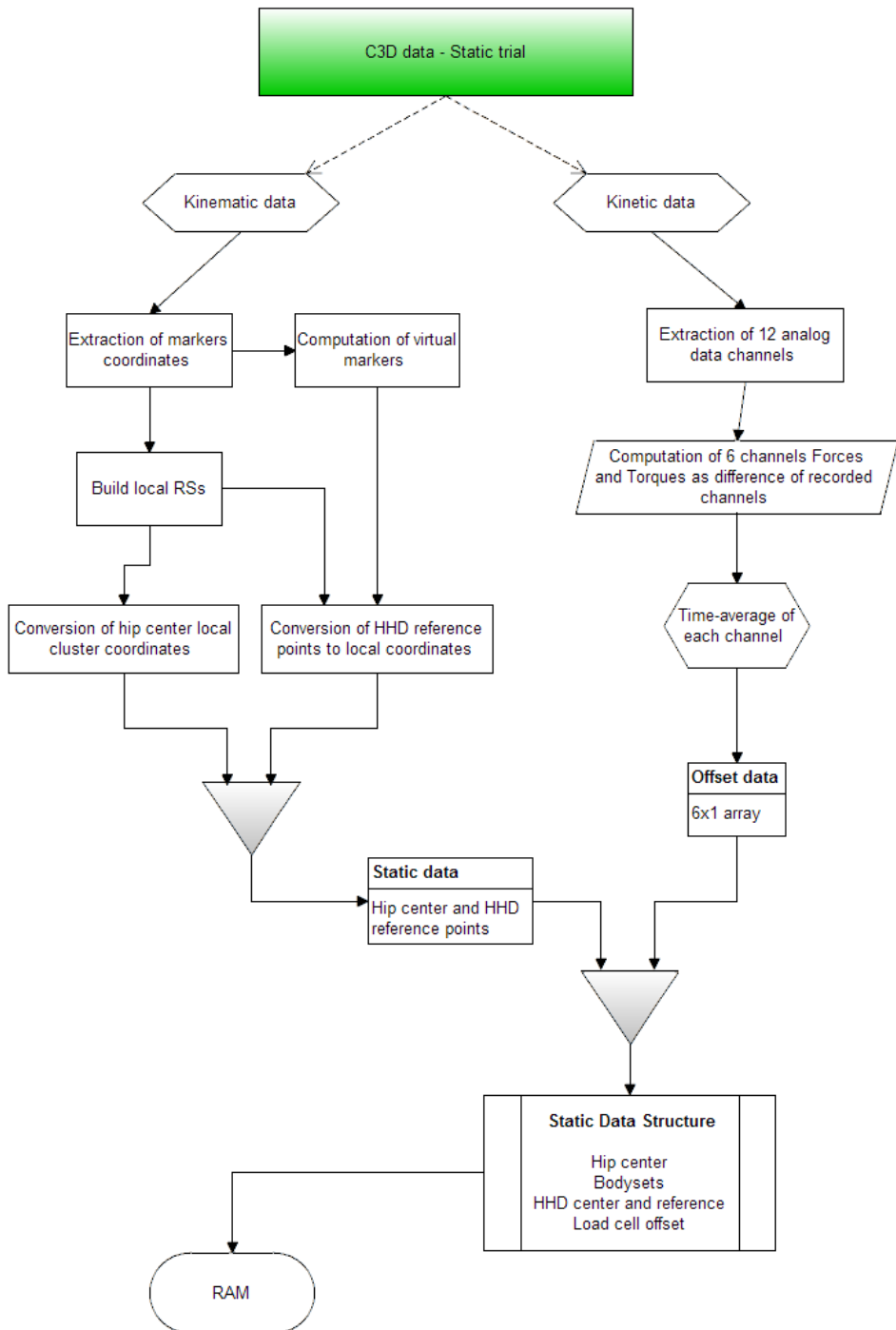
Figure 2.5.2: *Flowchart for the static processing script .*
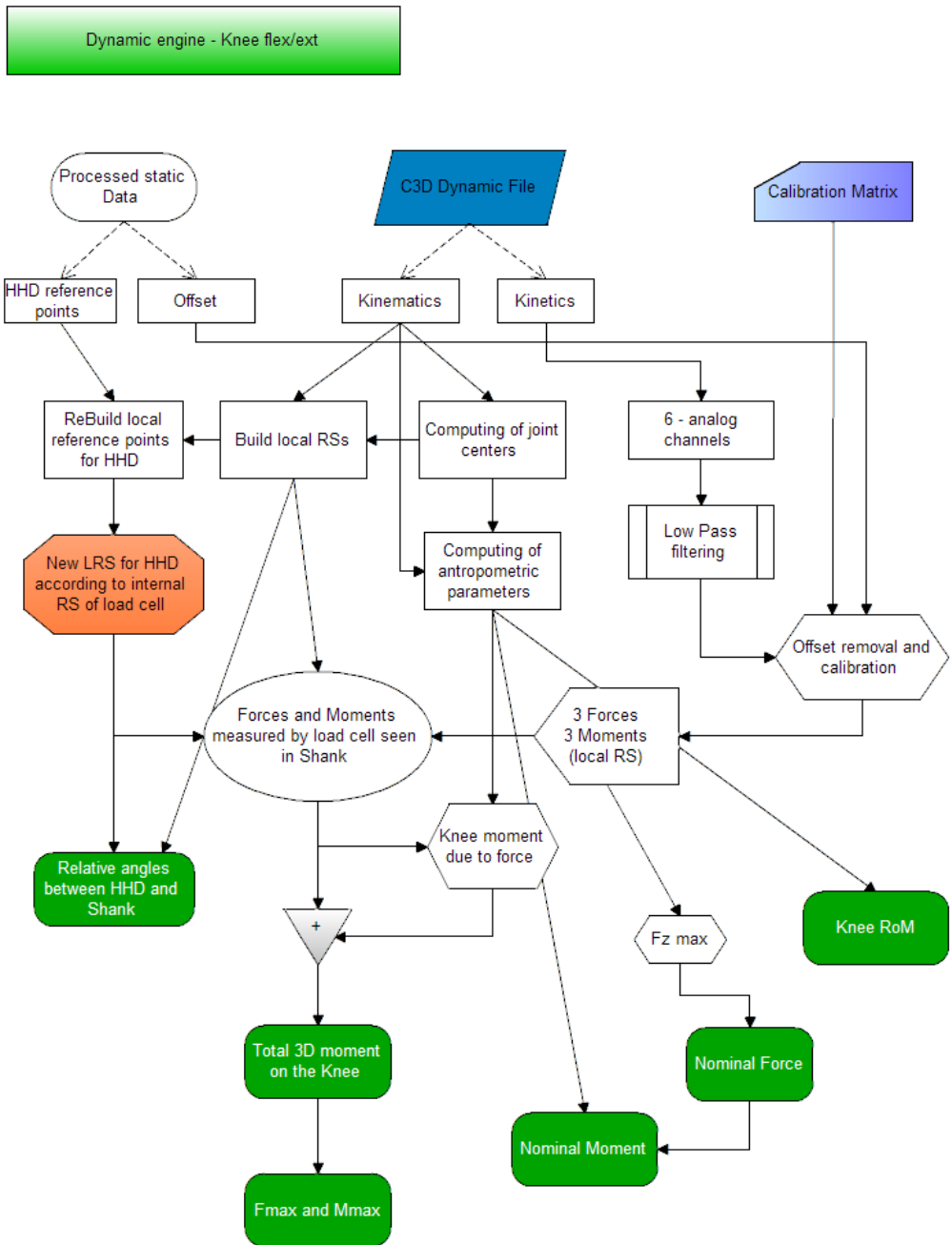
Figure 2.5.3: *Flowchart for the dynamic processing script .*
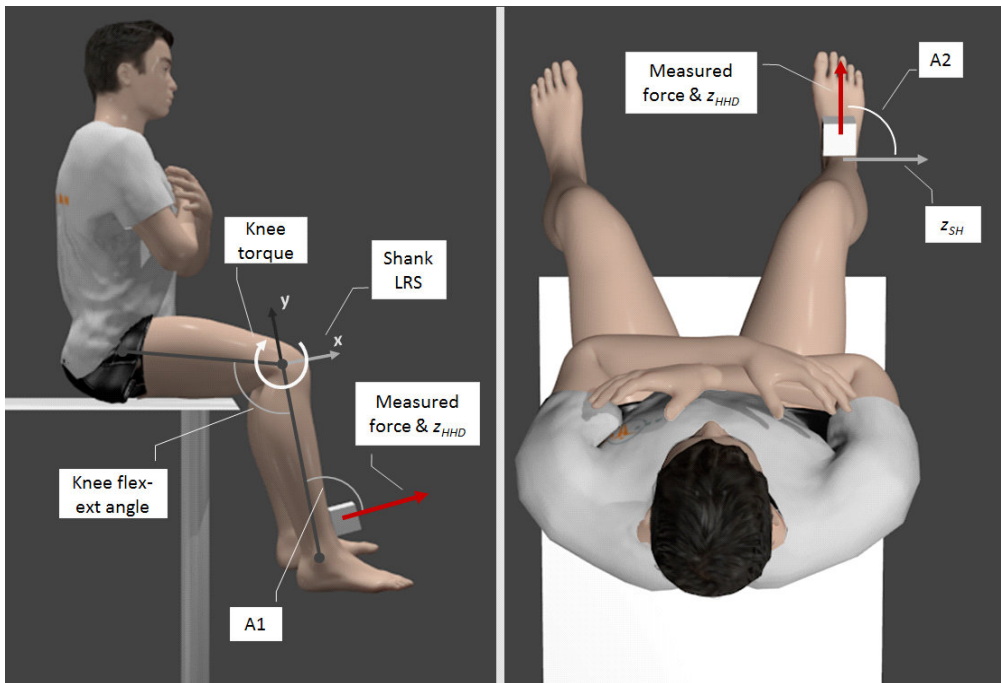
Figure 2.5.4a: *3D rendering representing subject's position, local reference systems and computed parameters. Lateral view and top view.*
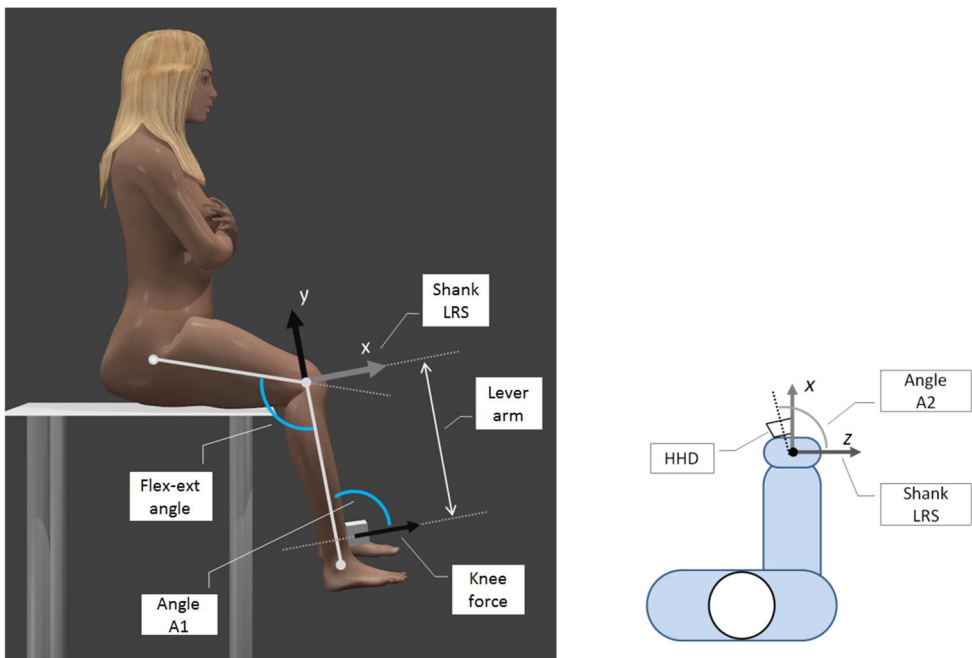
Figure 2.5.4b: *Alternative rendering and detailed drawing explaining the definition of A1 and A2 angles, knee angle and lever arm.*

In order to assess repeatability of kinematic measurements we computed the Coefficient of Variation (CV) for each parameter, addressed as CV_{RoM}, $CV_{\delta A1}$ and $CV_{\delta A2}$. The CV was defined as the % ratio between the standard deviation (SD) and the mean value between the five repetitions for each subject.

Regarding the kinetic data, we evaluated forces and moments acting on the knee joint center and reported in LRS_{SH} ($^{SH}\mathbf{F}$ and $^{SH}\mathbf{M}$, respectively):

$$^{SH}\mathbf{F} = {}^{SH}\mathbf{R}_{HHD} \cdot {}^{HHD}\mathbf{F} \tag{1}$$

$$^{SH}\mathbf{M} = {}^{SH}\mathbf{R}_{HHD} \cdot {}^{HHD}\mathbf{M} + {}^{SH}\mathbf{o}_{HHD} \times {}^{HHD}\mathbf{F} \tag{2}$$

Where $^{HHD}\mathbf{F}$ and $^{HHD}\mathbf{M}$ are the outputs of the HHD, $^{SH}\mathbf{R}_{HHD}$ is the rotational matrix that rotates vectors from coordinate system LRS_{HHD} to LRS_{SH}, and $^{SH}\mathbf{o}_{HHD}$ is the origin of LRS_{HHD} represented in LRS_{SH}.

The <u>kinetic</u> indices were:

- F_M, defined as the maximum value of $^{SH}F_y$, which represents the strength measurement;

- F_T the transverse component of the force exerted by the subject. It allows the quantification of the intensity of lateral force that cannot be acquired with the usual clinical measurements conducted with a uniaxial load cell:

$$F_T = \sqrt{{}^{SH}F_y{}^2 + {}^{SH}F_z{}^2} \tag{3}$$

- M_M, defined as the maximum value of the knee flexion-extension moment, that is $^{SH}M_z$, when the strength measurement is conducted;

- M_T the transverse component of the knee moment. It represents the moment components not-assessable if a uniaxial load cell was used to measure the knee moment:

$$M_T = \sqrt{{}^{SH}M_x{}^2 + {}^{SH}M_y{}^2} \tag{4}$$

All the computed indices were referred to the time instant when the maximum force was acquired and they were averaged between the five repetitions for each subject. Moreover, each kinetic index was computed for both knee extension and knee flexion trials.

In order to estimate the operator-dependent inaccuracy, we evaluated also the nominal knee strength ($\hat{F}$) and the nominal knee moment ($\hat{M}$) as they are usually measured in clinical routine. Specifically, we considered that clinicians evaluate the force exerted by subjects with a uniaxial HHD and they estimate

knee moment multiplying $\hat{F}$ by the distance between the HHD and the lateral malleolus usually determined with a tape measure. Thus, we simulated a uniaxial HHD by focusing only on the $^{HHD}F_z$ force component. In addition, we considered only $^{SH}\mathbf{o}_{HHD}$ that is the distance between the knee epicondyle and the HHD positioning as the nominal lever arm for the evaluation of knee moment (Eq. 5 and Eq.6).

$$\hat{F} = {}^{HHD}F_z \tag{5}$$

$$\hat{M} = {}^{SH}\mathbf{o}_{HHD} \cdot \hat{F} \tag{6}$$

The inaccuracies related to both the strength and the knee moment were evaluated as the Root Mean Square Error (RMSE) of the differences between actual values (F_M and M_M) and the nominal ones ($\hat{F}$ and $\hat{M}$); RMSEs were also normalized at the maximum values of $\hat{F}$ and $\hat{M}$ (Eq. 7).

$$RMSE_F = \sqrt{\frac{\sum_{i=1}^{N}\left(F_M^i - \hat{F}_i\right)^2}{N}} \cdot \frac{100}{max_i(\hat{F}_i)} \ [\%]$$

$$RMSE_M = \sqrt{\frac{\sum_{i=1}^{N}\left(M_M^i - \hat{M}_i\right)^2}{N}} \cdot \frac{100}{max_i(\hat{M}_i)} \ [\%] \tag{7}$$

where N is the number of repetitions of the trials. Thus, RMSE values permitted the overall quantification of strength inaccuracy in knee moment measurements performed in the clinical routine.

To assess measurement repeatability, we also computed the Coefficient of Variation (CV) for $\hat{F}$ and $\hat{M}$, addressed as $CV_{\hat{F}}$ and $CV_{\hat{M}}$.

Finally, to give an overall quantification of the quality of strength measurement, we proposed a novel synthetic quality index Q_{index}. It was defined to take into account both the angular misplacements of HHD (δA_1 and δA_2) expressed as a percentage of 90°, and the transverse component of moment (M_T) expressed as percentage of the maximum value of the knee moment (M_M). We considered the transverse component of moment representative of the quality of the measurement because it takes into account both the effects induced by the HHD incorrect positioning and the transversal force components.

$$Q_{index} = 100\left(1 - \sqrt{\left(\frac{\delta A_1}{90}\right)^2 + \left(\frac{\delta A_2}{90}\right)^2 + \left(\frac{M_T}{M_M}\right)^2}\right) \tag{8}$$

An *ideal* strength measurement implies δA_1, δA_2 and M_T equal to zero, that is Q_{index} equal to 100 %. Thus, Q_{index} values lower than 100% indicate a worsening of the strength measurements.

Statistics

Descriptive statistic was computed for each index among the subjects. All data were tested for normality by the Shapiro-Wilk test. The significance level was set at 0.05 for all statistical tests. The paired t-test was then computed to check differences of all parameters between the knee extension and the knee flexion trials.

To study the influence of incorrect positioning of the HHD on the measurements of strength and knee moment, we computed the Pearson product-moment correlation coefficient between the kinematic indices (δA_1, δA_2 and RoM) and the indices directly related to the inaccuracy of the strength measurement ($RMSE_F$, $RMSE_M$, F_T and M_T). The coefficient r ranges from -1 to 1 (values close to 1 or -1 represent a strong correlation between the variables). The following categorization for the Pearson coefficient r was considered, as suggested in literature (Dancey and Reidy 2004): $|r|=1$: perfect; $0.7 \leq |r| \leq 0.9$: strong; $0.4 \leq |r| \leq 0.6$: moderate; $0.1 \leq |r| \leq 0.3$: weak; $|r|=0$: zero.

Software implementation

The workflow for processing strength trials was implemented entirely in MatLab (The MathWorks, USA).

Processing strength trials requires processing a static (calibration) trial for the subject and the dynamic (measure of strength) trials. Each trial, after recording by the Vicon System, was preprocessed (noise filtering, labelling, etc.) by the Vicon Nexus software and then stored within a C3D file, i.e. a file format serving as container for motion capture data.

C3D file for static trial and dynamic trials were imported into MatLab by means of some ad hoc designed libraries and then processed according to the numerical algorithms previously described.

Software was developed according to a <u>modular criterion</u>: a "main" script accepts filenames and identifies calibration trial and dynamic trials. Then uses C3D accessing libraries (implemented as external function) to extract relevant tracks from containers and store them in a memory structure. After the details of the trial are identified (left or right side, extension, flexion, etc.) data is passed to another external script that does the processing according to the specific kind of trial.

Results of processing are stored within another memory structure and then passed to other modules (MatLab functions) that are designed to: (i) format and export processed data to CSV and Excel format, (ii) visualize data trough plots, (iii) arrange a visual report that summarize both the numerical and graphical results and (iv) do further processing on data, such as descriptive statistics.

The processing software was arranged in the form of a Graphical User Interface (GUI) (Figure 2.5.5) in order to speedup multiple trial loading, selection of the kind of trial and export of the processed results. The GUI is meant to be used by clinicians for routine strength measurements in order to achieve fast and reliable data processing as well as a fast export of results in the form of a clinical report (Figure 2.5.6).

3D data visualization was obtained by integrating into the GUI the Open Source code "Mokka" (Barre and Armand 2014) that allows an accurate viewing of 3D tracks and simultaneous visualization of analog data (Figure 2.5.7).

An issue that was encountered in data processing was the identification of the "trial start" and "trial end" events within the recording. In fact, in order to correctly process the force tracks, it was necessary to identify the starting time of the force profile (raising from zero), the ending time (approaching zero) and time at the peak value. Identification was made difficult by the noise superimposed to the analog tracks. As a first step, this issue was solved by asking the user to manually identify the events. The force profile and the distance between the HHD and the limb were shown on screen and the user had to click on starting point (force rising and distance approaching minimum) and ending point (force approaching zero and distance increasing).

This method was proved to work fine, but it significantly slowed data processing. In order to shorten data processing time and the need of user intervention, an algorithm for the automatic identification of events was developed. The algorithm requires: (i) noise filtering of force track, (ii) automatic removal of artifacts by means of thresholds, (iii) computing of the first order derivative of the force profile, (iv) identification of the rising and decreasing parts of force profile. This algorithm worked on most trials, but sometimes it failed. The most adverse conditions were observed for the tracks with low signal to noise ratio or tracks with strong artifacts on force profile, such as the accidental application of force on the sensible surface of the load cell before starting the measurement. For this reason, the possibility to manually identify events was kept in the final implementation of the GUI (Figure 2.5.5).
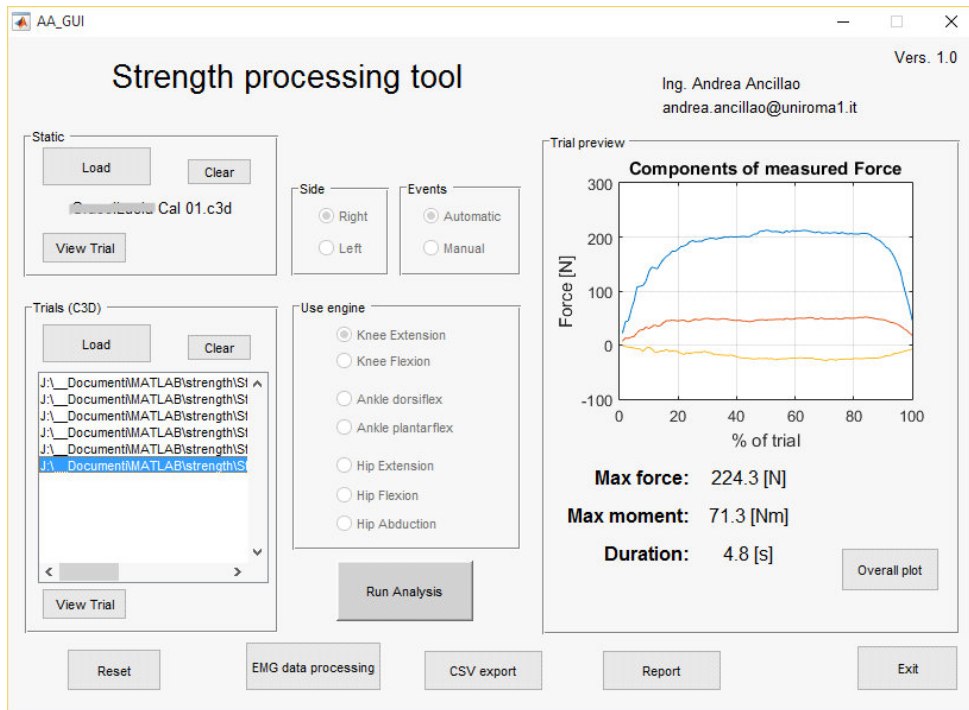
Figure 2.5.5: *GUI designed for strength data processing, export and visualization. Calibration (static) and six dynamic trials were processed and results were displayed.*
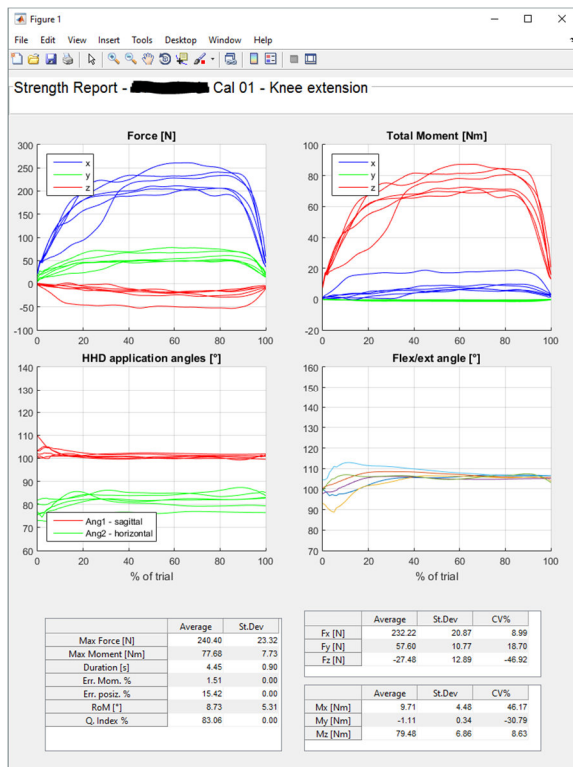
Figure 2.5.6: *Example of a Clinical Report. Results from repeated measurements are visualized as well as average and peak values of the parameters.*
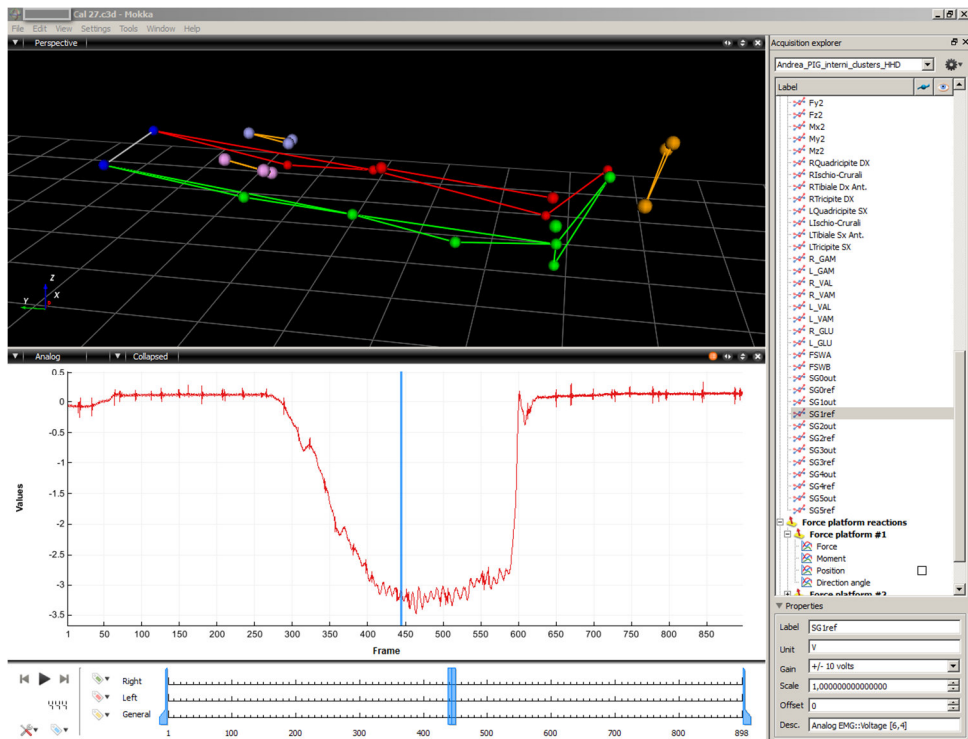
Figure 2.5.7: *3D visualization of an ankle plantarflexion strength trial. The RAW force profile is shown at the bottom.*

In order to visually explain the measurement setup in published papers, presentations, and also this book, several fine artworks were made. High quality three-dimensional representations of human characters were obtained by means of "Make Human" Open Source graphic software (http://www.makehuman.org/), in the form of high resolution meshes (.stl, .mhx, .dae formats).

Characters were posed, dressed and rendered by using "Blender" Open Source 3D CAD software (www.blender.org). Examples of character posing and scene creation for illustrating the knee strength measurements are shown in Figure 2.5.8.
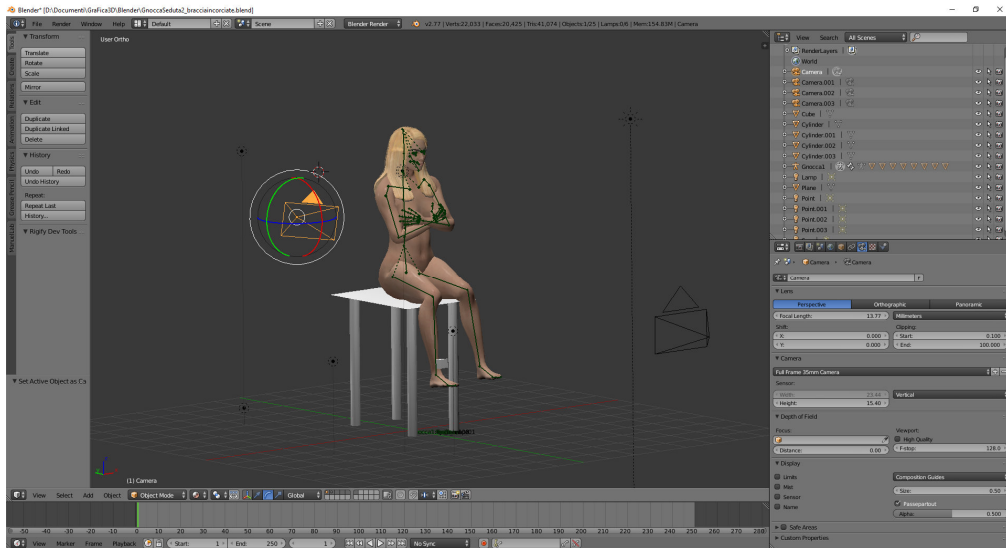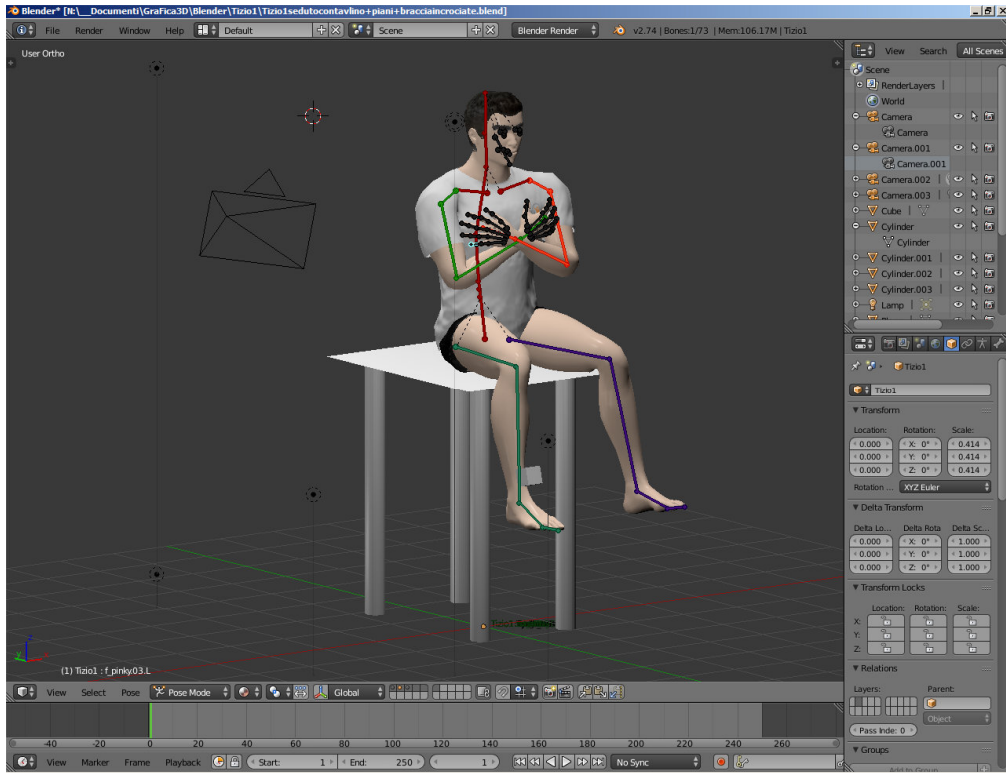
Figure 2.5.8: *Screenshots of Blender software illustrating the graphical design, workflow and rendering of human characters performing a knee strength measurement.*

2.6 – Results and discussion

Results are reported in Tables 2.6.1-2 as average and SD among the subjects included in the study; p values of t-test are also reported. The Shapiro-Wilk test showed that kinetic and kinematic indices had a normal distribution, therefore parametric statistics were applied.

Results of kinematic parameters are reported in Table 2.6.1. The observed RoM, i.e. the angular variation of the knee flexion/extension angle across the trial, was never close to 0° and was statistically higher for the extension movement than the extension one. Moreover, the standard deviation of RoM was higher for knee extension.

	Extension	**Flexion**	**t-test**
RoM [°]	21.7 (9.8)	15.5 (6.4)	0.005 *
δA_1 **[°]**	5.7 (3.4)	6.1 (3.8)	0.712
δA_2 **[°]**	9.3 (6.0)	15.1 (8.3)	0.014 *
CV_{RoM} **[%]**	23.2 (12.4)	23.5 (11.0)	0.919
$CV_{\delta A1}$ **[%]**	5.0 (3.7)	2.1 (1.2)	0.002 *
$CV_{\delta A2}$ **[%]**	4.8 (2.4)	3.3 (1.3)	0.013 *

Table 2.6.1: *KINEMATIC INDICES, mean (SD) values for the kinematic indices measured for the knee extension and flexion. * indicates a statistically significant difference between extension and flexion (p<0.05). The p values are reported in the t-test column.*

Positioning error δA_1 showed comparable values between knee flexion and extension. Instead, δA_2 assumed higher values for knee flexion. Values of δA_2 were always higher than δA_1 for both flexion and extension. As regards the coefficients of variation, no differences between flexion and extension were observed for the CV_{RoM}. It showed higher values than the coefficients of variation obtained for the positioning errors, i.e. $CV_{\delta A1}$ and $CV_{\delta A2}$. Both $CV_{\delta A1}$ and $CV_{\delta A2}$ were found statistically different between flexion and extension.

Results of kinetic indices are reported in Table 2.6.2.

Force and moment parameters $\hat{F}$, $\widehat{M}$, F_T, F_T, M_M and M_T, were found significantly higher for knee extension than the knee flexion. All RMSEs values were less than 5% (except for RMSE$_M$ of knee flexion that was slightly higher).

A statistical significant difference was observed for RMSE$_M$ of knee flexion that was higher than knee extension. RMSE$_F$ were lower than RMSE$_M$ and no significant differences were observed between the two rotations. Considering the coefficients of variation, $CV_{\hat{F}}$ and $CV_{\widehat{M}}$ were always lower than 10%. Both *CVs* were higher for knee extension, anyway no significant differences were observed. Average Q_{index} was relatively high for both extension and flexion. It was slightly lower for knee flexion. The difference was close to significance.

	Extension	Flexion	t-test
$\widehat{F}$ [N]	249.4 (27.3)	146.4 (23.9)	<< 0.001 *
$\widehat{M}$ [Nm]	88.4 (12.4)	49.9 (8.3)	<< 0.001 *
F_M [N]	242.5 (28.8)	145.1 (26.4)	<< 0.001 *
F_T [N]	63.0 (22.8)	37.5 (14.1)	<< 0.001 *
M_M [Nm]	87.8 (12.5)	48.7 (9.5)	<< 0.001 *
M_T [Nm]	14.6 (8.4)	9.4 (4.7)	0.018 *
RMSE$_F$ [%]	3.0 (2.6)	3.3 (1.7)	0.613
RMSE$_M$ [%]	4.0 (1.7)	5.2 (2.4)	0.035 *
$CV_{\widehat{F}}$ [%]	8.1 (6.0)	5.9 (3.2)	0.092
$CV_{\widehat{M}}$ [%]	8.2 (5.9)	5.8 (3.0)	0.068
Q_{index} [%]	82.8 (11.2)	75.3 (14.1)	0.069

Table 2.6.2: *KINETIC INDICES, mean (SD) values for the kinetic indices measured for the knee extension and flexion. RMSE values were evaluated between one-component and six-component measurements. * indicates a statistically significant difference between extension and flexion (p<0.05).*

Results of correlation analysis between the misplacement parameters (δA_1 and δA_2) and RoM, and the ones directly related to the inaccuracy of the strength measurement (RMSE$_F$, RMSE$_M$, F_T and M_T) are reported in Table 2.6.3.

No correlation was observed between RoM and the kinetic parameters for both extension and flexion. For the knee extension, a strong correlation was observed between δA_2 and F_T, M_T, RMSE$_F$ parameters. Correlation was strong also between δA_1 and F_T, RMSE$_F$ while it was moderate between δA_1 and M_T. Low correlations with RMSE$_M$ were observed for each misplacement parameters. As concerns the knee flexion, significant correlations were observed only for the δA_2. Specifically the correlation was strong with M_T while it was moderate with the other parameters.

		F_T	M_T	RMSE$_F$	RMSE$_M$
Knee Ext	RoM	-0.1	0.0	-0.1	0.1
	δA_1	0.8 **	0.5 *	0.7 **	0.1
	δA_2	0.7 **	0.8 **	0.9 **	0.3
Knee Flex	RoM	0.0	0.0	0.0	-0.1
	δA_1	0.2	0.0	0.3	-0.1
	δA_2	0.5 *	0.8 **	0.5 *	0.4 *

Table 2.6.3: *CORRELATION COEFFICIENTS, Pearson correlation coefficients (r) between kinematic indices and kinetic indices for knee extension and knee flexion. * indicates a moderate correlation (0.4≤|r|≤0.6), ** a strong correlation (0.7≤|r|≤0.9).*

Dependency of the strength measurements on the operator's ability

In order to test the operator dependant inaccuracies, when performing a strength measurement as a "make test" method, we measured the knee RoM that should be ideally close to 0°, as the subject's limb should remain still across the trial.

Analyzing the RoMs and the coefficient of variation CV_{RoM}, values higher than 0° were measured for both extension and flexion. Moreover, knee RoM was statistically higher for extension trials, in which the force exerted was higher, than flexion ones (Table 2.6.2), indicating that the operator was not able to completely counteract the participant's force and therefore he was not able to hold the limb completely still with poor repeatability across the trials.

Considering the errors in the HHD placement, positioning error δA_1 showed comparable values between knee flexion and extension, implying the same difficulty level for the operator in correctly positioning the HHD on the sagittal plane during the two types of trial. The index variability was relatively low, indicating a good repeatability in the angular positioning of HHD on the sagittal plane. δA_2 was found higher than δA_1 and was statistically higher for knee flexion, indicating that the most relevant source of inaccuracy was the HHD misplacement on the horizontal plane especially in the case of knee flexion. This may be due to the uncomfortable position that the operator had to assume to hold the HHD behind subject's ankle in knee flexion trials. It follows that the operator has to pay a special attention to avoid the rotation of the HHD on the horizontal plane.

Considering the coefficients of variation CV of the outputs of the strength measurements ($CV_{\hat{F}}$ and $CV_{\hat{M}}$) a low level of variability was observed (≤ 5 %) showing a good intra-subject repeatability of measurements for both knee flexion and knee extension trials, in agreement with the literature outcomes (Kim et al. 2014; Martin et al. 2006; Phillips et al. 2000). Moreover, $CV_{\hat{F}}$ and $CV_{\hat{M}}$ of knee flexion were lower than knee extension, indicating that knee extension trials had more inherent critical issues with respect to knee flexion ones. This finding can be interpreted by observing that the force $\hat{F}$ and the moment $\hat{M}$ values exerted by the subjects involved in the present study were higher during the extension trial than the flexion one implying a greater difficulty for the operator to maintain still the participant's limb. This finding is in agreement with the results of (Laing et al. 1995) that showed higher quality of the trials achieved by fixing the HHD in contrast to HHD freely held by the operator.

In conclusion, even though the operator was not able to keep the limb of the subject perfectly still and the HHD actual orientation was different with the desired one, the measurement outputs were reliable and accurate enough for both knee flexion and extension.

Comparison between 6-component and 1-component HHD

The inaccuracy associated to uniaxial HHD in comparison with the values collected via a 6-component HHD could be quantified by F_T, M_T, RMSE$_F$ and RMSE$_M$. The first two indices represented the lateral components of the force and moment that are commonly neglected when a uniaxial HHD is used. RMSE$_F$ and RMSE$_M$, instead, allowed us to quantify the accuracy of strength and knee moment measurements performed with the uniaxial HHD in the clinical routine comparing them with the actual ones obtained by a 6-component HHD and the OS.

Focusing on F_T and M_T values, the highest values were obtained during the extension trials confirming the above reported findings on the higher complexity of extension trials. RMSE$_F$ and RMSE$_M$ were relatively low, always ≤ 5.2 %, for both knee flexion and knee extension. We can therefore speculate that the uniaxial HHD is reliable and accurate enough for use in clinical contexts, according to the dataset acquired in the present study.

In order to synthetically describe the quality of a strength measurement, according to the previously discussed parameters, we computed a synthetic quality index Q_{index}. The average of Q_{index} value was high for both knee extension and knee flexion, without statistical difference. This finding supported the conclusions that the inaccuracies due to both the positioning of the HHD and the lateral force and moment components can be considered negligible. The Q_{index} is also useful for application "on the field", as it provides an overall quantification of the quality of a single trial and may help the clinician to identify trials to be discarded.

Correlation between operator's ability and strength measurement accuracy

Correlation between kinematic an kinetic parameters was analyzed to investigate the influence of the HHD misplacement and the accuracy of the uniaxial HHD in the strength measurements.

For the knee extension, a strong correlation was found between the misplacement indices δA_2, δA_1 and F_T, M_T, RMSE$_F$ while the correlation was low with RMSE$_M$. It can be stated that the angular misplacements had effect on the lateral undesired components of force and moment, while the error on the actual moment was not affected by an incorrect orientation of HHD. The misplacements affected influenced in a greater extent the force measurement than the moment one. The RoM had no influence on the lateral components of force/moment or effect on the RMSEs. This means that the range of motion, if it is maintained within the values observed in this work, does not affect the measurements in terms of lost information due to lateral components, which are not measured by commercial HHDs in clinical practice.

Concerning knee flexion trials, that are characterized by a lower exerted force, correlations were observed only between δA_2 and all the parameters. Specifically, the correlation was strong only versus M_T, while it was moderate towards the other parameters. The strong correlation between δA_2 and M_T, observed also for the extension trial, demonstrated that the main misplacement of the HHD is on the horizontal plane and an increase of δA_2 could drastically affect the quality of strength measurements performed with an uniaxial HHD. In fact, it had effect mainly on the lateral components of moment and it is therefore a critical positioning parameter to pay attention while gathering data. Conversely, the absence of correlation for δA_1 and RoM may be connected to the lower forces and moments exerted in the case of knee flexion. As in the knee extension, the RoM of knee flexion does not affect the lateral components of force and moment if it is maintained within the values found in the present study. The HHD misplacement quantified via the δA_2 index appears to be the main critical parameter for the quality assessment of a strength measurement.

2.7 – Conclusion

The aim of this project was to study the quality of the knee strength measurements by measuring the effects of sources of inaccuracies occurring when using a single component HHD.

The validation methodology was based on the concurrent use of a six-component HHD and an optoelectronic system. More precisely we analysed the effects induced on the strength measurement by: (i) the therapist ability both in positioning the HHD and in keeping it still in place and (ii) the current use of a single component HHD which does not collect both moments and transversal components of force. Moreover, we studied the inaccuracy causes in the strength measurements analysing their dependence with the kinematic parameters of HHD misplacement.

Healthy adult subjects were enrolled in the study because they represent the most aversive case for the operator due to the relatively high force they can exert.

This study showed that the limb of subjects did not remain perfectly still during knee strength measurements and it represents a not-negligible source of inaccuracy. From our measurements, we concluded that the use of uniaxial

HHDs can be assumed as reliable and accurate enough for both knee flexion and extension, if lower limb displacements and HHD misplacement are kept within the values found in the present study (see Table 2.6.1). The more critical measurements are in the knee extension, where the most affecting index was the HHD angular incorrect positioning on the horizontal plane.

According to the data collected for this study, the use of an uniaxial HHD for the strength measurement, in place of a six-component one, can be considered a reliable method when a maximum value of inaccuracy equal to 6% is considered acceptable.

The results here discussed may lead to a better understanding of HHD measurements and provide directions to the clinicians for the proper use of the instrument.

Further steps may involve analysis of inaccuracies associated to different anatomical districts and the quality analysis of strength measurements conducted on patients with pathology.

The main limitations of this study were: the absence of a gold-standard reference, such as the Isokinetic Dynamometer, to compare the values of force measured by HHD, and the absence of an inter-operator repeatability study. Further study may therefore involve the analysis of inter-operator repeatability by comparing the kinematic and kinetic parameters obtained by different expert operators. Moreover, this study was conducted on healthy adult subjects but other positioning difficulties and inaccuracies may occur in case of pediatric and pathologic subjects.

Part 3:

Gait Analysis Data Interpretation by means of Synthetic Descriptors

This section contains the description and the results of the research work about gait analysis data interpretation and pattern recognition on subjects with pathology. This study followed a previous research about gait analysis data storage, representation and indexing, conducted within the MD-Paedigree Project. Gait analysis exam is described within Part 1, chapter 1.5.

The most common synthetic indices were reviewed in this section. In this work, modern indices were implemented as numerical code and applied to gait analysis of subjects with Cerebral Palsy in order to study gait variation pre and post treatment. A novel index was designed, tested and applied to those subjects as well. The results provided a detailed biomechanical analysis of the effects of surgical treatment on the walking pattern and the effectiveness of the indices in quantifying gait deviation.

This project was sponsored by the "MD-Paedigree" European Project – Work Packages 13, 15 and 16, regarding gait analysis data processing, sematic representation and indexing.

This project was conducted in partnership with Department of Rehabilitation Medicine, MOVE Research Institute, VU University Medical Center, Amsterdam, NL.

3.1 – Introduction

Gait Analysis (GA) is a multifactorial and powerful tool that provides a quantitative description of normal and pathological gait patterns. It is therefore widely adopted as a routine exam in clinical centres (Carriero et al. 2009; Whittle 1996). As examples, GA was used to study and characterize: Parkinson's disease (PD) (Sale et al. 2013), Down Syndrome (Galli et al. 2008), Ehlers-Danlos syndrome (EDS-HT) (Rigoldi et al. 2012), Cerebral Palsy (CP) (Carriero et al. 2009; van den Noort et al. 2013) and it was applied to validate the effects of novel treatments in subjects with neurological disorders (Camerota et al. 2015; Sale et al. 2013; Vismara et al. 2016).

Clinical decisions, rehabilitative treatments and follow-up are often based on the results of GA exams (Assi et al. 2009; Whittle 1996), especially in the case of CP and spastic paresis that may result in serious motor disorder at different levels. Very different gait patterns were observed in these patients (Galli et al. 2010; Piccinini et al. 2011).

Focusing on population affected by CP, the resulting walking pattern strongly depends on which muscles or joints are involved, and therefore each condition needs a specific clinical study and treatment. Some examples are: the equinus gait pattern, that involves alteration of ankle joint functionality (van der Krogt et al. 2009); crouch gait, that involves abnormal knee flexion (van den Noort et al. 2013); and pelvis abnormal anti-retroversion with overall range of motion limitation due to spasticity (van den Noort et al. 2013).

GA is often used to validate the outcome of surgical treatments of CP and to monitor improvements in the gait pattern overt time (Galli et al. 2009). Moreover, children with CP showed different kinetic gait pattern if walking barefoot on the ground or on a treadmill (van der Krogt et al. 2015).

GA exams consist in the integration of data from different sources, i.e. kinematic data, kinetic data, video recording, EMG, etc. Thus, a single GA exam contains a large volume of data, that is composed of highly informative parameters, such as velocity, cadence, anatomical angles, peak flexion, forces, moments, etc., involving different joints and positions. All these parameters are usually presented in the form of a clinical report, i.e. a collection of tracks and numerical parameters (Stebbins et al. 2014; Whittle 1996), that are necessary to characterize specific gait strategies and to evaluate specific functional issues. On the other side, as the clinical report contains many different parameters, it is sometimes difficult to read and requires a specific training of

the clinicians. Thus, the clinical need of a quantitative evaluation and classification of the overall gait emerges.

Following this aim, many research studies focused on the validation of synthetic descriptors that could classify and quantify the severity of a pathological gait pattern, by testing if an observed pattern falls into a normality range. Such synthetic numbers may be used for follow up evaluation of the natural evolution of the gait pattern over time (Galli et al. 2012).

Gillette Gait Index (GGI)

A frequently used and well known index is the Gillette Gait Index (GGI), known also as Normalcy Index (Romei et al. 2004; Schutte et al. 2000). The GGI uses the principal component analysis on a set of 16 independent kinematic variables, providing a global evaluation of patient's gait. It was demonstrated efficient in categorizing pathologies and clinically applicable and repeatable (Assi et al. 2009), especially if applied to subjects with CP (Galli et al. 2012; Romei et al. 2004).

Hip Flexor Index (HFI)

The Hip Flexor Index (HFI) (Schwartz, Novacheck, and Trost 2000) has its focus on the hip functionality during gait. It uses principal component analysis applied to five kinematic and kinetic variables collected in a standard GA exam. A single number describing functionality of the hip is then derived. The HFI was demonstrated able to describe post-operative changes in hip functionality and it showed a good correspondence with subjective clinical observation (Schwartz et al. 2000).

Gait Deviation Index (GDI)

Recently, an overall, multivariate and comprehensive index, named Gait Deviation Index (GDI), was proposed as an alternative to the GGI (Schwartz and Rozumalski 2008). The GDI, is computed by using nine kinematic variables (pelvic and hip angles on the three planes, knee flex/extension, ankle dorsi/plantarflexion and foot progression) and comparing them to control data. GDI is a dimensionless parameter. If it is close to 100, it indicates the absence of gait pathology; each 10-point decrement below 100 indicates 1 standard deviation (SD) from normal kinematics (e.g. a GDI of 65 is 3.5 SD away from normal) (Schwartz and Rozumalski 2008). For this reason it is useful for a general measure of gait pathology (Baker et al. 2009; Galli et al. 2012).

In the literature, the GDI index was applied in participants with PD in order to classify gait patterns pre and post a levodopa treatment (Galli et al. 2012). The

conclusion was that the GDI was able to evaluate the effects of the treatment and to quantify a global gait improvement after the treatment. Similar results were observed by (Esbjörnsson et al. 2014) that computed GDI on subjects with rheumatoid arthritis, observing a GDI = 87.9 ± 8.7 significantly different from control. Therefore the GDI was assumed able to quantify the gait deviation from normality and could be assumed as an overall measure of GA (Esbjörnsson et al. 2014).

The GDI was applied to children with CP by Molloy at al. (Molloy et al. 2010), that validated this index for the classification of CP gait patterns and identified increasing levels of gait deviation in subjects with more severe pathology, concluding that the GDI captures both the functional and aesthetic components of walking.

Repeatability of GDI applied to CP was studied by (Massaad et al. 2014) by means of Monte Carlo simulations and test-retest study. They concluded that GDI correctly described the gait profile with an uncertainty of ±10. Observed errors could be linked to the errors that commonly occurred in GA exams, such as marker misplacement, noise, walking variability, etc. and the GDI could be considered robust, poorly sensitive to noise and able to discriminate between subjects with pathology and control. Anyway Massaad et al. (Massaad et al. 2014) pointed out that GDI could not be used to classify children with CP, since to different observed abnormalities corresponded similar GDI values, but it could anyway give information about the severity of impairments once the pathology was classified. In other words, GDI is useful to evaluate intervention outcomes and follow-up but it cannot give information about the location of the impairment or the nature of changes (Massaad et al. 2014).

A further work on CP was conducted by Cimolin et al. (Cimolin et al. 2011) that computed the GDI in pre- and post-surgery conditions. In this case, the GDI allowed the quantification of gait changes and improvement occurring in subjects with CP after gastrocnemius fascia lengthening. The results showed that before surgery the observed GDI was 70.4 ± 14.8 that changed to 82.9 ± 7.4 after surgery, indicating an improvement towards control group i.e. 100. The conclusion of this study was that GDI was an useful measure for the evaluation of effects of surgical treatments.

On the other side, Rose et al. (Rose et al. 2010) applied GDI on untreated CP patients over time, in order to study the natural evolution of gait pattern. They observed no significant change in gait deviation index over time, that demonstrated a lack of accuracy of the GDI in the detection of small changes due to natural evolution of patients.

The main limitation of GDI is that, even if it is useful to assess the overall gait pattern, it cannot provide information about the location of the impairment (Massaad et al. 2014).

Movement Analysis profile (MAP) and Gait Profile Score (GPS)

The limitations of the GDI were partially overcome by a newer method, the Movement Analysis Profile (MAP) (Baker et al. 2009).

MAP requires the computation of a deviation index, named Gait Variable Score (GVS), for each of nine relevant kinematic variables (Figure 3.1.1). The GVSs, quantify the deviation from normality for each gait feature and they can be averaged into an overall index, namely the Gait Profile Score (GPS).

GPS was shown to be strongly correlated to GDI and it is a good synthetic measurement of the overall deviation of kinematic parameters from a normative set of data (Baker et al. 2009).
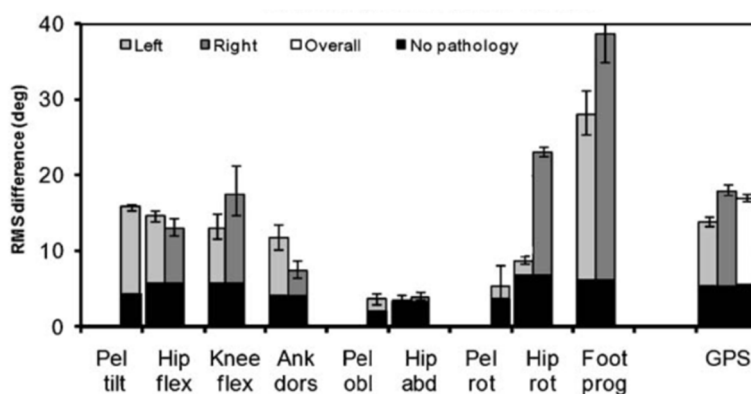
Figure 3.1.1: *Example of a Movement Analysis Profile (Baker et al. 2009). Each column corresponds to a kinematic variable. Its height represents the RMS average difference across time between a specific gait cycle and the average gait cycle from people with no gait pathology. The black area at the foot of the columns represents the average value for people with no gait pathology. The GPS for left side, right side and overall gait pattern are displayed in the rightmost column.*

As GDI, the GPS was used for the characterization of gait in children with CP and other neurological-orthopaedic disorders, showing also good correlation with other qualitative ratings of kinematic gait deviation (Beynon et al. 2010).

GPS was applied to the classification of gait pattern in subject with Ehlers-Danlos Syndrome (Celletti et al. 2013), obtaining an average value of 8.9° ± 2.6°, that was statistically different from the GPS of the control group i.e. 4.6 ± 0.9, concluding that the GPS and the GVS are appropriate for the evaluation of functional gait limitation in patients with such kind of impairments.

Gait analysis of children with CP was studied by means of GPS by Rutz et al. (Rutz et al. 2013). They found a pre-operative GPS of 15.5°±3.9° that reduced to 11.2°±2.5° post orthopaedic intervention, concluding that the degree of improvement was higher in the patients with the worst initial conditions.

Even if the MAP is able to localize the anatomical joint or segment whose pattern deviates from normality, it fails to identify the cause of the deviation, e.g. the offset between curves, the scaling factor or a time-shift.

Linear Fit Method (LFM)

A different approach to compare gait features to reference data was proposed by Iosa et al. (Iosa et al. 2014). The method allows to assess similarity between the observed waveform and reference GA tracks, in terms of shape, amplitude and offset. It consists of the application of a linear fit method (LFM) to two time-normalized datasets.

The result of the LFM are: (i) the R^2 regression coefficient, that quantifies the strength of relationship between the tracks; (ii) the $a0$ coefficient, i.e. the constant term of polynomial regression that represents the scalar addition (shift) between the compared datasets; (iii) the $a1$ coefficient, i.e. the first coefficient of first order polynomial regression that represents the amplitude scaling factor. When this method is used to compare a GA exam to a GA control group, the R^2, $a0$, and $a1$, values can be considered synthetic indices of deviance from normality, anyway the $a0$ and $a1$ lose significance if R^2 is lower than 0.5 (Iosa et al. 2014).

The LFM method was tested on kinematic GA data of patients with cerebrovascular accident, concluding that it is a simple method to implement and, since it takes into account all the data point of GA tracks, it is appropriate and reliable to discriminate between subjects with pathology and healthy subjects, with good sensitivity and specificity (Iosa et al. 2014).

To the author's best knowledge, the LFM method was never used to assess gait after surgery in subjects with CP.
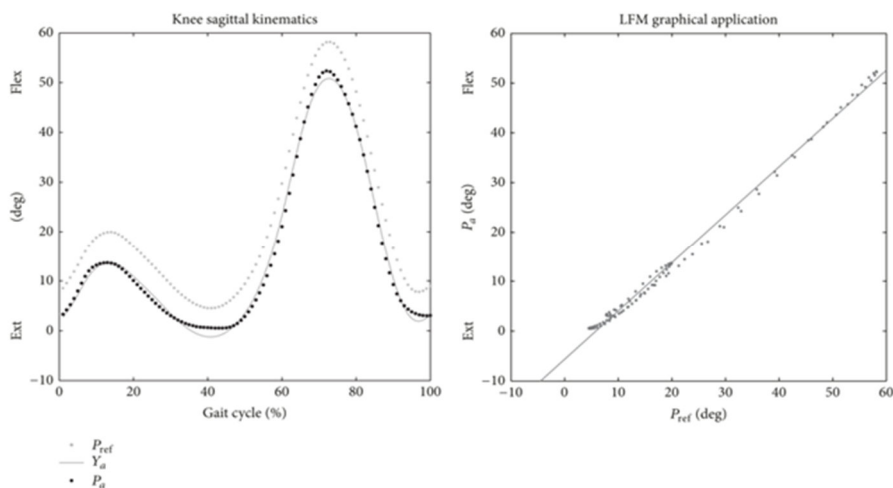
Figure 3.1.2: *Adapted from* (Iosa et al. 2014). *Two exemplificative knee sagittal kinematic datasets were compared in order to graphically illustrate the LFM. On the left are the points for the investigated dataset P_a (black dots) and for the reference dataset P_{ref} (grey dots). The grey line represents the reconstructed curve Y_a obtained by the parameters of the linear fit applied to the values of P_a when plotted versus P_{ref} (right plot).*

3.2 – Aim of the research

Children with CP are often treated by means of orthopaedic surgery to the lower limbs in order to improve their gait and, by consequence, their quality of life (Thomason et al. 2011). Orthopaedic surgery to the lower limbs usually involves muscle/tendon lengthening or transfer, bone resizing, bone rotation and reposition, as needed to improve the walking strategy (Delp et al. 1996; Thomason et al. 2011). Tight hamstrings, due to muscle spasticity or static contracture, are reputed to be the main cause of crouch gait, therefore persistent crouch is often treated by surgical lengthening of the hamstrings (Delp et al. 1996).

This kind of surgery, involving lengthening of the hamstrings, bone reposition and other orthopaedic corrections, takes the name of Single Event Multi Level Surgery (SEMLS) and often results in visible changes in the gait pattern.

The aim of this project was to study the changes in gait pattern occurring in children with CP that underwent SEMLS. The analysis was conducted by means of a quantitative method, i.e. the Gait Analysis, and by using synthetic descriptors in order to:

- reduce kinematic gait features to a set of synthetic parameters;
- quantify the deviation from normality;
- identify the affected anatomical districts;
- <u>simplify clinical interpretation of gait analysis.</u>

The MAP was applied to gait analysis exams pre and post intervention in order to identify and classify gait changes. In addition to the MAP, the LFM method was also applied to gait tracks in order to: (i) test the LFM on gait tracks of subjects with pathology; (ii) compare LFM results to MAP results; (iii) use the additional information provided by the LFM to identify the cause of change in the gait pattern.

From the preliminary analysis it emerged that for some gait features the abnormality was due to a pure offset between the observed track and the reference track. Therefore, we decided to design a modified version of the MAP, namely the OC-MAP, that separated the pure offset component from the gait deviation due to different curve shape.

Outcomes of the three different methods were compared.

3.3 – Description of the methods

Subjects

Ten children diagnosed with bilateral CP, age 10.9±2.3 years, 7 males, 3 females were enrolled in this study. All the subjects were patients followed by the Department of Rehabilitation Medicine of VUmc, Amsterdam, NL. All the subjects showed bilateral gait disorders and crouch gait (Figure 3.3.1). They were evaluated by means of Gross Motor Function Classification System (Palisano et al. 2008; Rosenbaum et al. 2008), at the time of admission, obtaining rankings from 2 to 3.

The subjects had no prior orthopaedic surgery and had no prior botulinum toxin treatment within the previous 16 weeks. All the subject underwent Single Event Multilevel Surgery (SEMLS), that consisted in bilateral hamstrings release (Figure 3.3.2) and orthopaedic surgery at the level of the femur associated to bone rotation and repositioning in some cases.

The subjects with CP were evaluated by Gait Analysis (GA) before treatment (pre) and one year after treatment (post).

Eleven typically developing children (TD), age 8.2±1.8 years, were included as a reference.

This study complied with the principles of the Declaration of Helsinki. All the subjects provided informed consent.
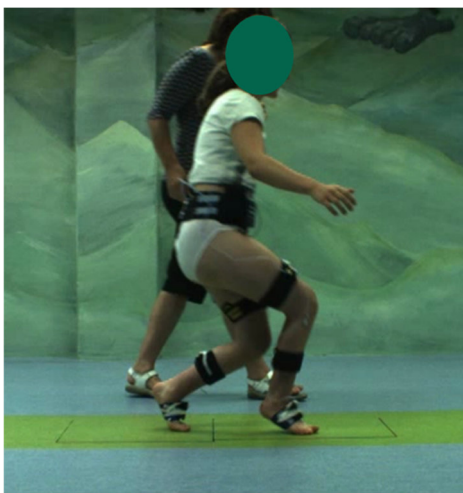
Figure 3.3.1: *Gait Analysis of a patient walking with persistent knee flexion (crouch gait).*

Figure 3.3.2: *The hamstring muscular groups.*

Equipment and procedures

GA data of both groups were collected in the Motion Analysis Laboratory (Figure 3.3.3) of the VU University Medical Center, dept. of Rehabilitation Medicine, Amsterdam, NL.

Kinematic data were collected by means of an Optotrak Optoelectronic System (Northern Digital, Waterloo, Ontario) composed of 3 racks, each one holding 3 cameras. Sampling frequency was 100 Hz. Marker protocol used was the CAST model (Cappozzo et al. 1995).

The protocol required a calibration trial to identify anatomical landmarks. Afterwards, the subjects were asked to complete some practice trials on the walkway to ensure they were comfortable with the experimental procedure. Then, a minimum of 5 walking trials were recorded for each subject. In each trial, subjects were asked to walk barefoot, at a self-selected speed, on the lab's walkway.

System calibration was performed before each acquisition session, according to manufacturer's instruction. The overall RMS error of marker reconstruction was ~1 mm.

Figure 3.3.3: *Motion Analysis Laboratory, VUmc, Amsterdam, NL.*

Data Processing

The laboratory-based data were processed by means of BodyMech (http://www.BodyMech.nl), a custom-made software based on MATLAB (The MathWorks, USA) in order to obtain joint angles and spatio-temporal parameters by solving the CAST model (Cappozzo et al. 1995). The results of each subject were then averaged across the 5 repetitions. From the GA datasets of each subject, 9 bilateral gait features were selected, as required to compute MAP (Baker et al. 2009). These included: pelvic tilt, obliquity and rotation; hip flexion, abduction and rotation; knee flexion; ankle dorsiflexion and foot progression angles (Figure 3.3.4).

Movement Analysis Profile

The computation of the GVSs for the nine gait features composing the MAP, was implemented as indicated by Baker et al. (Baker et al. 2009). The normality dataset obtained from the ND group was used as reference. A visual explanation about how a GVS is computed is shown in Figure 3.3.5.

More in details, a GVS is the RMS difference between a normalized *i*-th gait variable and the respective reference data (eq. 1):

$$GVS_i = \sqrt{\frac{\sum_{t=1}^{T}(x_{i,t} - \bar{x}_{ref,i,t})^2}{T}} \tag{1}$$

Where $x_{i,t}$ is the value of the i-th gait feature at the point t of gait cycle, T is the number of points in which the gait cycle has been divided and $\bar{x}_{ref,i,t}$ is the average value for reference population.

The GPS is then computed as RMS average of GVSs:

$$GPS = \sqrt{\frac{\sum_{i=1}^{N}(GVS_i)^2}{N}} \tag{2}$$

The GPS represents the overall deviation of patient's data from the reference dataset. Therefore, the higher the GPS value, the less physiological the gait pattern is.

GVS and GPS indices were computed for both left and right side of each subject. Statistical test showed no differences between left and right sides, therefore data were pooled in order to obtain one value for pre-surgery and one value post-surgery for each parameter. The pelvic parameters were not pooled to avoid doubling the data. In these cases only the right side was used. The average deviations from normality and their SDs were represented as bar plots (MAP). The final MAP contained 9 groups of bars representing the examined gait features, pre and post intervention, plus 1 group of bars representing the overall GPS, pre and post intervention.
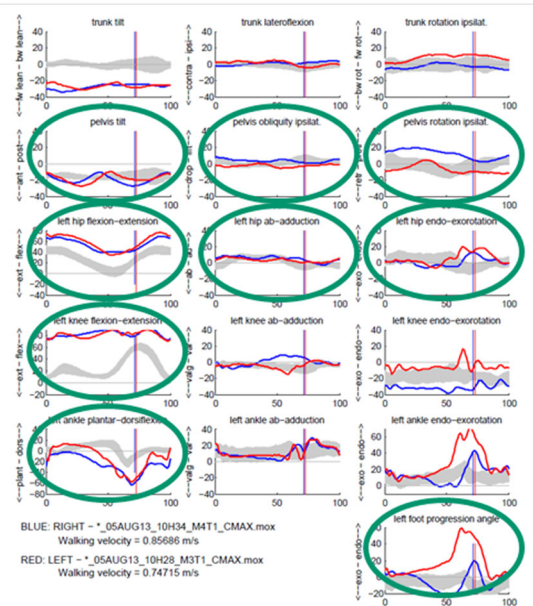
Figure 3.3.4: *Example of a gait report. The 9 gait features required for MAP computation are highlighted.*
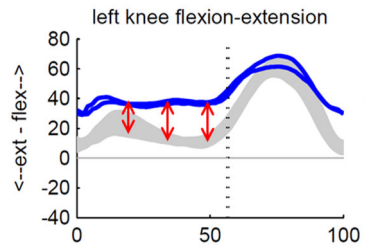
Figure 3.3.5: *Computing of a Gait Variable Score as point by point difference between observed track(s) and reference track(s).*

97

Offset Corrected Movement Analysis Profile

To take into account the effect of offset on kinematic gait features, we re-computed GVSs after removing the offset from waveforms. New indices were named OC-GVS, OC-MAP and OC-GPS.

Offset was defined as the distance between the average values of the gait features expressed as percentage of the gait cycle.

Offset for the i-th gait feature, x_i , was defined as:

$$offset_i = \bar{x}_i - \bar{x}_{ref,i} \tag{3}$$

Where $\bar{x}_i$ represented the average value of the i-th gait feature.

Equations 1 and 2 were re-implemented as:

$$\text{OC-GVS}_{\,i} = \sqrt{\frac{\sum_{t=1}^{T}(x_{i,t} - offset_i - \bar{x}_{ref,i,t})^2}{T}} \tag{4}$$

$$\text{OC-GPS} = \sqrt{\frac{\sum_{i=1}^{N}(\text{OC-GVS}_i)^2}{N}} \tag{5}$$

As in the MAP, the OC-GVSs and the OC-GPS were represented as bar plot, named OC-MAP. Also the offsets of gait features were represented as a bar plot, containing 10 groups of bars representing the examined gait features, pre and post intervention and the overall RMS of offset.

Linear Fit Method

The LFM method was implemented as described in Iosa et al. (Iosa et al. 2014). Coefficients were obtained according to the following equations:

$$a_1 = \frac{\sum_{t=1}^{N}(x_{ref,t} - \bar{x}_{ref}) \cdot (x_t - \bar{x})}{\sum_{t=1}^{N}(x_t - \bar{x}_{ref})^2} \tag{6}$$

$$a_0 = \bar{x} - a_1 \cdot \bar{x}_{ref} \tag{7}$$

$$R^2 = \frac{\sum_{t=1}^{N}(a_0 + a_1 \cdot x_t - \bar{x}_{ref})^2}{\sum_{t=1}^{N}(x_t - \bar{x}_{ref})^2} \tag{8}$$

Where x_t is the value at the point t of gait vector, N is the number of data points in the gait vector.

R^2 measures the strength of linear relationship between x and x_{ref}; *a1* represents the amplitude scaling factor; *a0* represents the scalar addition

(shift). In case of maximum similarity in waveforms, the parameters assume the following reference values:$R^2 = 1$; $a1 = 1$; $a0 = 0$.

LFM was computed as "overall" value on all the 9 gait features pooled in a single gait vector and compared to a normality gait vector built the same way (as in GDI). Then the LFM analysis was conducted for each of the 9 gait features.

Statistics

Descriptive statistics analysis was conducted on data from the three methods. The data groups were preliminary tested for normality by means of the Shapiro-Wilk test, with an alpha level of 0.05. As data were found to be normally distributed, the paired t-test was used. As preliminary analysis, data were tested for differences between left and right legs. Since no statistically significant differences were found, data from both sides were pooled into a single column, for each parameter. Then, data were tested to assess differences between means pre-post intervention for the all the parameters. A significance level of p<0.05 was assumed.

The variations in gait features were quantified by computing pre-post differences for each GVS and OC-GVS. The differences were then compared to the GPS Minimally Clinical Important Difference (MCID) (Baker et al. 2012), i.e. 1.6°. The average among subject for the variation of each GVS was computed.

Regression plots of the pre-post difference vs. GVS pre intervention were computed , as suggested by Rutz et al. (Rutz et al. 2013), in order to represent the improvement level associated to a certain GVS score.

A correlation analysis was also conducted between the respective MAP, OC-MAP, Offset and LFM parameters to study relation between the different indices. To compute correlation, data from pre and post analyses were pooled. The results were presented in the form of a correlation table. The following categorization for the Pearson coefficient R was considered, as suggested in literature (Dancey and Reidy 2004): |R|=1: perfect; 0.7≤|R|≤0.9: strong; 0.4≤|R|≤0.6: moderate; 0.1≤|R|≤0.3: weak; |R|=0: zero.

Statistical analysis was conducted by means of MS Excel software.

Software implementation

Basic gait analysis tracks, i.e. joint angle kinematics, were computed on RAW data by means of BodyMech (http://www.BodyMech.nl), a custom-made software based on MatLab. The basic gait features and parameters computed by BodyMech were exported to a MatLab structure. The name of the patient

was not saved within the data structure, obtaining anonymous data files that could be exported to external database, in accordance with MD-Paedigree requirements.

Anonymous data files, containing basic gait features stored within MatLab structures, were further processed in order to compute synthetic descriptors and statistical analysis. The workflow for processing gait data was implemented entirely in MatLab (The MathWorks, USA).

Software was developed according to a <u>modular criterion</u>. The "main" script accepts a list of files to access and process. Each data structure is passed sequentially trough external scripts, designed to compute the indices required for this study (MAP, OC-MAP, LFM, GPS, ecc.).

After computing the requested parameters, data are passed to other scripts for graphical visualization, export to CSV/excel spreadsheets and statistical analysis.

The modular development allowed a fast debugging of the code, fast implementation and the possibility to expand the software in the future.

A graphical user interface (GUI) was developed for the main script (Figure 3.3.6). The GUI design was aimed to speed up the process of trial selection (loading), data visualization, quick batch processing and preview for fast trial identification, generation of detailed plots, data export and last and foremost: make data processing easier and faster for the clinicians who need to quickly process a large amount of data.
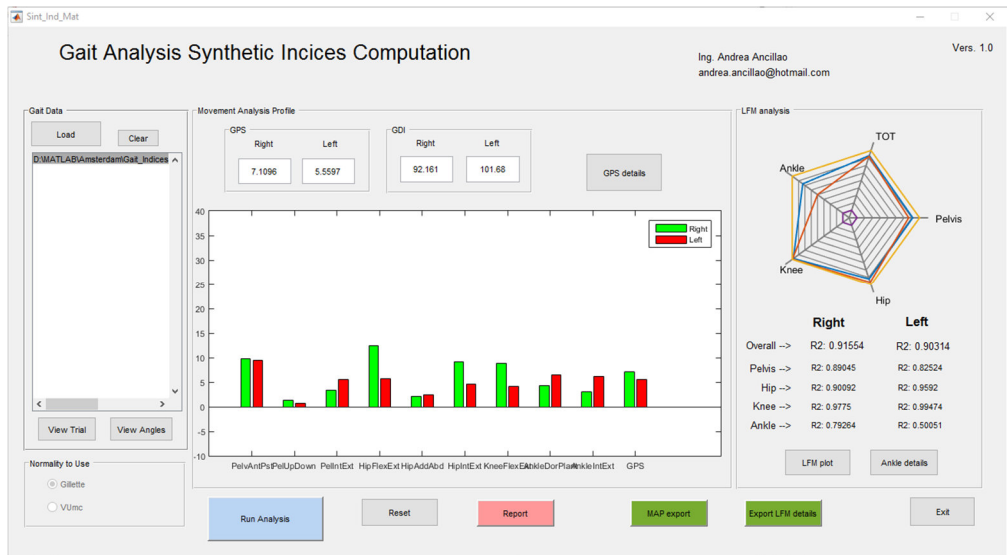
Figure 3.3.6: *Screenshot of the GUI designed for gait analysis data processing, export and visualization. In this example, data from a control subject is being processed.*

An example of gait analysis data visualization, including both kinematics and kinetics, is shown in Figure 3.3.7.

Figures 3.3.8 and 3.3.9 depict examples of graphs generated by the GUI for the selected trial. In these examples, data from a control subject is being processed. The results of LFM computing are shown in Figure 3.3.10. Such detailed view allows to determine the correctness and reliability of the linear fitting for each anatomical district, as well as the similarity between the observed gait feature and the reference track.
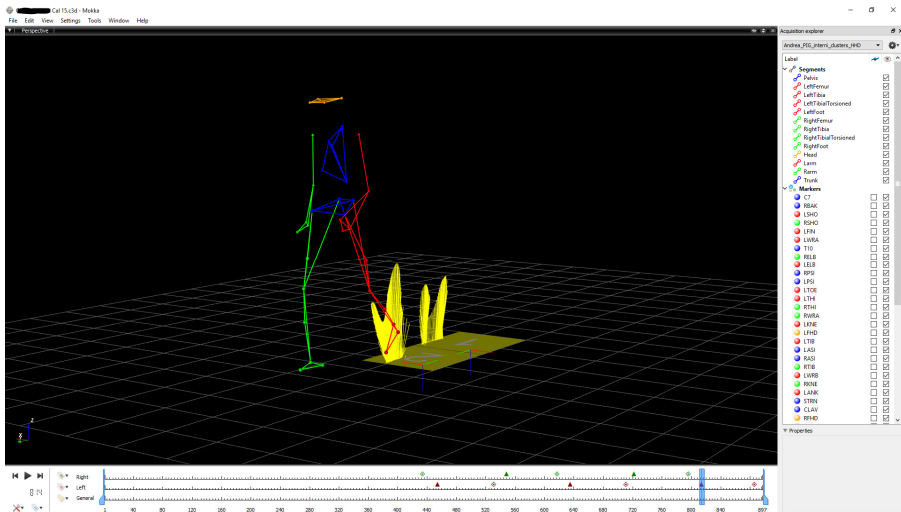
Figure 3.3.7: *Gait analysis data visualization by using the developed GUI.*
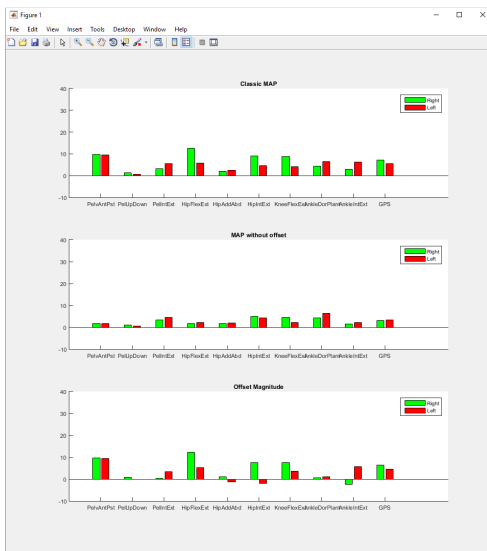
Figure 3.3.8: *Detailed graphs of MAP and OC-MAP generated by the GUI for the selected trial (control subject).*
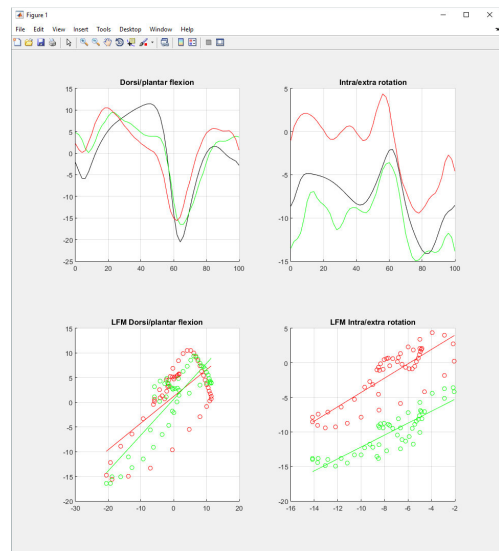
Figure 3.3.9: *Visualization of left (red) and right (green) ankle kinematics and the computing of LFM.*
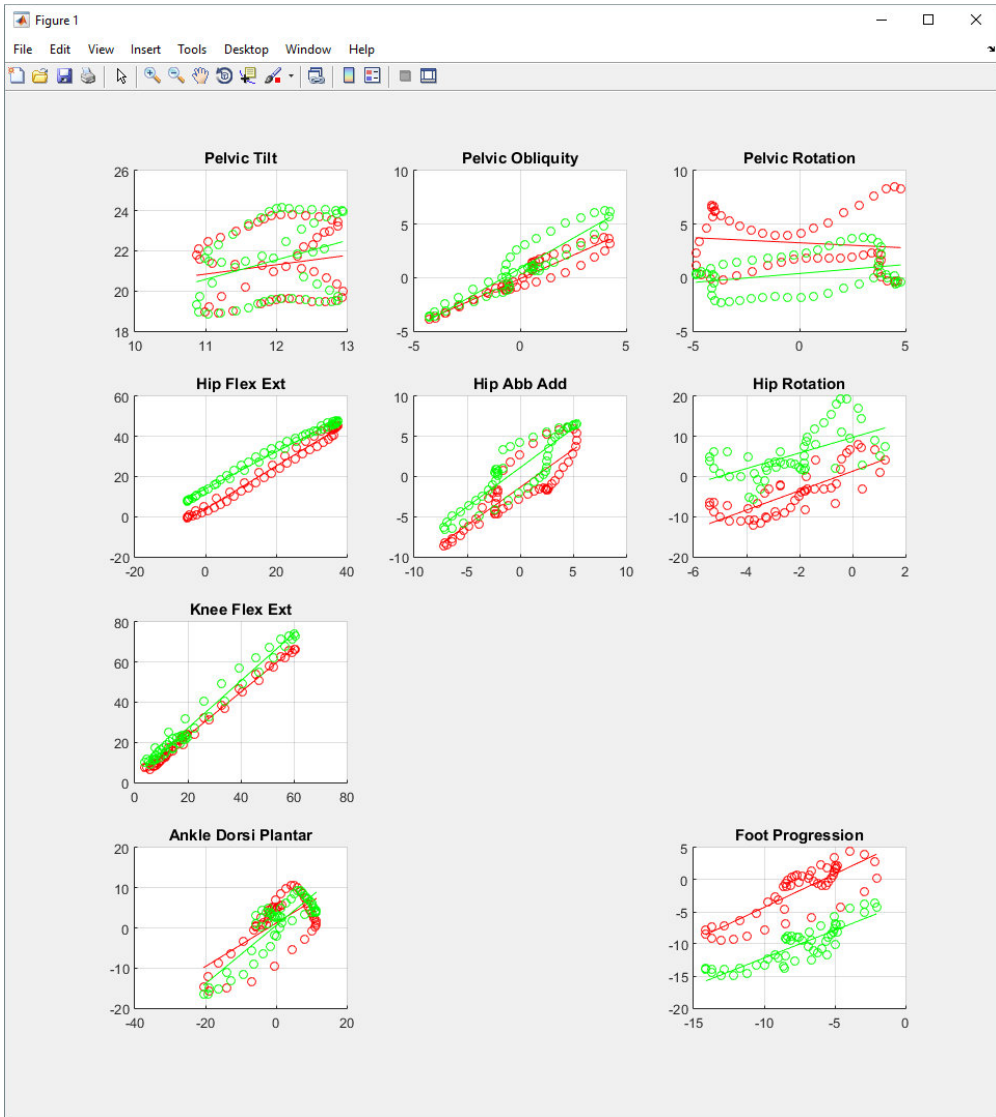
Figure 3.3.10: *Detailed visualization of the results from the LFM method. All the anatomical districts and reference planes were represented according to the standard layout of clinical reports. Red: left side, green: right side. Columns: anatomical reference planes (sagittal, frontal, horizontal). Rows: anatomical districts (pelvis, hip, knee, ankle.)*

3.4 – Results and discussion

Movement Analysis Profile

Average values and SDs of GVSs are displayed through bar graphs (MAP) in Figure 3.4.1 and reported in detail in Table 3.4.1, which includes differences pre-post.

Figure 3.4.1: *Movement Analysis Profile containing average values and SDs of GPS and GVS of 9 examined gait features, pre and post intervention. * significant differences (p<0.05).*

MAP	Pre		Post		Difference		p-value
	Mean	*SD*	*Mean*	*SD*	*Mean*	*SD*	
GPS	16.7	4.6	11.7	3.2	5.0 §	4.4	<<0.01 *
Pel. Tilt	8.2	4.8	10.5	4.4	-2.3 §	6.7	0.33435
Pel. Obl.	8.0	6.1	5.2	2.9	2.8 §	5.5	0.19863
Pel. Rot.	11.8	6.0	10.1	7.1	1.8 §	4.0	0.17468
Hip Flex	12.8	6.8	11.7	4.7	1.2	5.9	0.40325
Hip Abd.	10.1	5.9	6.9	3.1	3.2 §	5.6	0.01374 *
Hip Rot.	17.5	11.2	12.1	6.6	5.4 §	11.0	0.10843
Knee Flex.	27.6	12.7	15.8	7.1	11.8 §	12.4	<<0.01 *
Ankle Dors.	15.0	7.1	10.3	4.2	4.7 §	7.2	0.01000 *
Foot Prog.	17.1	10.1	11.7	7.4	5.3 §	9.4	0.03037 *

Table 3.4.1: *Numerical parameters of MAP, pre and post intervention. Positive differences means improvement. § pre-post higher than the MCID (i.e. 1.6°). * significant differences (p<0.05).*

Absolute values of pre-post differences were higher than the MCID for all parameters, except hip flexion. An improvement towards normality was observed in all the parameters, with exception of pelvic tilt, for which a worsening was observed. The highest improvement was observed for the knee flexion.

In Figure 3.4.2., GPS and GVS of sagittal gait features pre intervention are plotted against their changes between pre and post. A positive value of the difference means an improvement in the respective gait feature. In each case a linear trend could be observed. To higher GVSs pre intervention (most severe conditions) corresponded the higher improvements. Several negative variations were observed for Pelvis tilt and hip flexion. The highest correlation was observed for the knee sagittal kinematics (Figure 3.4.2, last row).
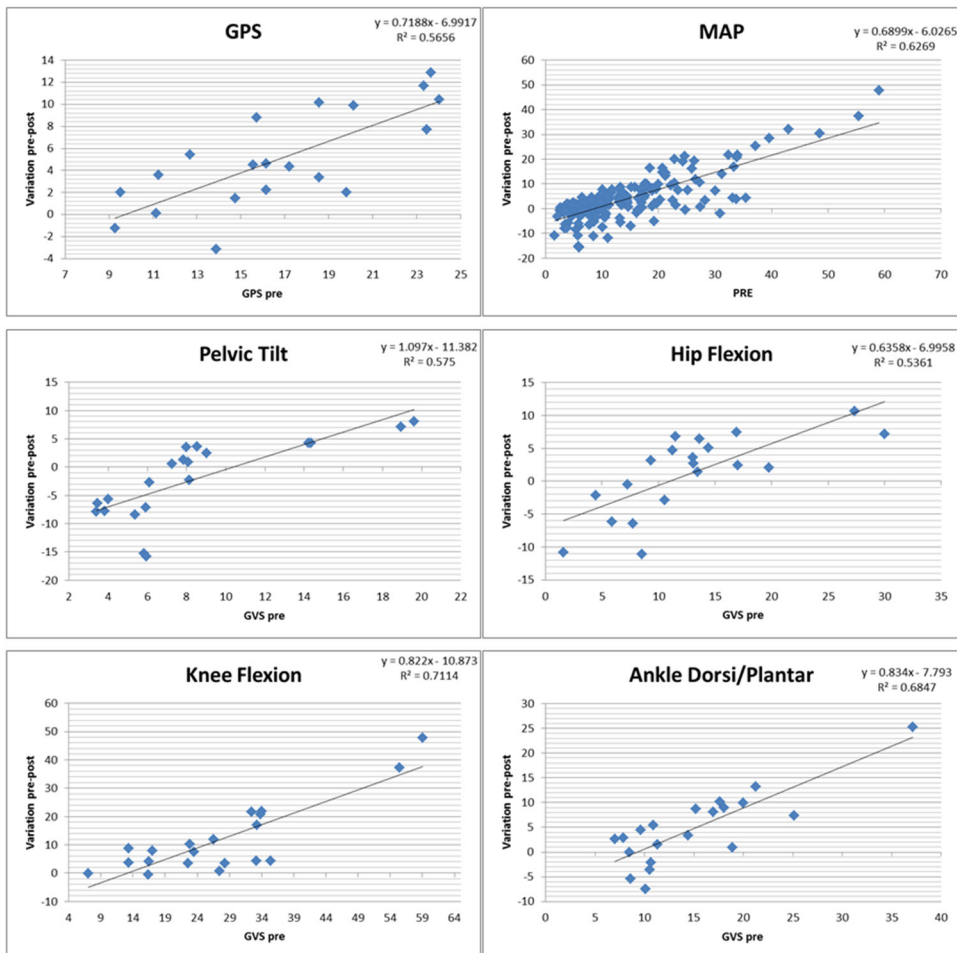
Figure 3.4.2: *Linear regression analysis between variation of GPS/GVS scores and their values pre intervention. In the first row: GPS and the GVSs of all the gait features (MAP). Second and third rows: GVSs of gait features relative to the sagittal kinematics.*

Offset Corrected Movement Analysis Profile

Average values and SDs of OC-GVSs are displayed in the OC-MAP reported in Figure 3.4.3. Numerical details are shown in Table 3.4.2. Offset values for the gait features are depicted in Figure 3.4.4 and reported in detail in Table 3.4.3.
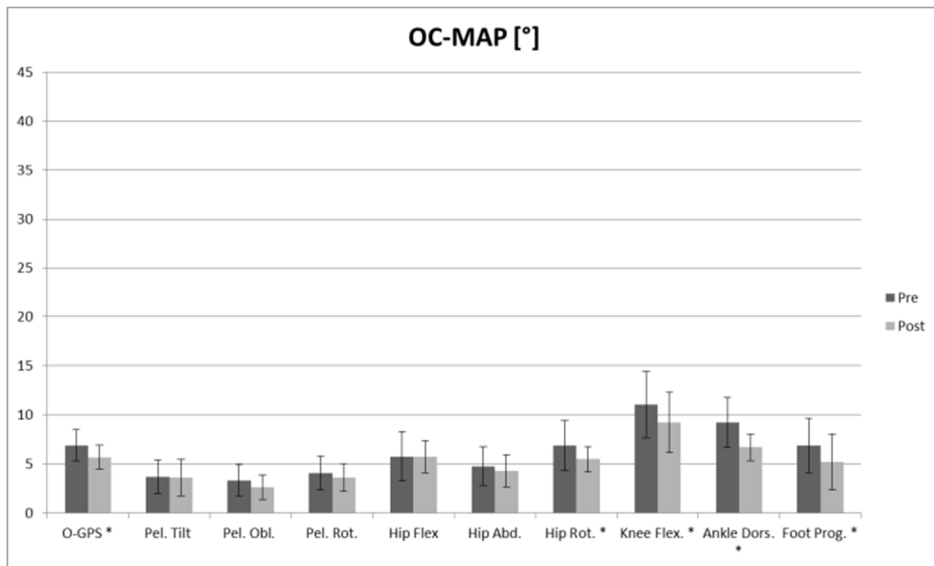
Figure 3.4.3: *Offset Corrected Movement Analysis Profile containing average values and SDs of OC-GPS and OC-GVS of 9 examined gait features, pre and post intervention. * significant differences (p<0.05).*
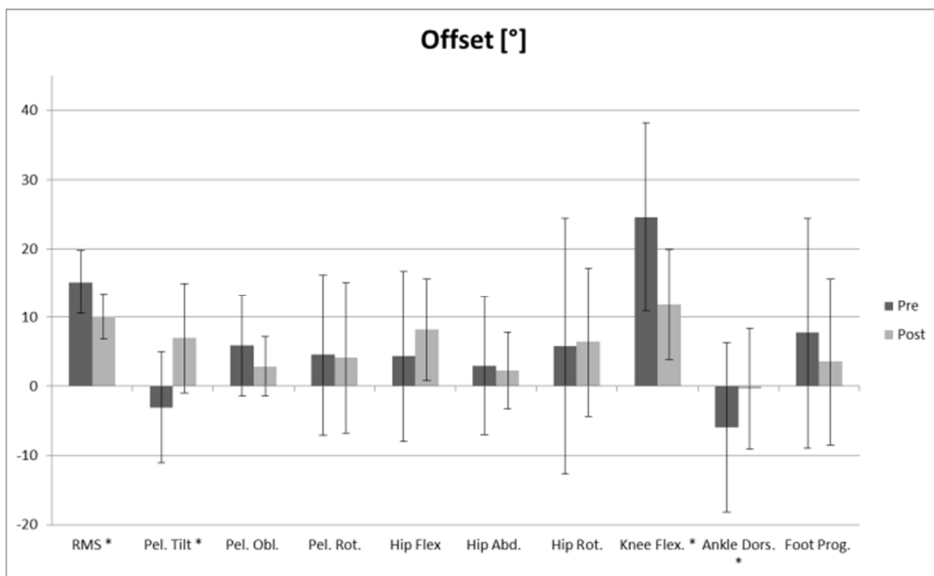
Figure 3.4.4: *Average values and SDs of measured Offset for the gait features, pre and post intervention. * significant differences (p<0.05).*

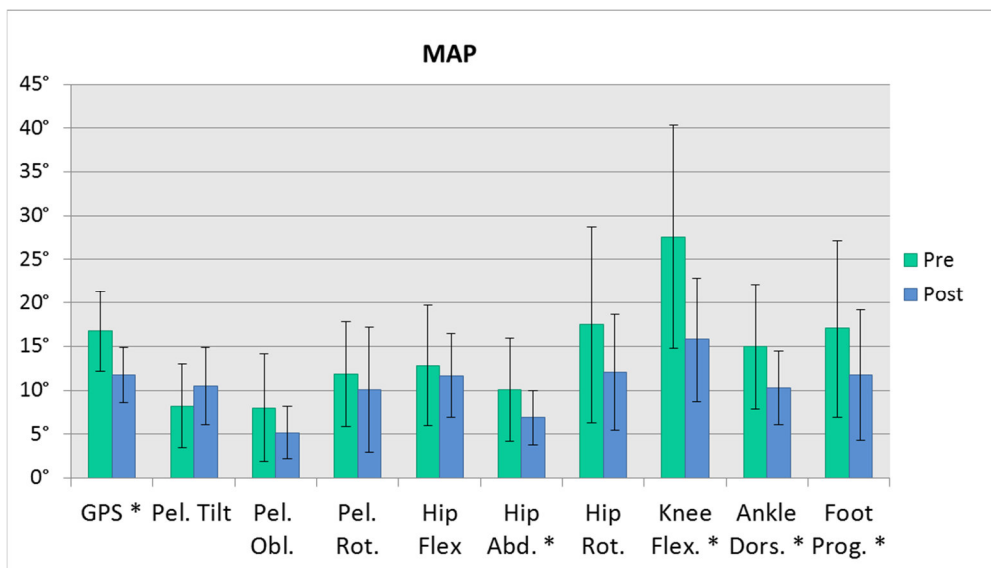| OC-MAP	Pre		Post		Difference		p-value
	Mean	*SD*	*Mean*	*SD*	*Mean*	*SD*	
OC-GPS	6.9	1.6	5.7	1.2	1.2	1.5	0.00245 *
Pel. Tilt	3.7	1.7	3.6	1.9	0.1	1.0	0.82243
Pel. Obl.	3.3	1.6	2.6	1.3	0.7	1.4	0.18772
Pel. Rot.	4.1	1.7	3.6	1.4	0.5	1.0	0.24024
Hip Flex	5.8	2.5	5.8	1.6	0.0	2.2	0.98621
Hip Abd.	4.8	1.9	4.3	1.6	0.5	1.4	0.14540
Hip Rot.	6.9	2.5	5.5	1.3	1.4	2.1	0.00898*
Knee Flex.	11.0	3.4	9.2	3.0	1.8 §	2.5	0.00537*
Ankle Dors.	9.2	2.5	6.7	1.3	2.5 §	2.9	0.00170*
Foot Prog.	6.9	2.7	5.2	2.8	1.6	3.1	0.04380*

Table 3.4.2: *Numerical parameters of OC-MAP, pre and post intervention. Positive differences means improvement. § pre-post higher than the MCID (i.e. 1.6°). * significant differences (p<0.05).*

Offset	Pre		Post		Difference		p-value
	Mean	*SD*	*Mean*	*SD*	*Mean*	*SD*	
RMS	15.2	4.6	10.1	3.3	5.1	4.3	0.03128 *
Pel. Tilt	-3.1	8.0	7.0	8.0	-10.1	9.1	<0.01 *
Pel. Obl.	5.9	7.3	2.9	4.3	3.0	7.2	0.21135
Pel. Rot.	4.6	11.6	4.2	10.9	0.4	5.0	0.81097
Hip Flex	4.4	12.4	8.3	7.4	-3.9	10.1	0.11110
Hip Abd.	3.0	10.0	2.3	5.6	0.7	7.3	0.67063
Hip Rot.	5.8	18.5	6.4	10.8	-0.6	14.7	0.86455
Knee Flex.	24.5	13.7	11.9	8.0	12.7	14.5	0.00120 *
Ankle Dors.	-5.9	12.2	-0.3	8.8	-5.6	8.7	0.01102 *
Foot Prog.	7.7	16.7	3.6	12.0	4.2	11.3	0.12465

Table 3.4.3: *Measured Offset and variation between pre and post. * significant differences (p<0.05).*

The OC-MAP analysis showed lower values than the MAP. A significant improvement was observed for OC-GPS, hip rotation, knee flexion, ankle dorsiflexion and foot progression. The highest improvements were observed at the knee flexion and ankle dorsiflexion.

The offset changed significantly from pre to post for the pelvic tilt, knee flexion and ankle dorsiflexion. Moreover the RMS average showed a significant overall improvement in the offset. A significant worsening was observed for the pelvic tilt, while high improvements where observed for the knee and ankle (Figure

3.4.4). The highest offset effect was observed on the knee flexion (Figure 3.4.4 and Table 3.4.3).

Linear Fit Method

Results of LFM analysis are shown in Figure 3.4.5. The R^2 parameter showed an improvement, from pre to post, in the overall kinematics and in the sagittal kinematics of knee and ankle. It also suggested an improvement in foot progression, but the difference was not statistically significant.

The *a0* coefficient showed that the highest offsets were observed on the pelvic tilt and knee flexion. Statistically significant improvements were observed for knee flexion and ankle dorsiflexion.

The knee flexion showed a statistically significant improvement also in terms of scaling (*a1* coefficient), that was closer to 1 in the post (Figure 3.4.5, third graph). A significant improvement was also observed, in terms of offset, for the ankle dorsiflexion.

The lowest value for R^2 were observed for pelvic tilt and hip rotation, suggesting that the associated *a0* and *a1* were not strongly meaningful. Moreover, the pelvic tilt showed a very high SD across subjects (Figure 3.4.5).
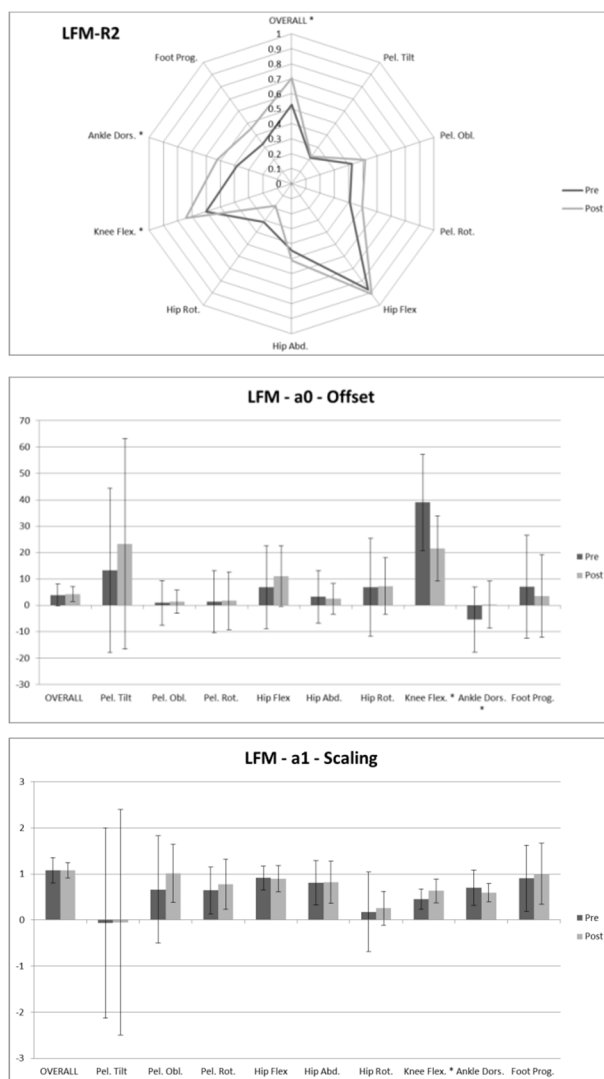
Figure 3.4.5: *Results of LFM analysis, averaged across subjects.*

	GPS / MAP	Pel. Tilt	Pel. Obl.	Pel. Rot.	Hip Flex	Hip Abd.	Hip Rot.	Knee Flex.	Ankle Dors.	Foot Prog.
	GPS					**MAP**				
R²	-0.759	-0.195	-0.126	-0.126	-0.214	-0.376	-0.094	-0.551	-0.443	-0.038
a0	0.371	0.174	0.834	0.535	0.605	0.048	0.581	0.978	-0.419	0.418
a1	0.194	-0.142	-0.331	-0.247	-0.187	-0.113	-0.137	-0.707	0.172	0.320
	OC-GPS					**OC-MAP**				
R²	-0.607	-0.390	-0.572	-0.780	-0.729	-0.605	-0.155	-0.919	-0.623	-0.570
a0	0.046	0.677	-0.072	0.030	0.036	-0.195	0.202	0.712	-0.300	-0.177
a1	0.139	-0.728	-0.306	-0.497	-0.190	0.139	-0.417	-0.919	0.320	-0.077
	RMS					**Offset**				
R²	-0.742	0.243	0.167	-0.349	-0.009	-0.048	0.076	-0.428	0.074	0.509
a0	0.405	-0.157	0.976	0.994	0.852	0.998	0.999	0.953	0.999	0.973
a1	0.194	0.436	-0.150	-0.398	-0.202	-0.150	-0.021	-0.608	-0.317	0.537

Table 3.4.4: Correlation table between the MAP, OC-MAP, Offset and the parameters compued from Linear Fit Method. Pearson's R coefficients for each gait feature are shown. Back color indicates strong and moderate levels of correlation.

108

Results of correlation analysis are reported in Table 3.4.4 as the Pearson correlation coefficients R, computed between the respective results from MAP/OC-MAP/Offset and LFM components (R^2, *a0* and *a1*) for each gait feature. GPS, OC-GPS and RMS average of the offsets were compared to the R^2, *a0* and *a1* resulting from the overall LFM computing.

A strong correlation was observed for: the Overall R^2 of LFM and GPS/RMS; the *a0* and the *Offset* of each gait feature, with exception of pelvic tilt; all the LFM parameters of knee flexion and the respective MAP and OC-MAP; the *a0*, *a1* of the pelvic tilt and the respective OC-MAP. Moderate correlations were also observed between R^2 and some gait features of OC-MAP.

The correlation between the GPS and the overall R^2 computed by LFM is shown in Figure 3.4.6 as scatterplot and regression line. The same plot was made for knee flexion, comparing the GVS and the a0 (Figure 3.4.7).
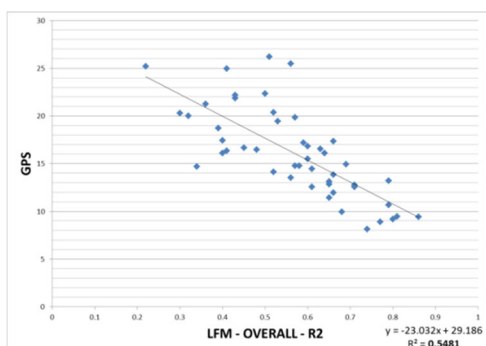
Figure 3.4.6: *Results of correlation analysis between the GPS and R^2 of LFM*
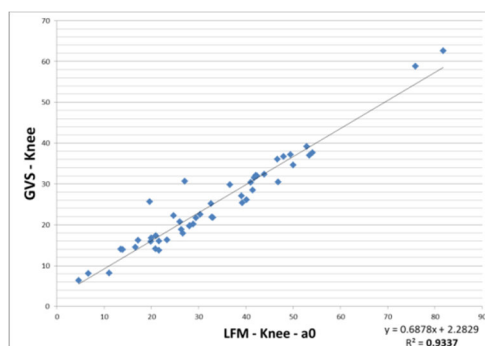
Figure 3.4.7: *Results of the correlation analysis between the GVS of knee flexion and a0 of LFM.*

Gait Report

In order to integrate and supplement the presentation of results, a complete kinematic gait report of one subject is presented here. In Figure 3.4.8 is depicted the kinematic gait report pre-treatment. The gait tracks post treatment are shown in Figure 3.4.9. Graphs are arranged according to the standard gait reporting directions: rows represent the anatomical districts of pelvis, hip, knee and ankle; columns represent anatomical planes sagittal, frontal and horizontal.

The subject, whose gait report is shown here, can be assumed as representative of the cohort of subject involved in this study.

The detailed kinematic report allowed us to visualize each gait feature for both left and right sides. The deviation from normality for each feature is clearly identified along the stride phases.
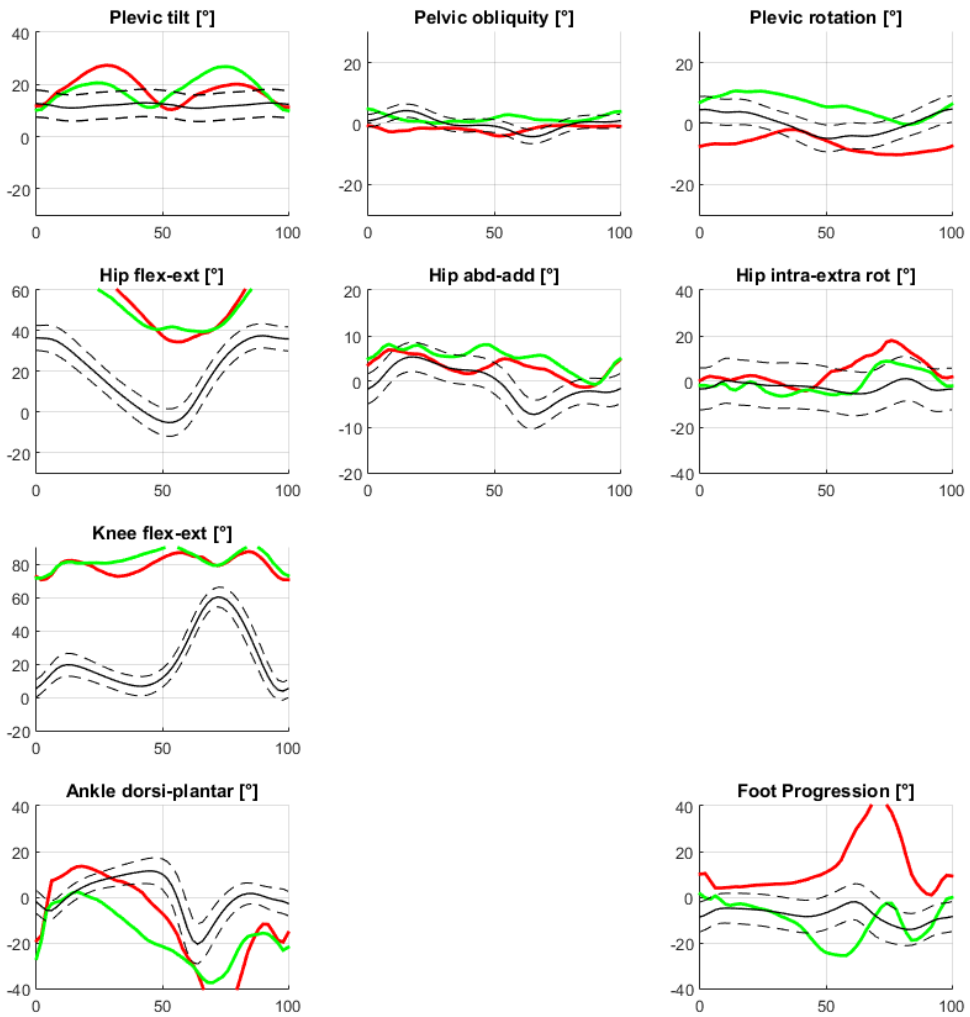
Figure 3.4.8: *Gait kinematics of a subject with CP,* **PRE** *treatment. Red: left side, green: right side, black: reference.*
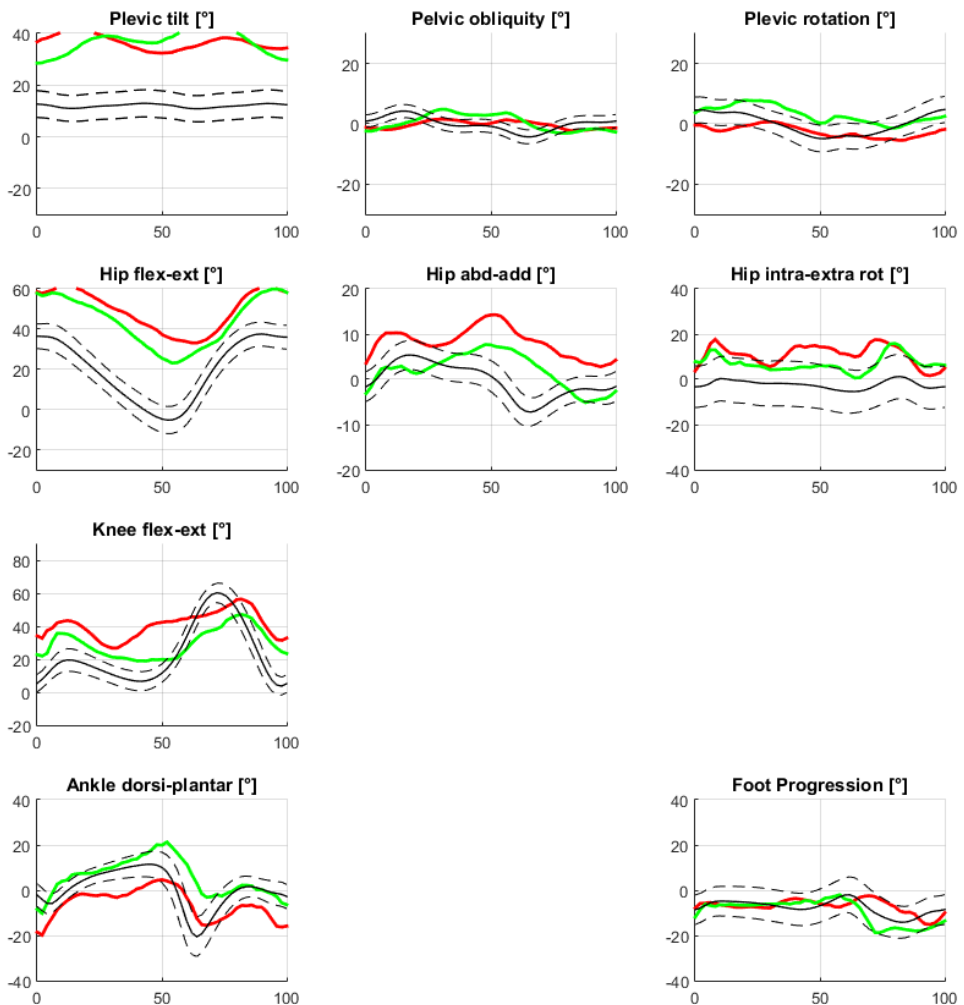
Figure 3.4.9: *Gait kinematics of a subject with CP,* ***POST*** *SEMLS treatment. Red: left side, green: right side, black: reference.*

In the pre-treatment (Figure 3.4.8) it is clear the condition of crouch gait, suggested by a persistent knee flexion, hip flexion and ankle plantarflexion. Pelvic tilt has a normal baseline but shows an abnormal pattern. On the horizontal plane, it is documented an internal foot rotation on the left side and foot rotation abnormalities on the right side.

Post treatment evaluation (Figure 3.4.9) suggests an improvement of the gait pattern. Knee flexion approached normality and the shape was regularized. Also hip flexion improved even though a persistent flexion remained. Ankle plantarflexion approached normality bilaterally, both in terms of offset and shape. Foot progression improved bilaterally. A worsening was observed for the pelvic tilt that deviated towards anterior flexion. This variation in the pelvic tilt may be a consequence to the hamstring lengthening, that was already documented in the literature (Delp et al. 1996; Hoffinger, Rab, and Abou-Ghaida 1993).

Discussion of the results

In this study, we observed an improvement in GPS (decrease in value) post treatment of 5.0°±4.4° that was comparable to the value found in subjects with CP by Rutz et al. (Rutz et al. 2013), that was 4.3°±3.7°.

MAP, OC-MAP and LFM showed an overall improvement in the gait pattern after surgery, that was represented by the reduction of GPS and OC-GPS scores and the increase of the overall R^2 coefficient computed by LFM. Even though the GPS reduced significantly from pre to post, in the post it was still higher than normality, that is within the range of 5° (Baker et al. 2009), indicating that the walking pattern was still compromised. As it was already pointed out in other studies (Rutz et al. 2013), we observed that patients who had initial high deviations, representing the worst cases, benefitted more from the treatment (Figure 3.4.2). This was noticeable for the overall GPS index and the sagittal plane features (Figure 3.4.2), especially for knee flexion. Indeed, the highest improvement was observed for the GVS of knee flexion (Figure 3.4.1 and Table 3.4.1) that was represented by a statistically significant reduction of the index. This meant that the surgery had a strong positive impact on the kinematics of the knee. An improvement was observed also at the level of ankle (Figure 3.4.1 and Table 3.4.1), even though surgery was not performed on this district.

The improvement observed for hip rotation and foot progression suggested that the surgery improved the kinematics on the horizontal plane by correcting compensatory strategies that were adopted by the subjects.

The worsening observed in the kinematics of the pelvis could be explained as a consequence of SEMLS surgery that involved a lengthening of hamstring group (Delp et al. 1996; Hoffinger et al. 1993). No effect was observed at the hip flexion meaning that the improvement at the knee induced a postural compensation at the level of the pelvis.

OC-MAP and offset analysis (Figures 3.4.3 and 3.4.4) showed that offset played a significant role in deviation from normality. A limitation of the classical MAP analysis is the lack of information about the direction of the deviation, e.g. towards flexion or extension. This information is instead provided by the offset analysis, where the sign indicates the direction of the deviation.

The highest offset component was observed for the knee flexion pre intervention, that reduced significantly in the post. The positive offset indicated that a deviation remained towards the flexion (Figure 3.3.4 and Table 3.4.3).

The ankle dorsiflexion angle had a high negative offset in the pre, that reduced towards normality in the post. This suggested that the improvement at the knee also improved ankle angle, leading to a better posture. The offset in the pelvic tilt changed from a negative value, meaning a posterior flexion, towards an anterior flexion with a significant difference (Figure 3.4.4 and Table 3.4.3). This effect was not identified by the other methods. The increase in pelvic anterior flexion could be attributed to a compensatory effect resulting from the surgery on the hamstring group.

The observed improvement in the kinematics of knee and ankle could also be identified by the increase in the R^2 coefficient of LFM (first graph in Figure 3.4.5). The *a0* component (second graph in Figure 3.4.5) provided results similar as a trend to offset analysis shown in Figure 3.4.4. But absolute values were different. This confirmed that the offset component played an important role in the improvement of knee and ankle kinematics. The *a0* parameter was not reliable to describe the offset of pelvic tilt, as it showed a very high standard deviation (Figure 3.4.5). This is a known limitation of the LFM method, as *a0* coefficient is reliable only when the correlation between the tracks is relatively high (Iosa et al. 2014). Therefore *a0* cannot be considered as an absolute measurement of offset but it can document changes in offset pre and post treatment.

The scaling parameter *a1* documented abnormalities in the hip rotation and the pelvic tilt, that were different from the reference level, i.e. 1 (one). Moreover the pelvic tilt showed again a very high SD, meaning high variability across subjects and therefore this index is not capable of describing pelvic

pattern. The *a1* index was instead capable of detecting a pattern improvement, in terms of shape/scaling factor, for the knee flexion (Figure 3.4.5).

The correlation analysis (Table 3.4.4) showed a strong correlation between the overall R^2 and GPS, meaning that both indices provided similar information. A strong correlation was also observed between the *a0* and the Offset, for all the gait features with an exception for the pelvic tilt, for which no correlation was observed. This was attributed to the high variability observed across subjects and to the very low R^2 found for pelvic tilt (Figure 3.4.5).

The knee flexion also showed a strong correlation between parameters, indicating that all the indices were able to identify the changes in this feature.

It is interesting that a moderate correlation was observed between R^2 and OC-GPS for most features, confirming them being good indices rating the overall gait performance.

Based on the results here obtained, the OC-MAP analysis is the most reliable and provides information about the direction of the deviation. For the subject studied in this work, the offset was a significant component of deviation in gait pattern, therefore the OC-MAP method was an useful synthetic method to interpret data. The R^2 itself remains a good overall index of similarity and therefore it can be considered a synthetic index describing the quality of a gait pattern. Anyway, the intrinsic limitation of the LFM method makes it unreliable for the quantification of the offset in the gait features.

3.5 – Conclusion

This research project was aimed to the evaluation of the changes occurring in gait pattern for subjects with CP undergoing SEMLS treatment. The quantitative analysis was conducted by means of Gait Analysis

The MAP, OC-MAP and LFM are synthetic descriptors based on different assumption and different mathematical procedures, meaning that they provided different kind of information.

The MAP allowed the computation of a score for each gait feature allowing a detailed analysis but it's main limitation was identified as its inability to describe the causes of deviation from normality (Baker et al. 2009). The OC-MAP allowed to analyse separately the effect of the offset and the deviation from normality of the tracks, once purified by the offset. The results were

compared to another method that allowed the analysis of effects of offset and scaling, i.e. the LFM method (Iosa et al. 2014).

As pointed out in other studies (Rutz et al. 2013), we observed that patients who had initial high deviations, representing the worst cases, benefitted more from the treatment. The highest improvements were observed at the level of the knee (Figure 3.5.1) and ankle, while pelvic tilt changed towards anterior flexion (Figure 3.5.2). The improvement observed for hip rotation and foot progression suggested that the surgery improved the kinematics in the horizontal plane as well. The worsening observed in the pelvis kinematics could be explained as a consequence of SEMLS surgery that involved a lengthening of hamstring group. In fact, surgical lengthening of hamstrings may increase hip flexion during stance (Delp et al. 1996) and anterior pelvic tilt (Hoffinger et al. 1993).

The changes in gait pattern were observed mainly as changes in the offset between the observed gait features and the reference tracks (Figures 3.5.1 and 3.5.2).
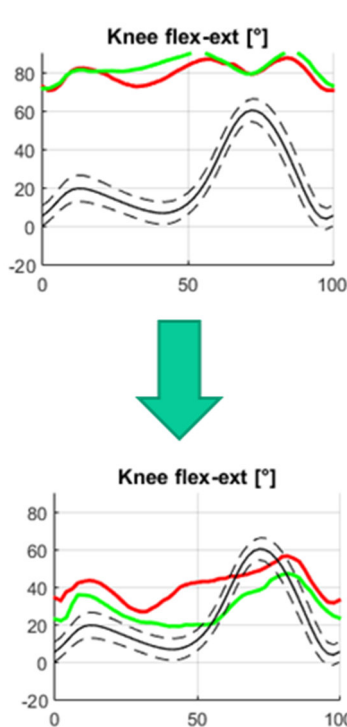
Figure 3.5.1: Improvement in knee flexion/extension angle observed as a change in the offset.
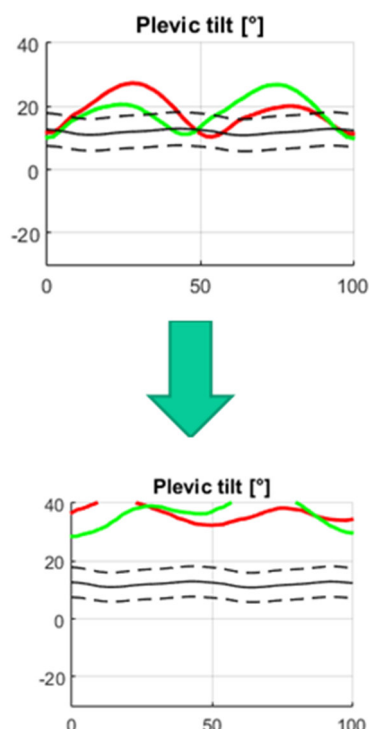
Figure 3.5.2: Worsening in pelvic tilt observed as a change in the offset towards persistent anterior tilt.

From this study it came clear that the MAP itself was not enough to describe the causes of deviation from normality, due to the absence of information about the direction of the deviation, e.g. towards flexion or extension or information about the cause of deviation (offset, shape, etc.).

OC-MAP and offset analysis demonstrated that offset could explain a larger part of the deviation from normality, as well as in correction after surgery. The deviation observed by MAP for pelvic tilt, knee flexion and ankle dorsiflexion was mainly due to offset. The observed improvements in the offset suggested a normalization of the sagittal plane kinematics, leading to a better posture.

Although R^2 can be considered a good overall index of similarity, when it is low, a0 and a1 lose their meaning, making LFM less suitable to assess gait features. Therefore the use of LFM is not recommended for interpreting gait of children with CP.

The OC-MAP method overcame a MAP limitation, by separating the offset component from the differences in the shape of the joint kinematics. As the offset was a significant component of deviation in gait pattern, the OC-MAP demonstrated being the most clinically meaningful synthetic method to interpret gait data in CP.

On the basis of the results observed in the present study, we recommend the use of the index here proposed, i.e. the OC-MAP, as a synthetic descriptor to investigate the effect of offset on gait features. Further work on larger cohorts of patients with CP and on other pathologies is recommended.

Summary and General Discussion

The study of movement has always fascinated artists, photographers and researchers. Across the years, several attempts to capture, freeze, study and reproduce motion were made.

Nowadays, motion capture plays an important role within many fields, from graphical animation, filmmaking, virtual reality, till medicine. In fact, movement analysis allows to measure kinematic and kinetic performance of the human body. The quantitative data obtained from measurements may support the diagnosis and treatment of many pathologies, allowing to take clinical decisions and supporting the follow-up of treatments or rehabilitation. This approach is nowadays named *evidence based medicine*.

In this work, motion capture techniques and advanced signal processing techniques were exploited in order to: (i) develop a protocol for the validation and quality assurance of the clinical strength measurements, (ii) develop an algorithm for clinical gait analysis data interpretation and identification of pathological patterns, and (iii) design user-friendly software tools to help clinicians using the novel data processing algorithms and reporting the results of measurements.

This work was divided into three sections:

Part 1 contains a survey about the history of motion analysis and a review of the earliest experiments in biomechanics. The review covered the first historical attempts, that were mainly based on photography, till the state-of-the-art technology used today, i.e. the optoelectronic system.

The working principle of optoelectronic system was reviewed as well as its applications and modern setups in the clinical practice.

Some modern functional evaluation protocols, aimed to the quantitative evaluation of physical performance and clinical diagnosis of motor disorders, were also reviewed. Special attention was paid to the most common motion analysis exam that is nowadays worldwide standardized, i.e. the Gait Analysis. Examples of Gait Analysis studies on subjects with pathology and follow-up were reviewed.

Part 2 concerns the design of an experimental setup, involving motion analysis, for the quality assurance of clinical strength measurements.

Measurements of force are popular in the clinical practice as they allow to evaluate the muscle weakness, health status of patients and the effects of therapies. A variety of protocols was proposed to conduct such measurements, implying the acquisition of forces, angles and angular velocities when the maximum voluntary force is exerted. Hand held dynamometry (HHD), based on single component load cell, was extensively used in clinical practice; however, several shortcomings were identified. The most relevant were related to the operator's ability.

This work was aimed to investigate the inherent inaccuracy sources in knee strength measurements when are conducted by a single component load cell. The analysis was conducted by gathering the outputs of a compact six-component load cell, comparable in dimension and mass to clinical HHDs, and an optoelectronic system.

Quality of measurements was investigated in terms of quantifying, by an *ad-hoc* metrics, the effects induced in the overall inaccuracy by: (i) the operator's ability to place and to hold still the HHD and (ii) ignoring the transversal components of the force exchanged between the patient and the experimenter.

The main finding was that the use of a single component HHD induced an overall inaccuracy of 5% in the strength measurements, when operated by a trained clinician and angular misplacements are kept within the values found in this work (≤15°) and with a knee ROM ≤ 22°.

Even if the measurement outputs were reliable and accurate enough for both knee flexion and extension, extension trials were the most critical due to the higher force exerted, i.e. 249.4±27.3 N vs. 146.4±23.9 N of knee flexion. The most relevant source of inaccuracy was identified in the angular displacement of HHD on the horizontal plane.

A dedicated software, with graphical user interface, was designed and implemented. The purposes of this software were to: (i) speed up data processing, (ii) allow user to select the proper processing workflow, and (iii) provide clinicians with a tool for quick data processing and reporting.

Part 3 concerns the research study about gait analysis on subjects with pathology.

Gait analysis is often used for the assessment of the gait abilities in children with cerebral palsy and to quantify improvements/variations after a treatment. To simplify GA interpretation and to quantify deviation from normality, some synthetic descriptors were developed in literature, such as the Movement Analysis Profile (MAP) and the Linear Fit Method (LFM).

The aims of this work were: (i) to use synthetic descriptors in order to quantify gait variations in subjects with Cerebral Palsy that underwent surgery involving bone repositioning and muscle/tendon lengthening at the level of the femur and hamstring group (SEMLS); (ii) test the effectiveness of a recently proposed index, i.e. the LFM, on such patients; (iii) design and implement a novel index that may overcome the limitations of the previous methods.

Gait Analysis exams of 10 children with Cerebral Palsy, pre and post treatment, were collected. Data were analysed by means of MAP and LFM indices. To overcome the limitations observed for the methods, another index was designed as a modified version of the MAP, namely the OC-MAP. It took into account the effect on deviation due to offset and allowed to compute the deviation from normality on tracks purified by the offset.

An overall improvement of the gait pattern was observed for most of the subjects after surgery. The highest effect was observed for the knee flexion/extension angle. Patients who had initial high deviations also had the largest improvements. Worsening in the kinematics of the pelvis could be explained as a consequence of SEML involving a lengthening of hamstring group. Pre-post differences were higher than the Minimally Clinical Important Difference for all parameters, except hip flexion.

An improvement towards normality was observed for all the parameters, with exception of pelvic tilt for which a worsening was observed. LFM provided results similar to OC-MAP offset analysis but could not be considered reliable due to intrinsic limitations.

As offset in gait features played an important role in gait deviation, OC-MAP synthetic analysis is recommended to study gait pattern of subjects with Cerebral Palsy.

A dedicated software, with graphical user interface, was designed and implemented. The purpose of this software was to compute the synthetic descriptors on a large amount of data, to speedup data processing and to provide clinicians with a quick access to the results.

About the Funded Projects

The experimental setups, study design, instrumentation and software design as well as the results of the experiments here described were funded by the projects:

- MD-Paedigree European Project.
- PRIN 2012 Project.

MD-Paedigree European Project

The MD-Paedigree Project, or "Model-Driven Paediatric European Digital Repository", is a project funded by the European Commission under FP7 - ICT Program.

The project involves 22 European partners: Universities, Research centers, Hospitals and Corporates (Figure 4.1).

Figure 4.1: *European partners of the MD-Paedigree Project.*

The main goals of the project are:

- Develop an open access, large-scale repository of data and models;
- Develop and share robust and reusable multi-scale models;
- Integrate and share biomedical information using the biomedical semantic Web;
- Develop holistic search strategies to index and navigate a digital repository;
- facilitate collaboration between research centers.

The MD-Paedigree project aims to answer the clinical need for integrating information from heterogeneous sources, unifying existing scattered modelling efforts, and translating the results into clinical practice. This applies in particular to paediatrics, in which therapeutic decisions have long-term consequences and where the foundation for a healthy adult life is laid.

MD-Paedigree validates and brings to maturity patient-specific computer-based predictive models of various paediatric diseases, thus increasing their potential acceptance in the clinical and biomedical research environment by making them readily available not only in the form of sustainable models and simulations, but also as newly-defined workflows for personalised predictive medicine at the point of care. These tools can be accessed and used through an innovative model-driven infostructure powered by an established digital repository solution able to integrate multimodal health data, entirely focused on paediatrics.

MD-Paedigree involves four mayor research areas:

- Cardiomyopathies;
- Cardiovascular Diseases;
- Juvenile idiopathic arthritis (JIA);
- Neurological and neuromuscular diseases (NND).

Patients from the JIA and NND groups were tested with Clinical Gait Analysis in order to study and identify characteristic walking patterns. Patients from the NND group were also tested with the strength protocol in order to assess muscular functionality and maximal force exerted.

As all the data gathered within the project, coming from different clinical centers, has to be merged within the same database (namely "Infostructure"), quality assurance criteria as well as data storage, reduction, indexing, search and pattern recognition criteria were requested to be implemented by the different work packages of the project.

Figure 4.2 illustrates the concept for the architecture of the big data infrastructure designed for the MD-Paedigree project. It is based on a mixed usage of a Distributed Architecture (DA) and an Hybrid Architecture (HA), where DA sites are automatically replicated with transactions guarantying databases' integrity, whereas HA sites do access their corresponding DA provider (Hub) to benefit from immediate storage and querying of networked data. Servers are hosted by the research centres involved in the project.

The pillars of this infrastructure lie in the two main sites, i.e. Rome and Taormina, which are both deployed using the DA solution. These two sites provide high quality of services upon accesses to the data by connected sites. Metropolitan sites, such as Palidoro, San Paolo and Santa Marinella host their own database and share with the rest of the OPBG network. On the other hand, the associated HA sites share and access the Children's Hospital Bambino Gesù network throughout the two (respectively Roman and Sicilian) hubs. These hubs can also accept new connections from external sites, such as new collaboration hospitals and clinical centres interested in sharing data and accessing the state-of-the art in related research applications.
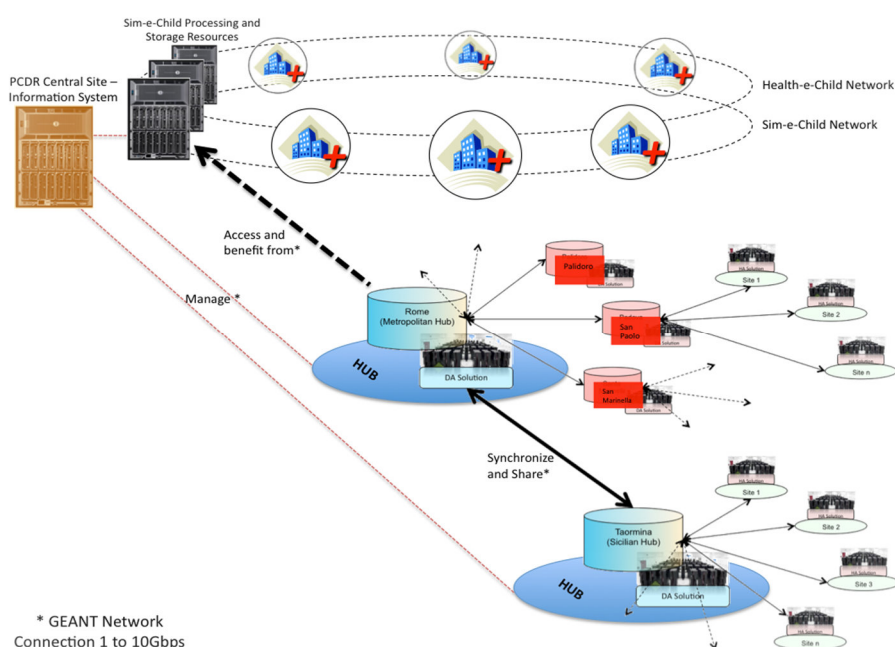

Figure 4.2: Architecture of the big data infrastructure for data storage and sharing among partners of the MD-Paedigree Project.

PRIN 2012 Project

The PRIN 2012 or "Programmi di Ricerca di Rilevante Interesse Nazionale, year 2012" is a project funded by Italian Ministry of Education, Universities and Research (MIUR).

Within this project, "Sapienza" University of Rome was commissioned to carry out the research entitled: "*Mechanical measurements for the musculoskeletal apparatus: novel and standardizable methodologies for metrological assessment of measurement systems*".

Project funding started on March 2014.

The aims of this project were: (i) the development and implementation of instrumental procedures to test the quality of the measurements conducted in motion analysis laboratories; (ii) to define standard methodologies to be adopted in motion analysis laboratories in order to obtain repeatable and reproducible measurements.

The types of measurements considered by this project were:

- Human kinematics and gait analysis, conducted through a Motion Capture System (OS);
- Forces, conducted through force plates and force sensors;
- Mechanics of breathing and respiratory volumes by optoelectronic plethysmography (OEP).

Therefore, the work conducted within this project was aimed to:

- Develop a method for calibration and uncertainty evaluation of **optoelectronic systems**, where used for:
  - ➢ Gait analysis;
  - ➢ Mechanical ventilation/breathing analysis;
  - ➢ Movement analysis and clinical measurements in general;
  - ➢ Synchronization between devices and multifactorial measurements.
- Develop a method for calibration and uncertainty evaluation of **force platforms** and **clinical dynamometers.**

- Propose a **standard procedure** to test quality of measurements in movement analysis laboratories.

This project was an extension of some Work Packages that had to be exploited by Sapienza in the four-year project funded by the 7th Framework Programme entitled "MD-Paedigree" and that started in March 2013.

The research was conducted in partnership with "Roma Tre" and "Campus Biomedico" Universities of Rome which provided their skills about force measurements and optoelectronic plethysmography. They also provided

access to their laboratories and instrumentation in order to conduct experiments.

This research also benefited from the network already established within the "MD-Paedigree" project, funded by the 7th Framework Programme, that involved 22 research groups in Europe and allowed to conduct research across different laboratories.

Assessing quality of measurements, as well as their reliability, repeatability and reproducibility is critical in clinical contexts, as clinical decisions are often taken on the basis of measurements. It is also important to determine if the variability in results, that is often observed in clinical trials, is due to patients' variability or intrinsic measurement error.

The expected results from this research will also have a potential application in rehabilitation, by allowing the development and validation of innovative functional evaluation protocols and supporting the development of tools, methods and statistics that provide a rapid, scientific and accurate clinical evaluation and the prediction of safety, effectiveness and quality of health technologies.

Conferences

The results of the research work described in this book were presented to the following international meetings and congresses:

- 25th ESMAC Annual Meeting, 29 September – 1 October 2016, Seville, ES.

- MD-Paedigree Third Annual Review, 15-17 February 2016, Rome, IT.

- MD-Paedigree Third Biannual Meeting, 1-2 October 2015, Crete, GR.

- Workshop on: Challenges of Big Data for Economic Modelling and Management: Tools from Efficiency Analysis, Sensitivity Analysis, Sensitivity Auditing and Physics of Complex Systems. 10-11 Nov. 2015, Sapienza University of Rome, Italy.

- IEEE 2015 International Symposium on Medical Measurements and Applications, 7-9 May 2015, Turin, IT.

- 1st Clinical Movement Analysis World Conference, (ESMAC-SIAMOC joint meeting), 1-4 October 2014, Rome, IT.

- IX Congress of MMT Group, 11-13 September 2014, Ancona, IT.

Awards

The work on quality assurance of knee strength measurements (Ancillao et al. 2015) has been awarded with the *"2015 Quarterly Travel Awards for Scientific Posters and Podium Presentation Abstracts"* by The Force and Motion Foundation, AMTI Inc. (www.forceandmotion.org).

Acknowledgments

Here it comes the end of this thesis. What you just read is the story of most of the research work conducted from January 2014 to December 2016.

At this point, I would like to spend some words to acknowledge the people that helped me out and took part to it, directly or indirectly. This thesis would not have been possible without them.

First and foremost, I sincerely acknowledge professor Paolo Cappa, that gave me the opportunity to start this adventure and go through with it. He prematurely passed away before seeing the conclusion of this work and I would like to take advantage of these lines to express my gratitude and esteem. After designing the earliest experiments, facing many difficulties, attending meetings abroad, spending many long days writing and reviewing the drafts for publications and conferences, he led me through the path to bring this project to its conclusion. The success of this work is mainly due to his help.

A big thank you goes also to professor Rino Del Prete, that helped me concluding this work and writing this thesis in the rush of the last months.

I would sincerely acknowledge professor Jaap Harlaar for giving me the opportunity to spend some enjoyable months at the VUmc University of Amsterdam, where I could improve my knowledge on motion analysis, learn new methods, pursue a challenging research project and, last but not least, meet many nice people and friends.

A heartfelt thanks goes to professor Giorgio Albertini and professor Manuela Galli that, in the years gone by, taught me the basis of functional evaluation and motion analysis, providing me with the method for the design and reporting of experiments in the field.

Finally, the biggest thank you goes to all the colleagues from Sapienza and from VUmc, that gave me a helpful support to this journey. We shared together many amazing moments.

Roma, February 2017

References

Accardo, A., M. Affinito, M. Carrozzi, and F. Bouquet. 1997. "Use of the Fractal Dimension for the Analysis of Electroencephalographic Time Series." *Biological Cybernetics* 77(5):339–50.

Allen, GM, SC Gandevia, and DK McKenzie. 1995. "Reliability of Measurements of Muscle Strength and Voluntary Activation Using Twitch Interpolation." *Muscle & Nerve* 18(1):593–600.

Ancillao, Andrea et al. 2012. "Temporomandibular Joint Mobility in Adult Females with Ehlers-Danlos Syndrome, Hypermobility Type (Also Known as Joint Hypermobility Syndrome)." *Journal of Cranio-Maxillary Diseases* 1(2):88–95.

Ancillao, Andrea et al. 2016. "Quantitative Evaluation of Facial Movements in Adult Patients with Hemiplegia after Stroke." *International Journal of Signal and Image Processing Issues* 2016(1):1–10.

Ancillao, Andrea, Manuela Galli, Chiara Rigoldi, and Giorgio Albertini. 2014. "Linear Correlation between Fractal Dimension of Surface EMG Signal from Rectus Femoris and Height of Vertical Jump." *Chaos, Solitons & Fractals* 66:120–26.

Ancillao, Andrea, Manuela Galli, Sara Laura Vimercati, and Giorgio Albertini. 2013. "An Optoelectronic Based Approach for Handwriting Capture." *Computer Methods and Programs in Biomedicine* 111(2):357–65.

Ancillao, Andrea, Stefano Rossi, and Paolo Cappa. 2017. "Analysis of Knee Strength Measurements Performed by a Hand-Held Multicomponent Dynamometer and Optoelectronic System." *IEEE Transactions on Instrumentation and Measurement* 66(1):85–92.

Ancillao, Andrea, Stefano Rossi, Fabrizio Patanè, and Paolo Cappa. 2015. "A Preliminary Study on Quality of Knee Strength Measurements by Means of Hand Held Dynamometer and Optoelectronic System." Pp. 595–99 in *IEEE - MeMeA2015*.

Aper, R. L., C. L. Saltzman, and T. D. Brown. 1996. "The Effect of Hallux Sesamoid Excision on the Flexor Hallucis Longus Moment Arm." *Clinical Orthopaedics and Related Research* (325):209–17.

Aprahamian, Ivan, José Eduardo Martinelli, Anita Liberalesso Neri, and Mônica Sanches Yassuda. 2010. "The Accuracy of the Clock Drawing Test Compared to that of Standard Screening Tests for Alzheimer's Disease: Results from a Study of Brazilian Elderly with Heterogeneous Educational Backgrounds." *International Psychogeriatrics / IPA* 22(1):64–71.

Assi, Ayman, Ismat Ghanem, François Lavaste, and Wafa Skalli. 2009. "Gait Analysis in Children and Uncertainty Assessment for Davis Protocol and Gillette Gait Index." *Gait & Posture* 30(1):22–26.

Baader, Andreas P., Oleg Kazennikov, and Mario Wiesendanger. 2005. "Coordination of Bowing and Fingering in Violin Playing." *Brain Research. Cognitive Brain Research* 23(2–3):436–43.

Baker, Richard. 2007. "The History of Gait Analysis before the Advent of Modern Computers." *Gait & Posture* 26(3):331–42.

Baker, Richard et al. 2009. "The Gait Profile Score and Movement Analysis Profile." *Gait & Posture* 30(3):265–69.

Baker, Richard et al. 2012. "The Minimal Clinically Important Difference for the Gait Profile Score." *Gait & Posture* 35(4):612–15.

Bandinelli, S. et al. 1999. "Measuring Muscular Strength of the Lower Limbs by Hand-Held Dynamometer: A Standard Protocol." *Aging Clin. Exp. Res.* 11(5):287–93.

Barre, Arnaud and Stéphane Armand. 2014. "Biomechanical ToolKit: Open-Source Framework to Visualize and Process Biomechanical Data." *Computer Methods and Programs in Biomedicine* 114(1):80–87.

Beynon, Sarah, Jennifer L. McGinley, Fiona Dobson, and Richard Baker. 2010. "Correlations of the Gait Profile Score and the Movement Analysis Profile Relative to Clinical Judgments." *Gait & Posture* 32(1):129–32.

Bohannon, R. W. 1986. "Test-Retest Reliability of Hand-Held Dynamometry during a Single Session of Strength Assessment." *Physical Therapy* 66(2):206–9.

Bohannon, R. W. 1988. "Make Tests and Break Tests of Elbow Flexor Muscle Strength." *Physical Therapy* 68(2):193–94.

Bohannon, Richard W. and a Williams Andrews. 1987. "Interrater Reliability of Hand-Held Dynamometry." *Physical Therapy* 67(6):931–33.

Bohannon, RW. 1990. "Hand-Held Compared with Isokinetic Dynamometry for Measurement of Static Knee Extension Torque (Parallel Reliability of Dynamometers)." *Clinical Physics and Physiological Measurement* 11(3):217–22.

Brodaty, Henry and Cressida M. Moore. 1997. "The Clock Drawing Test for Dementia of the Alzheimer's Type: A Comparison of Three Scoring Methods in a Memory Disorders Clinic." *International Journal of Geriatric Psychiatry* 12(6):619–27.

Brunner, R. and E. Rutz. 2013. "Biomechanics and Muscle Function during Gait." *Journal of Children's Orthopaedics* 7(5):367–71.

Butler, Erin E. et al. 2010. "Three-Dimensional Kinematics of the Upper Limb during a Reach and Grasp Cycle for Children." *Gait & Posture* 32(1):72–77.

Camerota, F. et al. 2015. "The Effects of Neuromuscular Taping on Gait Walking Strategy in a Patient with Joint Hypermobility syndrome/Ehlers-Danlos Syndrome Hypermobility Type." *Therapeutic Advances in Musculoskeletal Disease* 7(1):3–10.

Camerota, Filippo et al. 2013. "Neuromuscular Taping for the Upper Limb in Cerebral Palsy: A Case Study in a Patient with Hemiplegia." *Developmental Neurorehabilitation* 8423(6):1–4.

Camomilla, Valentina, Andrea Cereatti, Giuseppe Vannozzi, and Aurelio Cappozzo. 2006. "An Optimized Protocol for Hip Joint Centre Determination Using the Functional Method." *Journal of Biomechanics* 39(6):1096–1106.

Capodaglio, Paolo et al. 2009. "Strength Characterization of Knee Flexor and Extensor Muscles in Prader-Willi and Obese Patients." *BMC Musculoskeletal Disorders* 10:47.

Cappozzo, A., A. Cappello, U. Della Croce, and F. Pensalfini. 1997. "Surface-Marker

Cluster Design Criteria for 3-D Bone Movement Reconstruction." *IEEE Transactions on Bio-Medical Engineering* 44(12):1165–74.

Cappozzo, A., F. Catani, U. Della Croce, and A. Leardini. 1995. "Position and Orientation in Space of Bones during Movement: Anatomical Frame Definition and Determination." *Clinical Biomechanics* 10(4):171–78.

Cappozzo, Aurelio, Ugo Della Croce, Alberto Leardini, and Lorenzo Chiari. 2005. "Human Movement Analysis Using Stereophotogrammetry. Part 1: Theoretical Background." *Gait & Posture* 21(2):186–96.

Carpinella, Ilaria, Johanna Jonsdottir, and Maurizio Ferrarin. 2011. "Multi-Finger Coordination in Healthy Subjects and Stroke Patients: A Mathematical Modelling Approach." *Journal of Neuroengineering and Rehabilitation* 8(1):19.

Carriero, Alessandra, Amy Zavatsky, Julie Stebbins, Tim Theologis, and Sandra J. Shefelbine. 2009. "Determination of Gait Patterns in Children with Spastic Diplegic Cerebral Palsy Using Principal Components." *Gait & Posture* 29(1):71–75.

Casellato, Claudia, Giovanna Zorzi, Alessandra Pedrocchi, Giancarlo Ferrigno, and Nardo Nardocci. 2011. "Reaching and Writing Movements: Sensitive and Reliable Tools to Measure Genetic Dystonia in Children." *Journal of Child Neurology* 26(7):822–29.

Celletti, Claudia et al. 2013. "Use of the Gait Profile Score for the Evaluation of Patients with Joint Hypermobility syndrome/Ehlers–Danlos Syndrome Hypermobility Type." *Research in Developmental Disabilities* 34(11):4280–85.

Cerveri, P. et al. 2008. "In Vivo Validation of a Realistic Kinematic Model for the Trapezio-Metacarpal Joint Using an Optoelectronic System." *Annals of Biomedical Engineering* 36(7):1268–80.

Charbonnier, Caecilia et al. 2014. "Sexual Activity after Total Hip Arthroplasty: A Motion Capture Study." *The Journal of Arthroplasty* 29(3):640–47.

Chiari, Lorenzo, Ugo Della Croce, Alberto Leardini, and Aurelio Cappozzo. 2005. "Human Movement Analysis Using Stereophotogrammetry. Part 2: Instrumental Errors." *Gait & Posture* 21(2):197–211.

Chiu, H. Y., S. C. Lin, F. C. Su, S. T. Wang, and H. Y. Hsu. 2000. "The Use of the Motion Analysis System for Evaluation of Loss of Movement in the Finger." *Journal of Hand Surgery (Edinburgh, Scotland)* 25(2):195–99.

Cimolin, Veronica, Manuela Galli, Sara Laura Vimercati, and Giorgio Albertini. 2011. "Use of the Gait Deviation Index for the Assessment of Gastrocnemius Fascia Lengthening in Children with Cerebral Palsy." *Research in Developmental Disabilities* 32:377–81.

Clark, Ross a et al. 2010. "Validity and Reliability of the Nintendo Wii Balance Board for Assessment of Standing Balance." *Gait & Posture* 31(3):307–10.

Della Croce, Ugo, Alberto Leardini, Lorenzo Chiari, and Aurelio Cappozzo. 2005. "Human Movement Analysis Using Stereophotogrammetry. Part 4: Assessment of Anatomical Landmark Misplacement and Its Effects on Joint Kinematics." *Gait & Posture* 21(2):226–37.

Csuka, Maryellen and Daniel J. McCarty. 1985. "Simple Method for Measurement of Lower Extremity Muscle Strength." *The American Journal of Medicine* 78(1):77–81.

Dancey, CP and J. Reidy. 2004. *Statistics Without Maths for Psychology*. Harlow: Pearson Education.

Davis, Roy B., Sylvia Õunpuu, Dennis Tyburski, and James R. Gage. 1991. "A Gait Analysis Data Collection and Reduction Technique." *Human Movement Science* 10(5):575–87.

Delp, Scott L., Allison S. Arnold, Rosemary A. Speers, and Carolyn A. Moore. 1996. "Hamstrings and Psoas Lengths during Normal and Crouch Gait: Implications for Muscle-Tendon Surgery." *Journal of Orthopaedic Research* 14(1):144–51.

Eek, MN, AK Kroksmark, and E. Beckung. 2006. "Isometric Muscle Torque in Children 5 to 15 Years of Age: Normative Data." *Archives of Physical Medicine and Rehabilitation* 87:1091–99.

Esbjörnsson, A. et al. 2014. "Quantifying Gait Deviations in Patients with Rheumatoid Arthritis Using the Gait Deviation Index." *Gait & Posture* 36(September):S53.

Ferrari, Alberto et al. 2008. "Quantitative Comparison of Five Current Protocols in Gait Analysis." *Gait & Posture* 28(2):207–16.

Fischman, Joshua. 1987. "Graphology : The Write Stuff?" *Psychology Today* 21(7):11.

Frankenburg, William K. and Josiah B. Dodds. 1967. "The Denver Developmental Screening Test." *The Journal of Pediatrics* 71(2):181–91.

Fulcher, Mark L., Chris M. Hanna, and C. Raina Elley. 2010. "Reliability of Handheld Dynamometry in Assessment of Hip Strength in Adult Male Football Players." *Journal of Science and Medicine in Sport* 13(1):80–84.

Galli, Manuela, Sara Laura Vimercati, et al. 2011. "A New Approach for the Quantitative Evaluation of Drawings in Children with Learning Disabilities." *Research in Developmental Disabilities* 32(3):1004–10.

Galli, Manuela, Veronica Cimolin, et al. 2011. "The Effects of Muscle Hypotonia and Weakness on Balance: A Study on Prader-Willi and Ehlers-Danlos Syndrome Patients." *Research in Developmental Disabilities* 32(3):1117–21.

Galli, Manuela, Veronica Cimolin, Marcello Crivellini, and Giorgio Albertini. 2009. "Long-Term Evaluation of Isolated Gastrocnemius Fascia Lengthening in Children with Cerebral Palsy Using Gait Analysis." *Journal of Pediatric Orthopaedics B* 18(5):228–33.

Galli, Manuela, Veronica Cimolin, Maria Francesca De Pandis, Michael H. Schwartz, and Giorgio Albertini. 2012. "Use of the Gait Deviation Index for the Evaluation of Patients With Parkinson's Disease." *Journal of Motor Behavior* 44(3):161–67.

Galli, Manuela, Veronica Cimolin, Chiara Rigoldi, Nunzio Tenore, and Giorgio Albertini. 2010. "Gait Patterns in Hemiplegic Children with Cerebral Palsy: Comparison of Right and Left Hemiplegia." *Research in Developmental Disabilities* 31(6):1340–45.

Galli, Manuela, Chiara Rigoldi, Reinald Brunner, Naznin Virji-Babul, and Albertini Giorgio. 2008. "Joint Stiffness and Gait Pattern Evaluation in Children with Down

Syndrome." *Gait & Posture* 28:502–6.

Gilboa, Yafit, Naomi Josman, Aviva Fattal-Valevski, Hagit Toledano-Alhadef, and Sara Rosenblum. 2010. "The Handwriting Performance of Children with NF1." *Research in Developmental Disabilities* 31(4):929–35.

Goodenough, F. L. 1928. "Studies in the Psychology of Children's Drawings." *Psychological Bulletin* 25(5):272–83.

Hartmann, Antonia, Ruud Knols, Kurt Murer, and Eling D. de Bruin. 2009. "Reproducibility of an Isokinetic Strength-Testing Protocol of the Knee and Ankle in Older Adults." *Gerontology* 55(3):259–68.

Hébert, Luc J. et al. 2011. "Isometric Muscle Strength in Youth Assessed by Hand-Held Dynamometry: A Feasibility, Reliability, and Validity Study." *Pediatric Physical Therapy : The Official Publication of the Section on Pediatrics of the American Physical Therapy Association* 23(3):289–99.

Higuchi, T. 1988. "Approach to an Irregular Time Series on the Basis of the Fractal Theory." *Physica D: Nonlinear Phenomena* 31:277–83.

Hoffinger, S. A., G. T. Rab, and H. Abou-Ghaida. 1993. "Hamstrings in Cerebral Palsy Crouch Gait." *Journal of Pediatric Orthopedics* 13(6):722–26.

von Hofsten, C. 1991. "Structuring of Early Reaching Movements: A Longitudinal Study." *Journal of Motor Behavior* 23(4):280–92.

von Hofsten, C. and L. Rönnqvist. 1993. "The Structuring of Neonatal Arm Movements." *Child Development* 64(4):1046–57.

Hughes, V. A. et al. 2001. "Longitudinal Muscle Strength Changes in Older Adults: Influence of Muscle Mass, Physical Activity, and Health." *The Journals of Gerontology. Series A, Biological Sciences and Medical Sciences* 56(5):B209–17.

Iosa, M. et al. 2014. "Assessment of Waveform Similarity in Clinical Gait Data: The Linear Fit Method." *BioMed Research International* 2014:1–7.

Janssen, Jessie C. and Lan Le-Ngoc. 2009. "Intratester Reliability and Validity of Concentric Measurements Using a New Hand-Held Dynamometer." *Archives of Physical Medicine and Rehabilitation* 90(9):1541–47.

Jastifer, James R. and Luis H. Toledo-Pereyra. 2012. "Leonardo Da Vinci's Foot: Historical Evidence of Concept." *Journal of Investigative Surgery* 25(5):281–85.

Jones, C. J., E. R. Rikli, and W. C. Beam. 1999. "A 30-S Chair-Stand Test as a Measure of Lower Body Strength in Community-Residing Older Adults." *Research Quarterly for Exercise and Sport* 70(2):113–19.

Katz, Michael J. 1988. "Fractals and the Analysis of Waveforms." *Computers in Biology and Medicine* 18:145–56.

Khalid, Puspa Inayat et al. 2010. "The Use of Graphic Rules in Grade One to Help Identify Children at Risk of Handwriting Difficulties." *Research in Developmental Disabilities* 31(6):1685–93.

Kim, Won Kuel, Don Kyu Kim, Kyung Mook Seo, and Si Hyun Kang. 2014. "Reliability and Validity of Isometric Knee Extensor Strength Test with Hand-Held Dynamometer Depending on Its Fixation: A Pilot Study." *Annals of Rehabilitation*

Medicine 38(1):84–93.

Klonowski, Wlodzimierz. 2000. "Signal and Image Analysis Using Chaos Theory and Fractal Geometry." *Machine Graphics and Vision* 9(1):403–31.

van der Krogt, Marjolein M., Caroline A. M. Doorenbosch, Jules G. Becher, and Jaap Harlaar. 2009. "Walking Speed Modifies Spasticity Effects in Gastrocnemius and Soleus in Cerebral Palsy Gait." *Clinical Biomechanics* 24(5):422–28.

van der Krogt, Marjolein M., Lizeth H. Sloot, Annemieke I. Buizer, and Jaap Harlaar. 2015. "Kinetic Comparison of Walking on a Treadmill versus over Ground in Children with Cerebral Palsy." *Journal of Biomechanics* 48(13):3577–83.

Laing, B. A., F. L. Mastaglia, S. K. Lo, and P. Zilko. 1995. "Comparative Assessment of Knee Strength Using Hand-Held Myometry and Isometric Dynamometry in Patients with Inflammatory Myopathy." *Physiotherapy Theory and Practice* 11(3):151–56.

Leardini, Alberto, Lorenzo Chiari, Ugo Della Croce, and Aurelio Cappozzo. 2005. "Human Movement Analysis Using Stereophotogrammetry. Part 3. Soft Tissue Artifact Assessment and Compensation." *Gait & Posture* 21(2):212–25.

Longstaff, M. G. and R. a. Heath. 2006. "Spiral Drawing Performance as an Indicator of Fine Motor Function in People with Multiple Sclerosis." *Human Movement Science* 25(4–5):474–91.

Lopes, R. and N. Betrouni. 2009. "Fractal and Multifractal Analysis: A Review." *Medical Image Analysis* 13(4):634–49.

Mahony, K., A. Hunt, D. Daley, S. Sims, and R. Adams. 2009. "Inter-Tester Reliability and Precision of Manual Muscle Testing and Hand-Held Dynamometry in Lower Limb Muscles of Children with Spina Bifida." *Physical and Occupational Therapy in Pediatrics* 29(1):44–59.

Marey, EJ. 1874. *Terrestrial and Aerial Locomotion.* New York: Appleton and company.

Marey, M. 1894. "Des Mouvements Que Certains Animaux Exécutent Pour Retomber Sur Leurs Pieds, Lorsqu'ils Sont Précipités D'un Lieu Élevé." *Acad. Sci.* 119:714–17.

Marmon, Adam R., Federico Pozzi, Ali H. Alnahdi, and Joseph a Zeni. 2013. "The Validity of Plantarflexor Strength Measures Obtained through Hand-Held Dynamometry Measurements of Force." *International Journal of Sports Physical Therapy* 8(6):820–27.

Marr, D. 1982. "Vision: A Computational Investigation into the Human Representation and Processing of Visual Information."

Martin, H. J. et al. 2006. "Is Hand-Held Dynamometry Useful for the Measurement of Quadriceps Strength in Older People? A Comparison with the Gold Standard Biodex Dynamometry." *Gerontology* 52(3):154–59.

Massaad, Abir, Ayman Assi, Wafa Skalli, and Ismat Ghanem. 2014. "Repeatability and Validation of Gait Deviation Index in Children: Typically Developing and Cerebral Palsy." *Gait & Posture* 39(1):354–58.

Maughan, RJ, JS Watson, and J. Weir. 1983. "Strength and Cross-Sectional Area of Human Skeletal Muscle." *The Journal of Physiology* 338:37–49.

Metcalf, Cheryl D., Scott V Notley, Phappell H. Chappell, Jane H. Burridge, and Victoria T. Yule. 2008. "Validation and Application of a Computational Model for Wrist and Hand Movements Using Surface Markers." *IEEE Transactions on Bio-Medical Engineering* 55(3):1199–1210.

Molloy, M., B. C. McDowell, C. Kerr, and A. P. Cosgrove. 2010. "Further Evidence of Validity of the Gait Deviation Index." *Gait & Posture* 31(4):479–82.

Morris, A. F., Susan E. Vaughan, and P. Vaccaro. 1982. "Measurements of Neuromuscular Tone and Strength in Down's Syndrome Children." *Journal of Mental Deficiency Research* 26(1):41–46.

Muybridge, Eadweard. 1878. "The Science of the Horse's Motions." *Scientific American* 39:241.

van den Noort, JC, A. Ferrari, AG Cutti, JG Becher, and J. Harlaar. 2013. "Gait Analysis in Children with Cerebral Palsy via Inertial and Magnetic Sensors." *Med Biol Eng Comput* 51(4):377–86.

Palisano, Robert et al. 2008. "Development and Reliability of a System to Classify Gross Motor Function in Children with Cerebral Palsy." *Developmental Medicine & Child Neurology* 39(4):214–23.

De Pandis, Maria Francesca et al. 2010. "A New Approach for the Quantitative Evaluation of the Clock Drawing Test: Preliminary Results on Subjects with Parkinson's Disease." *Neurology Research International* 2010:283890.

Phillips, Beverley A., Sing K. Lo, and Frank L. Mastaglia. 2000. "Muscle Force Measured Using 'break' testing with a Hand-Held Myometer in Normal Subjects Aged 20 to 69 Years." *Archives of Physical Medicine and Rehabilitation* 81(5):653–61.

Piccinini, Luigi et al. 2011. "3D Gait Analysis in Patients with Hereditary Spastic Paraparesis and Spastic Diplegia: A Kinematic, Kinetic and EMG Comparison." *European Journal of Paediatric Neurology* 15(2):138–45.

Riddle, D. L., S. D. Finucane, J. M. Rothstein, and M. L. Walker. 1989. "Intrasession and Intersession Reliability of Hand-Held Dynamometer Measurements Taken on Brain-Damaged Patients." *Physical Therapy* 69(3):182–94.

Rigoldi, Chiara et al. 2012. "Gait Strategy in Patients with Ehlers-Danlos Syndrome Hypermobility Type and Down Syndrome." *Research in Developmental Disabilities* 33(5):1437–42.

Rigoldi, Chiara, Manuela Galli, and Giorgio Albertini. 2011. "Gait Development during Lifespan in Subjects with Down Syndrome." *Research in Developmental Disabilities* 32(1):158–63.

Romei, M., M. Galli, F. Motta, M. Schwartz, and M. Crivellini. 2004. "Use of the Normalcy Index for the Evaluation of Gait Pathology." *Gait and Posture* 19:85–90.

Rose, G. E., K. A. Lightbody, R. G. Ferguson, J. C. Walsh, and J. E. Robb. 2010. "Natural History of Flexed Knee Gait in Diplegic Cerebral Palsy Evaluated by Gait Analysis in Children Who Have Not Had Surgery." *Gait & Posture* 31(3):351–54.

Rosenbaum, David. 2009. *Human Motor Control.* 2nd ed. Academic Press.

Rosenbaum, Peter L., Robert J. Palisano, Doreen J. Bartlett, Barbara E. Galuppi, and Dianne J. Russell. 2008. "Development of the Gross Motor Function Classification

System for Cerebral Palsy." *Developmental Medicine & Child Neurology* 50(4):249–53.

Rosenblum, Sara and Miri Livneh-Zirinski. 2008. "Handwriting Process and Product Characteristics of Children Diagnosed with Developmental Coordination Disorder." *Human Movement Science* 27(2):200–214.

Rutz, Erich, Susan Donath, Oren Tirosh, H.Kerr Graham, and Richard Baker. 2013. "Explaining the Variability Improvements in Gait Quality as a Result of Single Event Multi-Level Surgery in Cerebral Palsy." *Gait and Posture* 38(3):455–60.

Sale, P. et al. 2012. "The Relation between Parkinson's Disease and Ageing-Comparison of the Gait Patterns of Young Parkinson's Disease Subjects with Healthy Elderly Subjects." *European Journal of Physical and Rehabilitatation Medicine* 48:1–7.

Sale, Patrizio et al. 2013. "Robot-Assisted Walking Training for Individuals with Parkinson's Disease: A Pilot Randomized Controlled Trial." *BMC Neurology* 13(1):50.

Schutte, L. M. M. et al. 2000. "An Index for Quantifying Deviations from Normal Gait." *Gait and Posture* 11(1):25–31.

Schwartz, M. H., T. F. Novacheck, and J. Trost. 2000. "A Tool for Quantifying Hip Flexor Function during Gait." *Gait & Posture* 12(2):122–27.

Schwartz, Michael H. and Adam Rozumalski. 2008. "The Gait Deviation Index: A New Comprehensive Index of Gait Pathology." *Gait and Posture* 28(3):351–57.

Scott, S. H. and D. A. Winter. 1990. "Internal Forces of Chronic Running Injury Sites." *Medicine and Science in Sports and Exercise* 22(3):357–69.

Small, C. F. et al. 1996. "Validation of a 3D Optoelectronic Motion Analysis System for the Wrist Joint." *Clinical Biomechanics* 11(8):481–83.

Spink, Martin J. et al. 2011. "Foot and Ankle Strength, Range of Motion, Posture, and Deformity Are Associated With Balance and Functional Ability in Older Adults." *Archives of Physical Medicine and Rehabilitation* 92(1):68–75.

Stebbins, Julie et al. 2014. "Recommendations for Reporting Gait Studies." *Gait & Posture* 10–11.

Taub, Edward and AJ Berman. 1968. "Movement and Learning in the Absence of Sensory Feedback." Pp. 173–92 in *The neuropsychology of spatially oriented behavior*, edited by S. J. Freeman. Homewood, USA: Dorsey.

Thomason, Pamela et al. 2011. "Single-Event Multilevel Surgery in Children with Spastic Diplegia: A Pilot Randomized Controlled Trial." *The Journal of Bone and Joint Surgery (American)* 93(5):451–60.

Tsaopoulos, Dimitrios E., Vasilios Baltzopoulos, Paula J. Richards, and Constantinos N. Maganaris. 2011. "Mechanical Correction of Dynamometer Moment for the Effects of Segment Motion during Isometric Knee-Extension Tests." *Journal of Applied Physiology* 111(1):68–74.

Turner-Stokes, L. and K. Reid. 1999. "Three-Dimensional Motion Analysis of Upper Limb Movement in the Bowing Arm of String-Playing Musicians." *Clinical Biomechanics (Bristol, Avon)* 14(6):426–33.

Verschuren, O. et al. 2008. "Reliability of Hand-Held Dynamometry and Functional Strength Tests for the Lower Extremity in Children with Cerebral Palsy." *Disability and Rehabilitation* 30(18):1358–66.

Vimercati, S. L. et al. 2012. "Quantitative Evaluation of Graphic Gesture in Subjects with Parkinson's Disease and in Children with Learning Disabilities." *Gait & Posture* 35:S23–24.

Vimercati, S. L. et al. 2014. "Clumsiness in Fine Motor Tasks: Evidence from the Quantitative Drawing Evaluation of Children with Down Syndrome." *Journal of Intellectual Disability Research* 1–9.

Vimercati, Sara Laura, Manuela Galli, Chiara Rigoldi, Andrea Ancillao, and Giorgio Albertini. 2013a. "Feedback Reliance during an Arm-Tapping Task with Obstacle Avoidance in Adults with Down Syndrome." *Experimental Brain Research* 226(4):631–38.

Vimercati, Sara Laura, Manuela Galli, Chiara Rigoldi, Andrea Ancillao, and Giorgio Albertini. 2013b. "Motor Strategies and Motor Programs during an Arm Tapping Task in Adults with Down Syndrome." *Experimental Brain Research* 225(3):333–38.

Vismara, Luca et al. 2016. "Osteopathic Manipulative Treatment Improves Gait Pattern and Posture in Adult Patients with Prader–Willi Syndrome." *International Journal of Osteopathic Medicine* 19:35–43.

Wang, Ching-Yi, Sharon L. Olson, and Elizabeth J. Protas. 2002. "Test-Retest Strength Reliability: Hand-Held Dynamometry in Community-Dwelling Elderly Fallers." *Archives of Physical Medicine and Rehabilitation* 83(6):811–15.

Whittle, M. 1996. "Clinical Gait Analysis: A Review." *Human Movement Science* 15(3):369–87.

Willemse, Lydia et al. 2013. "Reliability of Isometric Lower-Extremity Muscle Strength Measurements in Children with Cerebral Palsy: Implications for Measurement Design." *Physical Therapy* 93(7):935–41.

Wuang, YP, JJ Chang, MH Wang, and HC Lin. 2013. "Test–retest Reliabilities of Hand-Held Dynamometer for Lower-Limb Muscle Strength in Intellectual Disabilities." *Research in Developmental Disabilities* 34:2281–90.